

**CHONDROCYTES ENCAPSULATION IN HYDROGEL BEADS AND
THEIR RESPONSE TO POLYPHOSPHATE INCORPORATION**

DENIS FABRICIO VIERA REY

Thesis submitted to the University of Ottawa

in partial Fulfillment of the requirements for the degree of

MASTER OF APPLIED SCIENCE

in Chemical Engineering

Department of Chemical and Biological Engineering

Faculty of Engineering

University of Ottawa

© Denis Fabricio Viera Rey, Ottawa, Canada, 2020

Abstract

In Canada, one in five people suffers from arthritis, of which the most common type is osteoarthritis (OA). OA is a group of joint diseases that cause pain and loss of range of motion and for which there is currently no cure. OA can be caused by numerous factors such as aging, genetics, environmental elements, and abnormal joint biomechanics (e.g., injury, obesity). These diseases are degenerative and lead to the progressive breakdown of joint cartilage, as well as changes in the underlying bone and other tissues of the joint over a period of years to decades. Articular cartilage incorporates a single type of resident cells, termed chondrocyte cells. These cells are entrapped within a dense extracellular matrix that limits their ability to proliferate and migrate to a site of injury, while the absence of blood vessels in the cartilage, amongst other factors, hinders the ability of progenitor cells to reach the site of injury, contributing to a limited capacity for intrinsic regeneration of the damaged tissue following an injury. As such, efforts to develop tissue engineering strategies that combine a biomaterial with bioactive signals to induce cells with the chondrogenic potential to regenerate tissue have been pursued actively. In this thesis, we investigate the potential of one such cartilage tissue engineering approach, whereby chondrocytes are encapsulated with alginate hydrogels incorporating inorganic polyphosphate (polyP), a promising chondrogenic signal. The driving hypothesis of the work was that polyanionic polyP would crosslink within the alginate hydrogel meshwork by ionic bonds with the multivalent cations used to form the hydrogel. Initial efforts focussed on optimizing the sterile chondrocyte encapsulation protocol for alginate beads, chondrocyte culture conditions to reduce proliferation – a response that is associated with dedifferentiation and a pathological state – and protocol for the incorporation of polyP in alginate bead when using calcium as a cationic crosslinker. We observed that polyP release from the calcium-alginate bead exhibited an important burst release to nearly

80% of the initial polyP loading within 24 hours of incubation in the culture medium. Increasing the alginate concentration led to approximately a 2.5-fold increase in polyP retention following the burst release. Subsequent incubation showed a more controlled release for at least 1 week. Efforts to reduce hydrogel swelling and increase its stability by substituting Ca^{2+} by Sr^{2+} as a crosslinker did not reduce the release rate during the burst release phase, nor did it increase the polyP retention following this initial stage. Other divalent cations including Mg^{2+} and Co^{2+} , and pre-loading the polyP-alginate solution with a small concentration of Ca^{2+} did not impact the release profile either. Chondrocytes encapsulated in calcium- and strontium-alginate beads showed decreased DNA content and increased sulfated glycosaminoglycan accumulation at 1 week when polyP was incorporated in the beads compared to controls without polyP; however, this effect was lost at longer time points. These results suggest that this new material may find applications as a vehicle for the short-term delivery of polyP in joints and other tissues. Further efforts to improve the polyP release profile from alginate beads lead to promising results with the use of polyethylenimine (PEI) as a cationic tethering molecule between polyP and alginate. This thesis aims to generate novel biomaterials that can be used to stimulate cartilage tissue regeneration and to eventually develop a treatment strategy for OA. The work presented here will serve as a basis for continued efforts to ensure the prolonged retention of exogenous polyP into the joint.

Résumé

Au Canada, une personne sur cinq souffre d'arthrite, dont le type le plus courant est l'arthrose. L'arthrose est un groupe de maladies articulaires qui provoquent des douleurs et une perte d'amplitude de mouvement et pour lesquelles il n'existe actuellement aucun remède. L'arthrose peut être causée par de nombreux facteurs tels que le vieillissement, la génétique, les éléments environnementaux et la biomécanique articulaire anormale (par exemple, les blessures et l'obésité). Ces maladies sont dégénératives et entraînent la dégradation progressive du cartilage articulaire, ainsi que des modifications des os sous-jacents et des autres tissus de l'articulation sur une période de plusieurs années à des décennies. Le cartilage articulaire incorpore un seul type de cellules résidentes, appelées cellules chondrocytaires. Ces cellules sont piégées dans une matrice extracellulaire dense qui limite leur capacité à proliférer et à migrer vers le site d'une blessure, tandis que l'absence de vaisseaux sanguins dans le cartilage, entre autres facteurs, entrave la capacité des cellules progénitrices à atteindre le site d'une blessure, contribuant ainsi à une capacité limitée de régénération intrinsèque des tissus endommagés. Des efforts pour développer des stratégies d'ingénierie tissulaire qui combinent un biomatériau avec des signaux bioactifs pour stimuler des cellules ayant un potentiel chondrogène à régénérer les tissus ont donc été activement poursuivis. Dans cette thèse, nous présentons les résultats d'une étude sur le potentiel d'une telle approche d'ingénierie tissulaire du cartilage, impliquant l'encapsulation de chondrocytes dans des hydrogels d'alginate incorporant du polyphosphate inorganique (polyP), un signal chondrogène prometteur. L'hypothèse centrale de cette thèse était que le polyP polyanionique serait réticulé dans le maillage hydrogel d'alginate par des liaisons ioniques avec les cations multivalents utilisés pour former l'hydrogel. Les premiers efforts se sont concentrés sur l'optimisation du protocole d'encapsulation stérile des chondrocytes dans les billes d'alginate, des conditions de culture des

chondrocytes pour réduire la prolifération - une réponse associée à la dédifférenciation et à un état pathologique - et du protocole d'incorporation de polyP dans les billes d'alginate. Nous avons observé que la libération du polyP des billes d'alginate de calcium était de près de 80% de la charge initiale de polyP après seulement 24 heures d'incubation dans un milieu de culture. L'augmentation de la concentration d'alginate a conduit à une augmentation d'environ 2,5 fois de la rétention de polyP après cette libération initiale rapide. L'incubation ultérieure a montré un taux de libération plus contrôlée pendant au moins 1 semaine. Les efforts pour augmenter la stabilité de l'hydrogel en substituant le Ca^{2+} par le Sr^{2+} comme agent réticulant n'a pas ralenti la libération du polyP pendant la phase de libération initiale, ni augmenté la rétention de polyP durant la phase subséquente. D'autres cations divalents, notamment le Mg^{2+} et le Co^{2+} , et le préchargement de la solution de polyP-alginate avec une petite concentration de Ca^{2+} n'ont pas eu d'impact sur le profil de libération non plus. Les chondrocytes encapsulées dans des billes d'alginate de calcium et de strontium ont montré une diminution de la teneur en ADN et une augmentation de l'accumulation de glycosaminoglycane sulfaté après 1 semaine d'incubation lorsque le polyP était incorporé dans les billes par rapport aux contrôles sans polyP; cependant, cet effet était perdu après des incubations plus longues. Ces résultats suggèrent que ce nouveau matériau peut trouver des applications comme véhicule pour la livraison à court terme de polyP dans les articulations et d'autres tissus. Des efforts supplémentaires pour améliorer le profil de libération du polyP à partir des billes d'alginate conduisent à des résultats prometteurs avec l'utilisation de polyéthylénimine (PEI) comme molécule de liaison cationique entre le polyP et l'alginate. Cette thèse vise à générer de nouveaux biomatériaux qui peuvent être utilisés pour stimuler la régénération des tissus cartilagineux et éventuellement développer une stratégie de traitement de l'arthrose. Les travaux

présentés ici serviront de base aux efforts continus pour assurer la rétention prolongée du polyP dans l'articulation.

Statement of Originality

All the contents presented in this thesis document are the product of the original work done by the author under the supervision of Dr. Jean-Philippe St-Pierre at the University of Ottawa in the Department of Chemical and Biological Engineering in partial fulfillment of the requirements for the degree of Master of Applied Science (Chemical Engineering) at the University of Ottawa. This work has been presented in/as:

1. Poster entitled “Chondrocytes encapsulation in alginate hydrogel beads functionalized with inorganic polyphosphate” by Mr. Denis Viera and Dr. Jean-Philippe St-Pierre at the Graduate Engineering poster competition held at the University of Ottawa on March 6, 2019.
2. Poster entitled “Chondrocytes encapsulation in alginate hydrogel beads functionalized with inorganic polyphosphate” by Mr. Denis Viera and Dr. Jean-Philippe St-Pierre at the 35th Annual Meeting of the Canadian Biomaterials Society in Quebec City on May 23, 2019.

Statement of contributions and collaborators

This thesis document was entirely written by the author and reviewed by his supervisor, Dr. Jean-Philippe St-Pierre. The work presented in the thesis was largely performed by the author. The studies on the investigation of polyP action on chondrocyte cells are entirely his work and involved support from Mr. Neelabh Rastogi as part of his NSERC Undergraduate Student Research Award. Early work toward polyP retention/quantification and alginate beads characterization involved support from Mr. Jordan Nhan as part of his NSERC Undergraduate Student Research Award; however, the data presented on this topic in this thesis was performed by the author.

I would like to dedicate this thesis to my family: my sweet Grace for her love, support and encouragement, and my loved Denis Emanuel for letting me learn how to be a better human being during this adventure.

Acknowledgment

I would first like to express my deep gratitude to my supervisor Dr. Jean-Philippe St-Pierre for his patient guidance, enthusiastic encouragement and useful critiques throughout my research work.

I would like to thank my lab colleagues, Janani Mahendran, Sietske Barnes, Jordan Nhan, Noor Ghadie, Nimrah Munir, Neelabh Rastogi, Jacob Boisvert, Maude Tremblay, Josh Yazbeck, Justin Quan, Jean-Pascal Bourassa, and Shreya Nagavalli for their help in my research and also for making it an enjoyable experience during these two years. I would also like to thank Dr. Xudong Cao and his students for all the support and predisposition to allow me to work in your laboratory, as well as Dr. Roberto Chica and Dr. Christopher Lan for the help provided. Thanks to all professors and members of the Department of Chemical and Biological Engineering for the guidance and timely support. I would also thank you to Secretaría de Educación Superior, Ciencia, Tecnología e Innovación (SENESCYT) from the Ecuadorian government for providing fundings during the time of this master. Finally, but not least I would like to thank my family: Grace Kelly Quirola Punin and Denis Emanuel Viera for always being my source of motivation. I would like to thank my mother Mary Dolores Rey Torres to whom I owe everything, my brother David Alexander Viera Rey, my relatives Rey who supported my family all the time, and every single person who contributed to the realization of this project.

Table of content

Abstract	ii
Résumé	iv
Statement of Originality	vii
Statement of contributions and collaborators	viii
Acknowledgment	x
List of Abbreviations	xv
List of Tables	xvii
List of Figures	xviii
CHAPTER 1 – INTRODUCTION AND RESEARCH OBJECTIVES	1
1.1 Introduction	1
1.2 Hypothesis.....	3
1.3 Thesis Objectives	4
1.4 Thesis Organization.....	4
CHAPTER 2 - LITERATURE REVIEW	5
2.1 Articular Cartilage.....	5
2.1.1 <i>Functions of Articular Cartilage</i>	5
2.1.2 <i>Composition of articular cartilage</i>	5
<u>2.1.2.1 Collagens</u>	6
<u>2.1.2.2 Proteoglycans</u>	7

<u>2.1.2.3 Chondrocyte Cells</u>	8
2.1.3 <i>Articular cartilage organization</i>	9
2.2 Osteoarthritis.....	10
2.2.1 <i>Causes and consequences</i>	11
2.2.2 <i>Diagnosis and current treatments</i>	12
<u>2.2.2.1 Conservative treatments</u>	13
<u>2.2.2.2 Surgical treatments</u>	15
<u>2.2.2.3 Implants</u>	19
2.3 Cartilage Tissue Engineering.....	20
2.3.1 <i>Inorganic Polyphosphate (PolyP)</i>	21
2.3.2 <i>Scaffolds and templates for cartilage tissue engineering</i>	23
<u>2.3.2.1 Hydrogels</u>	23
<u>2.3.2.2 Ionically crosslinked alginate hydrogels</u>	24
2.3.3 <i>Proposed Strategy</i>	26
CHAPTER 3 - MATERIALS AND METHODS	28
3.1 Materials.....	28
3.2 Alginate bead formation.....	28
3.3 Quantification of inorganic polyphosphate retention in beads.....	29
3.4 Alginate bead swelling and degradation.....	30
3.5 Compression test on alginate hydrogels.....	30

3.6 Chondrocyte cells isolation and culture	31
3.7 Biological assays	32
3.7.1 <i>Live/Dead viability test</i>	32
3.7.2 <i>Biochemical content of alginate beads</i>	32
<u>3.7.2.1 Papain digestion</u>	32
<u>3.7.2.2 DNA content assay</u>	33
<u>3.7.2.3 Sulfated DNA content assay</u>	33
3.8 Statistical analysis	34
CHAPTER 4 – RESULTS AND DISCUSSION PART 1:	35
4.1 Effects of the incorporation of polyP in calcium-alginate beads	35
4.2 Effects of culture conditions on chondrocytes encapsulated in ca-alginate beads.....	39
4.3 Effect of NaCl on chondrocytes morphology	42
4.4 Effect of bead formation on polyP content	44
4.5 PolyP release profile of calcium-alginate beads	46
4.6 Swelling of Alginate Beads.....	51
4.7 Mechanical properties of alginate gels in compression	58
4.8 Effect of polyP incorporation on the response of chondrocytes encapsulated in alginate beads.....	60
CHAPTER 5 – RESULTS AND DISCUSSION PART 2:	64
5.1 Investigation of other bioactive cations (Co ²⁺ and Mg ²⁺) as ionic crosslinkers.....	64

5.2 Effect of ethanol addition in crosslinking bath on polyP retention.....	66
5.3 Effect of polycationic polymers on polyP retention.....	67
5.3.1 Chitosan.....	67
5.3.2 Polyethylenimine	68
CHAPTER 6 – CONCLUSIONS, LIMITATIONS AND FUTURE WORK.....	74
6.1 Conclusions.....	74
6.2 Limitations	75
6.3 Future work.....	75
References.....	77

List of Abbreviations

M-block	1,4-linked B-D-mannuronic acid
2D	2-dimentional
ATP	Adenosine triphosphate
G-block	α -L-guluronic acid
AC	Articular cartilage
ACI	Autologous chondrocyte implantation
CA	Canada
CO ₂	Carbon di-oxide
CHs	Collagen hydrolysates
COX-I	Cyclooxygenase I
COX-II	Cyclooxygenase II
DNA	Deoxyribonucleic acid
ddH ₂ O	Distilled and deionized water
DAPI	Diamidino-2-phenylindole
DMMB	Dimethylmethylene blue
DMOADs	Disease modifying Osteoarthritis drugs
dsDNA	Double stranded deoxyribonucleic acid
DMEM	Dulbecco's Modified Eagle's Medium
EDTA	Ethylenediaminetetraacetic acid
ECM	Extracellular matrix
FBS	Fetal Bovine Serum
FITC	Fluorescein Isothiocyanate
GAG	Glycosaminoglycans
ITS	Insulin-transferrin-selenium
IA	Intra-articular
KL	Kellgren-Lawrence
MRI	Magnetic resonance imaging
MSM	Methylsulfonylmethane
μ g	Microgram
μ L	Microliter
μ m	Micrometer
nm	Nanometer
NSAIDs	Non-steroidal-anti-inflammatory drugs
OA	Osteoarthritis
OATS	Osteochondral autologous transfer system
PCM	Pericellular matrix
PBS	Phosphate buffered saline

PRP	Platelet-rich plasma
PDMS	Polydimethylsiloxane
polyP	Polyphosphate
PI	Propidium iodide
sGAG	Sulfated glycosaminoglycans
TRITC	Tetramethyl rhodamine
USA	United States of America

List of Tables

Table 1. Measured polyP content when polyP is mixed with PEI and control conditions.	71
Table 2. Measured polyP content in solution when polyP is mixed with PEI and alginate and control conditions at different solution pH.	71
Table 3. Measured polyP content in beads when polyP is mixed with PEI and alginate and control conditions at different solution pH.	72

List of Figures

Figure 1. Schematic representation of AC, cellular organization in the zones of AC, and the relative diameters and organization of collagen microfibrils. (Reprinted with permission from the Composition and Structure of Articular Cartilage: A Template for Tissue Repair ^[41] .)	9
Figure 2. Schematic step by step representation of the microfracture technique. (A) Debridement to create a stable cartilage margin, (B) removal of the zone of calcified cartilage, (C) microfracture penetrations, (D) well-anchored mesenchymal clot filling. Reprinted by permission of Clinical Orthopaedic Rehabilitation: a Team Approach (406), by G. Kelley, et.al., 2018, Elsevier Books ^[59]	17
Figure 3. Schematic representation of the autologous cartilage implantation (ACI) procedure. In a two-surgery procedure, cartilage is harvest, autologous cells are isolated and cultured to proliferate, and the cells are reinsertion by injection them underneath a sutured periosteal or collagen membrane. Reprinted by permission of Current Surgical Treatment of Knee Osteoarthritis (3), by K. Rönn, et.al., 2011, Switzerland, Hindawi Publishing Corporation ^[47]	18
Figure 4. Osteochondral autograft transplantation. (A) Shows one plug hole (B) shows multiple plugs used to fill the defect. (C)A sagittal section that shows how the osteochondral graft spaced to be filled. Reprinted by permission of Clinical Orthopaedic Rehabilitation: a Team Approach (406), by G. Kelley, et.al., 2018, Elsevier Books ^[59]	19
Figure 5. Chemical structure of inorganic polyphosphate (polyP).	22
Figure 6. Schematic representation of the different physical and chemical crosslinking method to form hydrogels. Reprinted with permission from N. Eslahi, M. Abdorahim, A. Simchi, Biomacromolecules 2016, 17, 3441. Copyright (2016) American Chemical Society ^[79]	24

Figure 7. Chemical structures of alternating alginate blocks of G-blocks and M-blocks. Reprinted with permission from *Alginate: Properties and biomedical applications* (108), by K. Yong Lee, et.al. 2012, United States, Elsevier. 25

Figure 8. Schematic representation of the main constituents in this study for cartilage tissue engineering. Bovine chondrocytes as native cell, polyP as the biomolecule and alginate beads as scaffold to provide an adequate 3-D environment. Adapted from *Cartilage Regeneration and Tissue Engineering* (369), by M. Sancho-Tello, et.al., 2019, Spain, Elsevier^[39]. 27

Figure 9. DNA content of chondrocyte-encapsulated alginate beads formed to incorporate 0.0, 1.0, and 2.5 mM polyP at days 0, 1, and 14 in culture. The experiment was performed in triplicates. Data are presented as means ± standard deviation..... 36

Figure 10. Calcium-alginate beads formed with different initial concentrations of polyp with chondrocytes entrapped in the 3D structure after different time points in culture. Red arrowheads highlight some of the large cell agglomerates that start appearing between 3 and 7 days in culture. 37

Figure 11. sGAG accumulation by chondrocytes encapsulated in alginate beads prepared with 0, 1, and 2.5 mM polyP at days 7, and 14. The sGAG data are normalized by the DNA content of the beads. The experiment was performed in triplicates. Data is presented as means ± standard deviation ($p < 0.05$; $n=3$). * indicates a statistically significant difference between the 2.5 mM and 0 mM polyP control condition. 38

Figure 12. DNA content of chondrocyte-encapsulated alginate beads cultured in 10% FBS, 2% FBS and 1% ITS culture conditions at days 0, 1, and 14. The experiment was performed in triplicates. Data are presented as means ± standard deviation. * indicates a statistically significant increase in DNA content at the control condition (10% FBS)..... 40

Figure 13. Calcium-alginate beads in different culture conditions (10% FBS, 2% FBS, and 1% ITS) with chondrocytes entrapped in the 3D structure after 7 days in culture. Red arrowheads highlight some of the large cell agglomerates that start appearing between 3 and 7 days in culture. 41

Figure 14. sGAG accumulation by chondrocytes encapsulated in alginate beads in 10% FBS, 2% FBS, and 1% ITS culture conditions at days 7, and 14. The sGAG data are normalized by the DNA content of the beads. The experiment was performed in triplicates. Data is presented as means \pm standard deviation ($p < 0.05$; $n=3$). * indicates a statistically significant difference compared to the control 10% FBS. 41

Figure 15. Morphology of bovine chondrocytes in monolayer culture on tissue culture plastic in DMEM alone or supplemented with different concentrations of NaCl imaged by light microscopy 24 hours after the introduction of the NaCl. 44

Figure 16. PolyP content within spiked an alginate solution (7.5 μ L) before forming the bead (solution) and after forming the bead in CaCl_2 for 30 minutes and washing once with PBS. PolyP was spiked at 2.5 and 25.0 mM. The experiment was performed in five replicates. Data are presented as means \pm standard deviation. * indicates a statistically significant difference compared to before gelation for 25.0 mM polyp condition. ** indicates a statistically significant difference compared to before gelation for 2.5 mM polyp condition 45

Figure 17. PolyP content within calcium-alginate beads prepared at different weight concentrations (1.0, 1.5, 2.0, 2.5, and 3.0 %wt.) after different times in DMEM. The initial polyP loading was 25 mM. The experiment was performed in quadruplets. Data are presented as means \pm standard deviation. * indicates a statistically significant difference compared to the other conditions. 47

Figure 18. PolyP cumulative release profile of calcium-alginate beads prepared at different CaCl₂ concentrations (0, 5, and 10 mM) after 24 hours in DMEM. The initial polyP loading was 25 mM. The experiment was performed in triplicates. Data are presented as means ± standard deviation. 49

Figure 19. Higuchi release profile of polyP from Ca-alginate beads. The first graph shows release until 6h while the second graph shows the release until 24h. 51

Figure 20. Hydrogel mass over time during incubation in PBS. Alginate beads formed by crosslinking with calcium and strontium cations (100 mM Ca, 50:50 Ca:Sr mM and 100 mM Sr) and alginate concentrations (1.0, 1.5, and 2.0 %wt.). The experiment was performed in triplicates from two different experiments. 52

Figure 21. Hydrogel mass over time during incubation in DMEM. Alginate beads were formed by crosslinking with calcium and strontium cations (100 mM Ca, 50:50 Ca:Sr mM and 100 mM Sr) and alginate concentrations (1.0, 1.5, and 2.0 %wt.). The experiment was performed in triplicates. 53

Figure 22. PolyP content within alginate beads prepared in crosslinking baths comprising different ratios of calcium and strontium after different times in DMEM. The initial polyP loading was 25 mM. The experiment was performed in quadruplets from 2 independent experiments. Data are presented as means ± standard deviation. * indicates a statistically significant difference compared to the Ca-alginate bead condition. 54

Figure 23. PolyP content inside strontium-alginate and calcium-alginate beads (7.5 μL) after gelation. Casting times of ~0, 15 and 30 min were investigated with and without a washing step with culture medium. A polyP concentration of 25 mM was used. The experiment was performed

in quadruplets. Data are presented as means \pm standard deviation. * indicates a statistically significant difference compared to the Ca-alginate bead condition for each time point. 55

Figure 24. Higuchi release profile of polyP from Sr-alginate beads. The first graph shows release until 6h while the second graph shows the release until 24h. Last graph shows the release profile for Sr-alginate and Ca-alginate bead..... 56

Figure 25. PolyP release profile from alginate beads crosslinked in baths with 50 mM and 250 mM. The experiment was performed in quadruples. Data are presented as means \pm standard deviation..... 58

Figure 26. Image of alginate disc compressed by an Instron instrument..... 59

Figure 27. Young's modulus in compression at 5 and 10 % strain of alginate gels prepared in crosslinking baths of 100 mM CaCl₂, 50:50 mM CaCl₂:SrCl₂ and 100 mM SrCl₂. Alginate concentrations used were 1, 2, and 3 %wt. The experiment was performed in nine replicates from three different experiments. Data are presented as means \pm standard deviation. 60

Figure 28. DNA content in three alginate beads (7.5 μ L) formed in crosslinking baths of 100 mM CaCl₂, 50:50 mM CaCl₂:SrCl₂, and 100 mM SrCl₂ and with or without 25 mM polyP at week 0, 1, 2, 3, and 4. The experiment was performed in triplicates. Data are presented as means \pm standard deviation. * indicates a statistically significant difference compared to treated conditions at week 1..... 62

Figure 29. sGAG/DNA content in three alginate beads (7.5 μ L) formed in crosslinking baths of 100 mM CaCl₂, 50:50 mM CaCl₂:SrCl₂, and 100 mM SrCl₂ and with or without 25 mM polyP at week 0, 1, 2, 3, and 4. The experiment was performed in triplicates. Data are presented as means \pm standard deviation. * indicates a statistically significant difference compared to untreated conditions at week 1..... 63

Figure 30. PolyP release profile from alginate beads formed in different crosslinking solution at 100 mM CaCl₂, 50:50 mM CaCl₂:CoCl₂, 100 mM CoCl₂, and 50:50 mM CaCl₂:MgCl₂. Each alginate bead was formed from a solution with 2.0 %wt. alginate and 25 mM polyP. The experiment was performed in triplicates. Data are presented as means ± standard deviation. 65

Figure 31. PolyP release profile from alginate beads formed in a 100 mM CaCl₂ crosslinking solution with different concentrations of ethanol. Each alginate bead was formed from a solution with 2.0 %wt. alginate and 25 mM polyP. The experiment was performed in triplicates. Data are presented as means ± standard deviation. 66

Figure 32. PolyP release profile from alginate beads formed in a 100 mM CaCl₂ crosslinking solution with different concentrations of chitosan. Each alginate bead was formed from a solution with 2.0 %wt. alginate and 25 mM polyP. The experiment was performed in triplicates. Data are presented as means ± standard deviation. 68

Figure 33. PolyP release profile from alginate beads formed in a 100 mM CaCl₂ crosslinking solution following the addition of polyP-PEI at a 0.9:1.0 charge ratio. Each alginate bead was formed from a solution with 2.0 %wt. alginate and 25 mM polyP. The experiment was performed in triplicates. Data are presented as means ± standard deviation. 69

Figure 34. Live/dead assay of Ca-alginate beads (A), polyP-Ca-alginate beads (B), PEI-Ca-alginate beads (C), and PEI-PolyP-Ca- alginate beads (D) at 1million cells per mL and after 24h incubation. 73

CHAPTER 1 – INTRODUCTION AND RESEARCH OBJECTIVES

1.1 Introduction

In Canada, nearly six million people suffer from the symptoms of arthritis, a group of joint diseases that cause pain, joint stiffness, and loss of range of motion to those afflicted. This number is expected to increase to 25% of Canadians by 2035, in part due to population aging^{[1][2]}. The most common type of joint diseases by far is osteoarthritis (OA), which can be defined as a group of degenerative joint diseases that lead to the progressive degeneration of the articular cartilage tissue in a joint, while also causing pathological changes to the other tissues in the joint including the subchondral bone located directly under the thin layer of cartilage. These changes and associated symptoms have a tremendous impact on the quality of life of patients^[3].

Articular cartilage is a connective tissue that is composed mainly of a dense and anisotropic extracellular matrix (ECM) that gives the tissue its unique mechanical properties^[4]. This tissue provides low friction surfaces for skeletal movements and facilitates load absorption and distribution in the joint. Articular cartilage differs from most other tissues in that it is avascular and aneural; hence, mass diffusion from the synovial fluid (a viscous liquid that consists in part of an ultrafiltrate of plasma^[5]) transfers nutrients through the articular cartilage layer to its resident cells. The avascular nature of articular cartilage contributes to a deficit in progenitor cells that can reach the site of injuries to drive repair processes, while the fact that chondrocytes are constrained by the pericellular matrix (PCM) encapsulating them hinders their ability to migrate and exacerbates repair issues^[6]. These chondrocytes constantly, albeit slowly, remodel the ECM in response to changes in their chemical and mechanical environment; however, certain conditions

can lead to a prolonged imbalance between catabolic (ECM breakdown) and anabolic (new ECM synthesis) and the progressive degeneration of the articular cartilage layer observed in OA^[7].

Some therapeutics and surgical procedures have been developed to treat patients with OA; however, there is currently no cure for the disease^[8]. For example, oral non-steroidal-anti-inflammatory drugs (NSAIDs) and injections with a viscosupplement are often prescribed to help patients manage the pain and improve their lifestyle, but these do not slow the progression of the disease. Cell- and tissue-based surgical interventions including marrow stimulation, autologous chondrocyte implantation (ACI), and mosaicplasty are also performed to repair or replace damaged articular cartilage^{[9][10]}. These procedures often provide temporary relief, but show some important drawbacks including a limited long-term benefits^[11]. Cartilage tissue engineering is an emerging field of study that aims to improve the outcome of cell-based surgeries through the careful design of biomaterials and inclusion of bioactive molecules that stimulate the repair process, with the ultimate goal of regenerating, rather than simply repairing, the damaged tissues. One approach that is receiving attention is the encapsulation of cells with chondrogenic potential within hydrogels, which are highly hydrated materials that replicate some of the micro-environmental features of tissues.

Previous work has demonstrated that inorganic polyphosphate (polyP), an understudied molecule in biology, despite having been identified in members of all branches of the phylogenetic tree of life^[12], is present in articular cartilage^[13] and stimulates the accumulation of major cartilage ECM components: sulfated glycosaminoglycan (sGAG) and collagen, in chondrocyte cultures^[14,15]. This polyanionic molecule composed of orthophosphate residues linked together by energy-rich phosphoanhydride bonds was also shown to cause a significant reduction in the histological signs of OA in a menisectomized guinea pig model of the disease when injected twice

weekly directly in the joint capsule^[16]; however, a major issue with the direct injection of bioactive molecules in joint capsules is the rapid turnover of the synovial fluid in a matter of hours, meaning that drugs get cleared from the joint rapidly^[17] and that relatively regular injections would likely have to be performed for any health benefit to be achieved.

There is therefore a need for the development of strategies that cause the prolonged retention of bioactive molecules like polyP in the joint in order to stimulate the formation of new ECM. One way to achieve this is to non-covalently crosslink polyP to a biomaterial that can release the biomolecule in a controlled manner over a prolonged period of time. For example, polyP could be incorporated within a cell-encapsulated hydrogel, such that it could stimulate new tissue deposition by these cells, thereby accelerating repair processes.

1.2 Hypothesis

In this study, **we hypothesized** that polyP can be retained for prolonged periods of time within ionically crosslinked cell-encapsulated hydrogels because of its polyanionic nature, thereby stimulating tissue formation.

To test this hypothesis, we have focused on the use of the ionically crosslinked alginate hydrogel system. Alginate is a polysaccharide that has been widely used to form hydrogels for several applications in tissue engineering and more broadly in biomedical and biochemical engineering^[18] because it is considered biocompatible, can easily and rapidly be formed into hydrogels through incubation with polycationic crosslinkers, has high charge density at neutral pH, and is inexpensive. Alginate is extracted from seaweed, and its structure is mainly composed of 1,4-linked B-D-mannuronic acid (M) and α-L-guluronic acid (G)^[19]. The ratio M/G ratio, the monomer sequence in the copolymer, and the affinity to some cations (G-block have more affinity

to Ca^{2+} , Ba^{2+} , and or Sr^{2+}) determine the mechanical properties and degradation profile of the hydrogel^{[20][21]}. The initial idea involved cross-linking polyP within the alginate meshwork through ionic bonds with Ca^{2+} , the intended crosslinker.

1.3 Thesis Objectives

This thesis focusses on 3 specific objectives towards testing our hypothesis:

1. To optimize a protocol for sterile chondrocyte encapsulation within alginate-based hydrogel beads.
2. To devise a strategy to enable the controlled release of polyP from alginate-based hydrogel beads.
3. To characterize biological responses of encapsulated chondrocytes to the incorporation of polyP within alginate beads.

1.4 Thesis Organization

This thesis is divided in 6 chapters. Chapter 2 will present details on articular cartilage, joint diseases and the clinical options for treating these conditions, as well as an overview of the literature on cartilage tissue engineering and polyP. Chapter 3 will detail all the procedures and methods employed to carry out this project. In chapter 4 and 5, the key results towards the specific objectives of the thesis will be presented and discussed in detail. Chapter 6 will state the important conclusions of the work, as well as future directions for the project.

CHAPTER 2 - LITERATURE REVIEW

2.1 Articular Cartilage

2.1.1 Functions of Articular Cartilage

Hyaline cartilage is a type of cartilage that provides mechanical support and flexibility to several parts of the body. When it is present on the articulating surfaces of bones, it is known as articular cartilage (AC). AC is a highly specialized connective tissue with whitish glassy appearance that serves as a load bearing and low friction surface in joints^[22]. Importantly, this tissue is aneural and, when healthy, does not incorporate vasculature. AC can absorb and distribute the applied loads through its surface, thus decreasing the peak stresses transmitted to the underlying bone. Even though AC is just a few millimetres in thickness (i.e., 2-5 depending on joint, location, loading, age, etc.), the tissue composition and organization confer it with sufficient stiffness and resilience for normal compression forces in the joint^{[23][24]}. AC presents a biphasic poroviscoelastic behaviour under compression loading, whereby the application of a load initially leads to interstitial (synovial) fluid pressurization, which is followed by relaxation associated with fluid flow out of the tissue if the load is maintained. In addition, in conjunction with the synovial fluid, it presents low friction surfaces to ensure the smooth articulation of the joint and minimize tissue damage.

2.1.2 Composition of articular cartilage

AC is composed primarily of interstitial fluid that includes water (approximately 80 %wt. of the tissue), ions and other soluble biomolecules, with ECM accounting for 95 to 99 %wt. of the solid phase. Meanwhile, only 1 to 5 %wt. is attributed to chondrocyte cells, the only cell type in AC. These cells are responsible for tissue homeostasis in response to changing mechanical demands by

ensuring the turnover of the ECM (i.e., synthesizing new ECM biomolecules and degrading damaged tissue components). The ECM is composed primarily of two components, proteoglycans (15-30 % of dry wt.; ground substance) and collagens (50-75% of dry wt.), of which collagen type II represents 95% of the total collagen content. A relatively small quantity of non-collagenous proteins is also present^[4]. One main mechanical function of the collagens is to resist shear and tensile stresses transferred to the tissue, while proteoglycans are shock absorbers because of their ability to attract water through the Donnan effect^[25]. This phenomenon takes place because of the highly negatively charged nature of the glycosaminoglycan (GAG) contained in proteoglycans. Indeed, this net negative charge attracts soluble cations in the tissue, which in turn cause increased osmotic pressure and tissue hydration. The high water content of AC is critical to its mechanical properties in compression. Tissue expansion is opposed by restrictions imposed by the collagen meshwork, such that the collagen:GAG ratio, ECM crosslinking, and the organization of the collagen meshwork play an important role in the tissue properties. The function and interactions of each component of AC is described below.

2.1.2.1 Collagens

Collagen is a protein that is secreted by cells such as chondrocytes as soluble procollagen molecules, which self-assemble as triple helices that requires subsequent enzymatic processing before being incorporated into the ECM. In the body, collagen types can be either globular or fibrillar. In hyaline cartilage, fibrillar collagens are the most common type. Collagens present more than 28 isoforms and all of them share a common set of repeating amino acid sequences: glycine-proline-X and glycine-Y-hydroxyproline, where X and Y are other amino acids than glycine, proline or hydroxyproline^[4]. Triple helical collagen molecules self-assemble into rope-like higher-order collagen fibrils and fibrils are assembled into larger diameter fibers.

The most abundant collagen in hyaline cartilage is collagen type II, which represents approximately 50% of the total cartilage dry weight, while others collagen types including type I, IV, V, VI, IX, X and XI are also present but in smaller proportion^[26]. Collagen type I is present only on the superficial zone of AC and is also produced by de-differentiated chondrocytes^[27]. Collagen type VI is found in relatively high levels in the pericellular matrix (PCM), a thin layer of ECM with distinct composition from the bulk of the tissue ECM directly apposed to each chondrocyte, and is assumed to contribute to cellular mechanotransduction^{[28][29]}. Collagens type IX and XI play important roles in collagen type II fibrillar and fiber assembly and as linkers of macromolecules^{[30][31]}. Collagen type X is found in the deep zone of the AC and appears to have a role in the mineralization of the deeper aspect of the tissue at the interface with subchondral bone^[32].

Collagen fibers are aligned in different principle orientations through the depth of AC as will be explained below and are attributed the tensile properties of the cartilage. They also contribute to counteracting the expansion of the tissue due to its high osmotic pressure. It appears that the zonal orientation, as well as changes in concentration and dimensions of the fibers across the depth of the tissue, are critical the tissue's ability to perform its complex functions.

2.1.2.2 Proteoglycans

Proteoglycans are comprised of a core protein such as aggrecan onto which polysaccharide (GAG) molecules are covalently bound to form a brush-like structure^[33]. GAG are long unbranched (linear) polymers of repeating disaccharide units linked through glycoside bonds^[34]. The most common GAG molecules found in AC are dermatan sulfate, keratan sulfate, chondroitin 4-sulfate, chondroitin 6-sulfate, and hyaluronan^[35]. Hyaluronan is the largest GAG secreted by chondrocytes and the only GAG that does not present negatively charged sulfate ester groups under

physiological conditions. Hyaluronan binds proteoglycan through interaction with the link protein to form aggregates of proteoglycan. These aggregates accumulate in depth dependent concentrations across the AC thickness and provide a compressive stiffness to the AC^[36].

2.1.2.3 Chondrocyte Cells

Chondrocytes are highly specialized cells found in AC that are characterized with very low to no proliferative activity in healthy joints^{[37][38]}. These cells are responsible for maintaining tissue homeostasis throughout life by secreting enzymes for matrix degradation (e.g., matrix metalloproteinases), and generating new ECM constituents, in a balanced manner^{[39][40]}. These cells account for as much as 10% of the total cartilage volume at birth, but this percentage decreases to 1-2% in adults for humans, which impacts the ability of the tissue to react to changing demands upon aging^[4]. These cells respond to a broad range of stimuli such as hydrostatic pressures, electric forces, mechanical loads, growth factors, and other soluble signaling molecules, as well as ECM components; however, chondrocytes rarely form cell-to-cell interactions contacts for direct communication and signal transduction between chondrocyte cells, because they are entrapped within dense PCM. The combination of chondrocyte and its PCM is referred to as the chondron^[39].

Depending on the anatomical regions of the AC and the depth from the surface of the tissue, the number, size and shape of chondrocyte cells vary. For example, in the superficial zone chondrocyte cells are small, elongated parallel to the surface and present at a high cell density, while in the deeper aspect of the tissue, chondrocytes are spherical, larger, and exhibit a relatively low cell density^{[23][41]}.

2.1.3 Articular cartilage organization

AC is a highly complex anisotropic tissue. It is organized in distinct zones with respect to depth from the articulating surface and from the chondrocyte. Figure 1 provides a schematic representation of these depth-dependent and distance-from-the-chondrocytes zonal aspects of the tissue. Depth dependent ECM composition, organization and cellular phenotype has been categorized into four completely different zones: the superficial, mid, deep and calcified zones, whereby each zone is characterized by distinct mechanical, structural and functional properties.

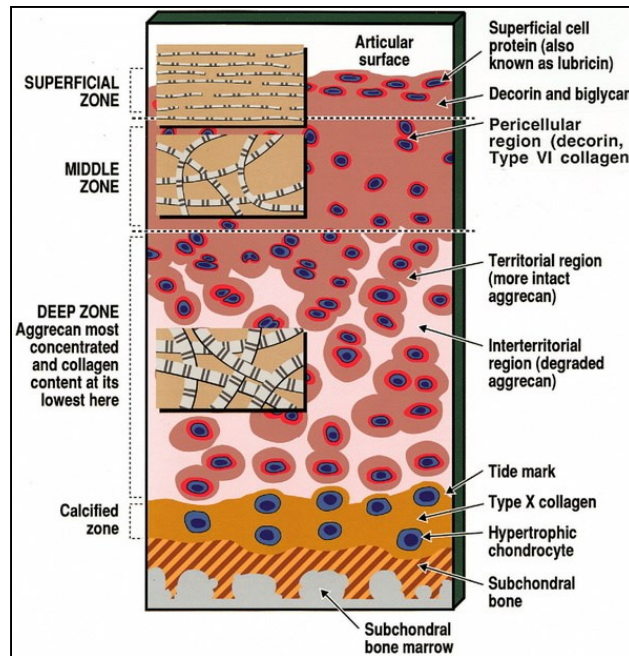


Figure 1. Schematic representation of AC, cellular organization in the zones of AC, and the relative diameters and organization of collagen microfibrils. (Reprinted with permission from the *Composition and Structure of Articular Cartilage: A Template for Tissue Repair*^[41].)

The superficial zone is the section that is in contact with the synovial fluid and contributes to most of the tensile properties. This thin section constitutes 10 to 20% of the total cartilage thickness, which has a low level of keratan sulfate GAGs and proteoglycans, but high levels of

collagen type II fibers arranged in parallel to the surface around flattened and elongated chondrocytes^[42].

In the middle or transitional zone, accounting for 40 to 60% of the total volume of cartilage, dispersed spherical chondrocytes can be found, surrounded by an ECM with a high level of proteoglycans and with thicker collagen fibers than in the superficial zone organized obliquely to the surface.

The radial or deep zone of the AC account for 30-40% of the total cartilage thickness and provides resistance to compressive forces during articulation. In this zone, chondrocytes are large, spherical and oriented in columns, while collagen fibers are thicker than in the middle zone and oriented perpendicularly to the surface. This zone also contains the highest level of proteoglycans.

Directly underneath the deep zone, a thin basophilic line termed the tidemark separates the mineralized layer from the deep zone. In this calcified zone, a few large chondrocyte cells are present and the collagen fibers from the deep zone bridge the non-calcified and calcified layers^[4]. The interface between the calcified cartilage and subchondral bone is termed the cement line and is undulated.

2.2 Osteoarthritis

In Canada, approximately six million people suffer from arthritis and it is estimated that this number will increase to nine million people by 2040^[1]. The most common type of arthritis is OA, with an estimated 60-70% of people older than 65 years suffering from this condition worldwide^[22]. OA is a degenerative disease of the joint that involves AC and the surrounding joint tissues, including the underlying bone. This disease causes pain, swelling, stiffness and less range

of motion, in large part due to the progressive degeneration of the AC tissue leading to bone-bone contact, whereby bone tissue incorporates nerves.

2.2.1 Causes and consequences

OA can be caused by a variety of factors that can be classified into systemic risk of factors (age, genetics, immune responses, estrogen deficiency, diet, race, bone density, etc.) and local factors (trauma, obesity, bone remodeling, muscle weakness, joint mechanics, etc.)^[43]. Although the pathological mechanisms involved in the progression of OA are not completely understood, one element that has been demonstrated is the fact that biochemical and/or biomechanical factors cause a prolonged imbalance between ECM synthesis (anabolism) and degradation (catabolism) in the AC ^{[44][45]}. The progressive degradation of the AC layer further impacts its ability to withstand the loads applied through the joint and perpetuates the imbalance. A number of intrinsic characteristics of AC contribute to the establishment of this imbalance between anabolic and catabolic processes. For example, chondrocytes are entrapped within their chondron and do not migrate to a site of injury to participate in repair following damage to the tissue. Further, they are characterized by a low metabolic activity, which limits their ability to ensure rapid turnover of the ECM. Similarly, the lack of vasculature in AC means that progenitor cells do not have direct access to a site of injury via the blood stream, unless a full thickness injury occurs that propagates to the subchondral bone^[46]. Finally, tears in the cartilage expose small polysaccharide molecules, which inhibit the ability of progenitor cells (from the surrounding joint tissues) to attach to the ECM and initiate repair.

2.2.2 Diagnosis and current treatments

OA is diagnosed by a doctor from the results of a physical exam (e.g., tenderness, redness, flexibility and pain), imaging tests (X-ray, and magnetic resonance imaging (MRI)), and lab tests (blood tests, and joint fluid analysis)^{[47][48]}. The Kellgren-Lawrence (KL) radiological classification is the most common system for knee OA grading and provides a determination of the severity of OA in a patient to help the surgeon make an assessment on the need for a surgical intervention. In the KL grading system (radiological findings), a grade of 0 indicates that the joint does not present features of OA, a grade of 1 indicates the presence of some osteophytes and/or joint space narrowing, a grade of 2 indicates the presence of osteophytes with a clear mild joint space narrowing, a grade of 3 indicates the presence of osteophytes, moderate joint space narrowing (50%) and in some cases cysts/sclerosis, and finally a grade of 4 indicates the presence of a possible deformity of bone ends and severe joint space narrowing^[43]. Of course, this approach only allows clinicians to diagnose fairly advanced cases of OA with observable macroscopic changes to the joint. It is important to emphasize that early detection methods for OA have yet to be implemented successfully in the clinic.

As was previously mentioned in this Chapter, there is currently no approved disease-modifying OA drug (DMOADs) available on the market. DMOADs is defined as “a drug that inhibits structural disease progression and ideally also improves symptoms and/or function”^[49]. A number of factors have been proposed as contributors to the fact that efficacious DMOADs have yet to be discovered and/or approved for broad clinical use, notably an incomplete understanding of the molecular and cellular mechanisms involved in the pathophysiology of the disease, the multivariate nature of OA, the lack of early-detection methods, and the fact that drugs and other molecules injected in a joint are typically cleared from the joint space within a matter of hours^[50].

Despite these factors, a number of potential candidates are currently in different stages of clinical trials^{[51][52]}.

In absence of an efficacious DMOAD candidate, a number of treatments focused on managing the symptoms of OA and improving joint mobility, repairing damaged articular surfaces, and replacing diseased joints with implants have been developed and implemented in clinical settings. Current treatments can be classified as conservatives, surgical and joint replacements with implants and each strategy has their own advantages and disadvantages^[53]. The following discussion will highlight the main options available to practitioners.

2.2.2.1 Conservative treatments

Conservative treatments are the first line of treatments recommended by a specialist to manage the symptoms of OA because they are non-invasive in nature since no surgery is required. These are favoured strategies to help patients maintain an active lifestyle and reduce their joint pain for mild and early cases of OA. Conservative treatments can be classified as non-pharmacological and pharmacologic.

Non-pharmacological strategies have allowed patients to improve their quality of life, and reduce the pain sensation associated with pathological changes in the joints including exposure of subchondral bone surfaces. These include lifestyle changes that lead to weight loss (obesity is a risk factor for OA), avoiding movements that can aggravate the condition, and the practice of low impact exercise to strengthen the joint structures and increase muscle mass around the joint so that these can participate in load bearing and relieve AC^[54]. Bracing and orthotics have also been employed as alternatives^{[55][56]}. Acupuncture has also been investigated as a therapy to manage pain and loss of joint function^[57,58].

Pharmacological treatments can also be prescribed to help manage the symptoms of patients with early signs of OA. These are classified as non-steroidal anti-inflammatory drugs (NSAIDs), selective cyclooxygenase II (COX-II) inhibitors, opioid pain killers and other non-opioid oral analgesic^[43].

NSAIDs are a chemically heterogeneous group of analgesics that act as non-specific inhibitors of the COX enzymes (COX-I and COX-II) and thus stop the biosynthesis of prostaglandin, which is the first step in inflammatory disorders. The COX-I enzyme is normally found in cells as a primary constitutive isoform, while COX-II is constitutively expressed in some areas of the brain and kidneys, but its expression can also be induced in other tissues by the presence of inflammatory cytokines and mediators. Some examples of non-specific Cox inhibitors are Ibuprofen, Meloxicam, and Aspirin. Selective COX-II inhibitors including Valdecoxib, Refexocib, and Celecoxib have also been employed. All of these can help patients manage pain; however they also elicit important side effects, particularly when used over long periods as is required for the management of OA symptoms. These side effects can include renal, cardiovascular and gastrointestinal issues, where orally administered drugs also distribute to these sites^[43].

Opioids are another category of analgesic agents that have been used to manage the symptoms of OA. These molecules are derived from opium and include codeine, morphine and many semi-synthetic derivatives. Opioids can be classified into short-acting, long-acting and partial agonists molecules and have the ability to inhibit directly the ascending transmission of nociceptive information from the spinal cord dorsal horn and simultaneously activate the pain control circuits that descend from the midbrain via the rostral ventromedial medullary tract to the spinal cord dorsal horn. These drugs are effective and used in KL grade 3 OA patients for whom at least a moderate joint space narrowing (50% minimum) is observed in the radiological findings;

however, they can create physical dependence, provide only limited pain relief and their long term use can lead to tolerance requiring increased dosages^[43]. Patients have also elicited increased sensitivity to pain over time.

Other drugs that are considered for OA treatment include acetaminophen (paracetamol), glucosamine, diacerin, nutraceuticals, collagen hydrolysates (CHs), methylsulfonylmethane (MSM) and antidepressants^[43]. There also exists other alternatives that are offered when simpler analgesics no longer provide symptoms management for the patients. For example, intra-articular (IA) injections of corticosteroids for pain relief, hyaluronic acid derivatives for viscosupplementation (i.e., as a synovial fluid substitute), platelet-rich plasma (PRP) – a concentrate of autologous platelets in a small volume of plasma to stimulate tissue regeneration as platelets are considered to be loaded with different growth factors – and stem cells^[43].

2.2.2.2 Surgical treatments

When conservative treatments are deemed ineffective for pain relief in a patient or if a cartilage injury or defect is deemed likely to develop into secondary OA because of patient-related factors (i.e., patient's comorbidities, age, physical activity), surgical treatments are considered. Surgical treatments aim to induce cartilage repair or replace the damaged tissues and vary considerably in invasiveness. These include arthroscopic debridement, cell and tissue based repair interventions, and total or unicompartmental knee arthroplasty^[47]. The most common of these techniques will be explained in detail in the following paragraphs.

The simplest surgical interventions available to clinicians are lavage and arthroscopic debridement performed on their own or simultaneously. Lavage involves the injection of a saline solution into the joint to essentially wash or rinse the joint. The fluid is then aspirated to remove any fluid, debris and blood present in the joint space. In theory, this approach also helps remove

inflammatory cytokines that cause synovitis in the joint. In a debridement intervention, the surgeon removes the damaged cartilage tissue, particularly the loose portions, to re-establish a “smooth” articular surface. These surgeries are typically performed as minimally invasive arthroscopic interventions; nevertheless, there is debate within the medical community as to the clinical benefits of these interventions for the patients^[47].

A number of cell-based surgical interventions have been developed to overcome limitations associated with the migration of cells with chondrogenic potential to the site of cartilage damage and to induce the formation of repair tissue. The most common intervention, and gold standard in the field of cartilage repair, is a group of methods termed marrow stimulation. These approaches take advantage of the “healing” potential of the body to induce chondral resurfacing with repair tissue. Different techniques are used to penetrate and/or fracture the subchondral bone at the site of a cartilage defect following debridement to access multipotent stem cells from the bone marrow that can promote some level chondrogenesis in the affected area. One common and simple technique currently used for bone marrow stimulation techniques is microfracture (see Figure 2), performed as an arthroscopic (i.e., minimally invasive) procedure during which small holes are created into the subchondral lamina and at a 3 to 4 mm distance from each other using an awl. The blood released into the defect clots to essentially form a scaffold into which bone marrow progenitor cells can migrate and deposit tissue. The main disadvantage of this technique remains the fact that the repair tissue formed is mostly fibrocartilage with increased collagen and decreased proteoglycan content compared to hyaline cartilage. This repair tissue does not respond to mechanical forces in the same way as the native tissues and often undergoes rapid functional deterioration, such that this strategy often only provides short term relief to the patients.

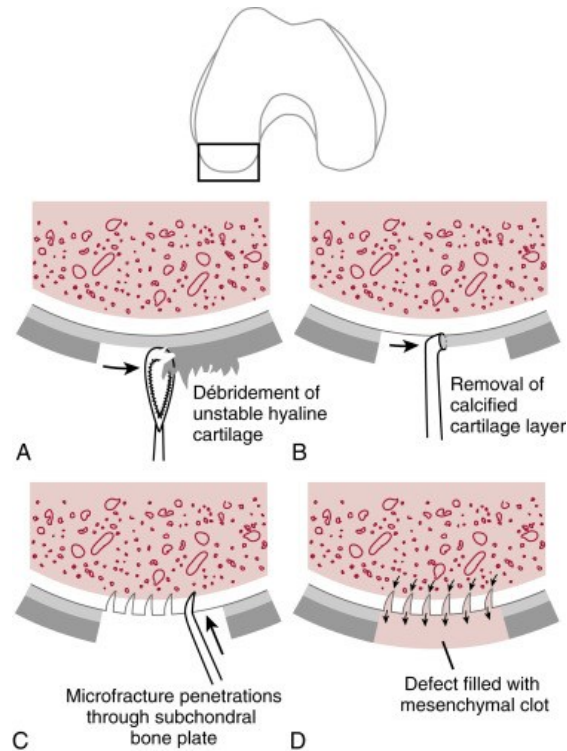


Figure 2. Schematic step by step representation of the microfracture technique. (A) Débridement to create a stable cartilage margin, (B) removal of the zone of calcified cartilage, (C) microfracture penetrations, (D) well-anchored mesenchymal clot filling. Reprinted by permission of Clinical Orthopaedic Rehabilitation: a Team Approach (406), by G. Kelley, et.al., 2018, Elsevier Books^[59].

Another cell-based surgical intervention is termed autologous chondrocyte implantation (ACI) (see Figure 3). This is a cartilage repair technique based on a two-stage procedure where small cartilage samples are excised from the joint at a non-loading area in a first surgery. The tissue is digested *in vitro* to extract autologous chondrocytes and these cells are cultured and proliferated over a 3 to 4 weeks period in monolayer culture flasks to produce a large number of cells with chondrogenic potential. Finally, these cells can be re-implanted underneath a periosteal flap or a collagen membrane sutured onto a debrided cartilage defect^[60]. This approach has been associated with the formation of some hyaline cartilage, although the culture of chondrocytes *in vitro* does

lead to their dedifferentiation and the formation of fibrocartilage in some cases. ACI has a similar success rate as microfracture at 2 years, but slightly better prognosis for the longer term. The elevated risks associated with a second surgery and the high costs associated with cell culture in vitro has limited the use of this technique. It is notably currently not performed in Canada.

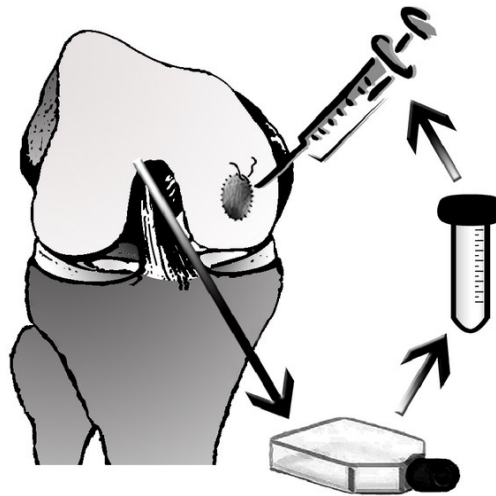


Figure 3. Schematic representation of the autologous cartilage implantation (ACI) procedure. In a two-surgery procedure, cartilage is harvest, autologous cells are isolated and cultured to proliferate, and the cells are reinsertion by injection them underneath a sutured periosteal or collagen membrane. Reprinted by permission of Current Surgical Treatment of Knee Osteoarthritis (3), by K. Rönn, et.al., 2011, Switzerland, Hindawi Publishing Corporation^[47].

Another cartilage repair technique involves osteochondral transplantation. This technique can involve the transplantation of multiple smaller autologous osteochondral grafts (mosaicplasty) or only one or two larger autologous grafts (osteochondral autologous transfer system; OATS). For small defects the procedure can be arthroscopic, while it will require larger incisions for large defects. Plugs from lower loading areas are extracted and then transferred to the site of defect. This is a technically difficult procedure that only leads to minimal integration of the grafts and is limited

by graft availability (an alternative is the use of allogeneic grafts); however, it does resurface the joint with native hyaline cartilage.

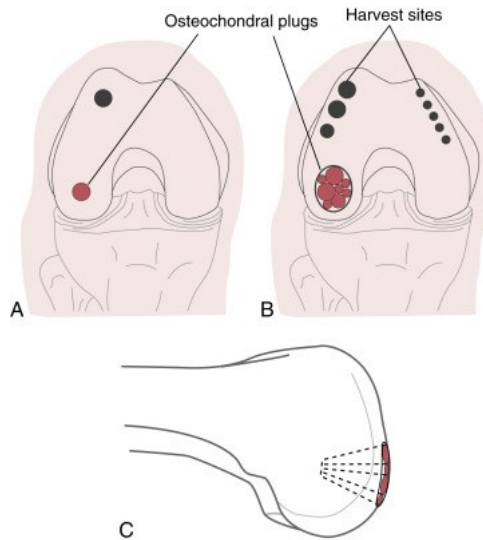


Figure 4. Osteochondral autograft transplantation. (A) Shows one plug hole (B) shows multiple plugs used to fill the defect. (C) A sagittal section that shows how the osteochondral graft spaced to be filled. Reprinted by permission of *Clinical Orthopaedic Rehabilitation: a Team Approach* (406), by G. Kelley, et.al., 2018, Elsevier Books^[59].

All of these techniques are meant to help reduce the pain suffered by a patient and enhance their range of motion; however, the outcomes of these techniques are limited to the short term for many patients such that alternatives are sought.

2.2.2.3 Implants

When all other therapeutic options have failed and the disease has progressed to a point where the quality of life of the patient is considerably affected, the ultimate surgical option for the patients is the replacement of the diseased joint(s) with permanent implants. A number of different designs based on metallic, metallic-ceramic, or metallic-polymer materials are used to replace affected joint sites. Implants are designed to balance basic criteria of biocompatibility and strength

requirements. This technology has been used for a long time. For example, knee implants have been used since the 1950s to help decrease pain related to OA and recover some range of motion in the affected articulations. Total joint replacements are quite successful at improving the quality of life of patients and many individuals are able to return to their pre-surgery level of activity. Nevertheless, some issues associated with the fixation of the implant in bone, the production of degradation products due to shear, and infection, to name a few have somewhat limited the long-term use of total joint replacement implants^[61]. Further, revision surgeries after the failure of the initial implant are much more complex and associated with lower success rates. Therefore, there is an urgent need for the development of strategies to improve the long-term outcome of cell-based surgical interventions and delay the need for total joint replacements in a broader spectrum of patients.

2.3 Cartilage Tissue Engineering

As was discussed in this Chapter, cell-based cartilage repair strategies provide short-term symptom relief for some patients with joint conditions, but they often fail to induce the regeneration of functional AC with properties that allow it to provide long term relief^[62]. In fact, current clinical cartilage repair strategies do not allow to replicate the complex and heterogeneous composition and organization of AC, nor do they yield tissue with the unique biomechanical properties of the native tissue they are trying to recreate^[63]. One promising strategy to promote the improved repair and possibly even the regeneration of damaged or diseased AC is tissue engineering. Tissue engineering is a multidisciplinary approach that integrates engineering and biological principles to coordinate the regeneration of damaged or diseased tissues and organs. The central tenet of tissue engineering is the combination of three components – a biomaterial, cells, and signaling factors

(i.e. chemical, mechanical, or structural signals) – to stimulate tissue regenerative processes^[64]. While a number of strategies termed tissue engineering employ only one or two of these constituents, the central goal of the field is to provide cells with an instructive environment that guides the regeneration of a tissue^{[65][66]}.

In this study, we are primarily interested in the potentials of a specific biomolecule termed polyP for applications in cartilage tissue engineering. The next section will provide insights into the reasons for using this intriguing and promising biomolecule.

2.3.1 Inorganic Polyphosphate (PolyP)

PolyP (Figure 5) is a linear polymer of orthophosphates linked by energy-rich phosphoanhydride bonds, such as those found in adenosine triphosphate (ATP). At physiological pH, polyP is polyanionic with each monomeric phosphate unit carrying a negative charge. It is generally considered ubiquitous in nature, because of the fact that it has been identified in members of all three branches of the phylogenetic tree of life^[14]. In mammals, it has been observed in a number of tissues and organs including the brain, heart, liver, lungs, and bone^[67]. Through enzymatic process, inorganic polyP is synthesized from ATP in a reversible reaction, while other enzymes can break down the polymer via cleavage of its end groups (exopolyphosphatases), or breakage of bonds in the middle of the molecule (endopolyphosphatases)^[68]. While much remains to be discovered about the roles played by polyP in mammal's biology, a number of functions have already been studied. For example, it has been involved with the modulation of tissue mineralization processes through physicochemical effects and by regulating gene expression profiles^{[69][70][71]}. It has also been implicated in blood coagulation^{[72][73]}, as well as in cell proliferation processes^{[74][75]}. Interestingly, the stimulation of mitogenic activity observed in

fibroblastic cells was linked to the physical and functional stabilization of fibroblast growth factors^[76].

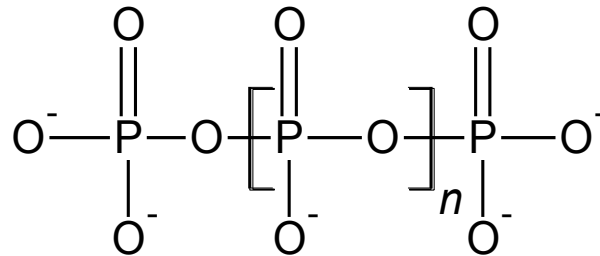


Figure 5. Chemical structure of inorganic polyphosphate (polyP).

St-Pierre et.al^[14,15], was the first to report on the positive effects of polyP on collagen and GAG accumulation by in vitro high density chondrocyte cultures and explanted AC cultured ex vivo. They reported that this effect was temporary, owing to the fact that polyphosphatases are expressed by chondrocytes, as well as concentration- and chain length-dependent. PolyP with an average polymer length of 45 phosphate units was deemed optimal for ECM accumulation. This study also showed that polyP treated chondrocyte cultures exhibit lower rate of cell number increase, likely because of the inhibition of cell proliferation pathways, in comparison with untreated cultures. This result was in contrast with other reports in the literature highlighted above that showed a positive effect of polyP on proliferation in other cell types. This inhibitory effect on chondrocyte proliferation was deemed positive as chondrocyte proliferation is a response associated with dedifferentiation and pathologies such as OA. In an unpublished study, St-Pierre and his colleagues also injected polyP intra-articularly in the menisectomized knee of guinea pigs to evaluate its effects on the development of OA. They found that this treatment leads to lower histological OA scores compared to the injection of saline only (carrier; control). As such, polyP was deemed promising for the treatment of OA and to exhibit chondroprotective effects in an

aggressive animal model of the disease. Indeed, its effects suggest that it might be an interesting candidate for DMOADs and that it could be used for cartilage tissue engineering applications.

2.3.2 Scaffolds and templates for cartilage tissue engineering

A broad array of different polymers from synthetic and biological origins have been investigated as base materials for the fabrication of scaffolds and templates for cartilage tissue engineering applications. These have been processed via a range of methodologies to produce structures with highly interconnected porosity for the culture of chondrocytes, and other cell types with chondrogenic potential. We recently wrote a book chapter describing the most commonly employed techniques for the fabrication of porous scaffolds, as well as their advantages and disadvantages^[77], which can be consulted for additional information on the subject.

2.3.2.1 Hydrogels

As was highlighted in our recent book chapter on scaffolds for tissue engineering applications, limitations associated with the ability of traditional porous scaffolds to replicate the native pericellular environment experienced by cells in tissues such as AC have led to a shift towards a class of materials termed hydrogels to stimulate the regeneration of tissues. Hydrogels are hydrophilic polymeric networks crosslinked together using a variety of approaches that can absorb and hold large quantities of water (see Figure 6). In that sense, they can be seen as replicating the hydrated ECM meshwork nature of native tissues. These materials offer intricate control over the biological, mechanical and degradative properties, through the careful selection of the base polymer, its functionalization, and the crosslinking strategy. A broad range of materials both synthetic and biological polymers have been used to form hydrogels for cartilage tissue engineering^[78,79], a topic that is regularly reviewed in the literature.

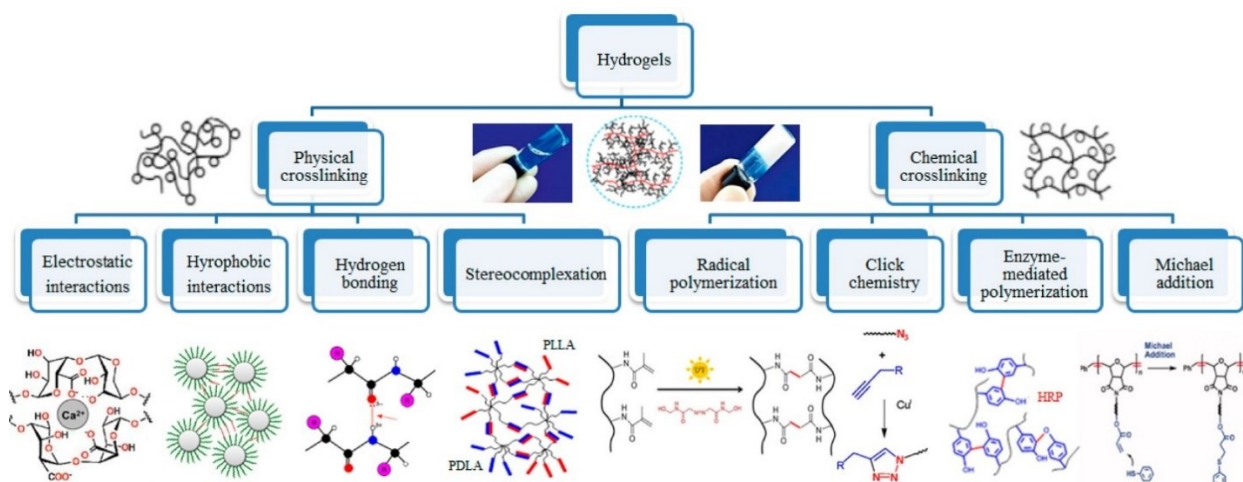


Figure 6. Schematic representation of the different physical and chemical crosslinking method to form hydrogels. Reprinted with permission from N. Eslahi, M. Abdorahim, A. Simchi, *Biomacromolecules* 2016, 17, 3441. Copyright (2016) American Chemical Society^[79].

2.3.2.2 Ionically crosslinked alginate hydrogels

One natural polymer that has been used substantially for cartilage tissue engineering strategies is alginate. Alginate is a polysaccharide composed of (1→4)-linked α -L-galuronic (G) and β -D-mannuronic (M) residues with a variety of sequences of G-, M-, and GM-blocks that depend on the source of the particular batch of polymer (see Figure 7)^[80]. Alginate is found in marine brown algae as a structural component and in soil bacteria as a capsular polysaccharide. There are at least 200 different types of alginates identified. Importantly, it is a polyanionic molecule at physiological pH.

Alginate is considered versatile as a biomaterial because of the simple, instantaneous and cost-effective method employed for its physical crosslinking into a hydrogel. In fact, dropping an alginate solution in a bath containing a polycationic molecule (typically Ca^{2+}) leads to the formation of ionic crosslinks via the negative charges on the alginate backbone and gelation into a structure with relatively high mechanical properties. Additionally, alginate entraps a large

quantity of water that makes this material an excellent microenvironment for cell encapsulation and biochemical factors entrapment^[80]. Further, approaches such as electrospraying, which consists of applying an electric field between a needle from which the alginate solution is dropped and the crosslinking bath facilitates the production relatively of small hydrogel beads of the order of a couple hundred microns or even smaller^[81], thereby making these gels injectable.

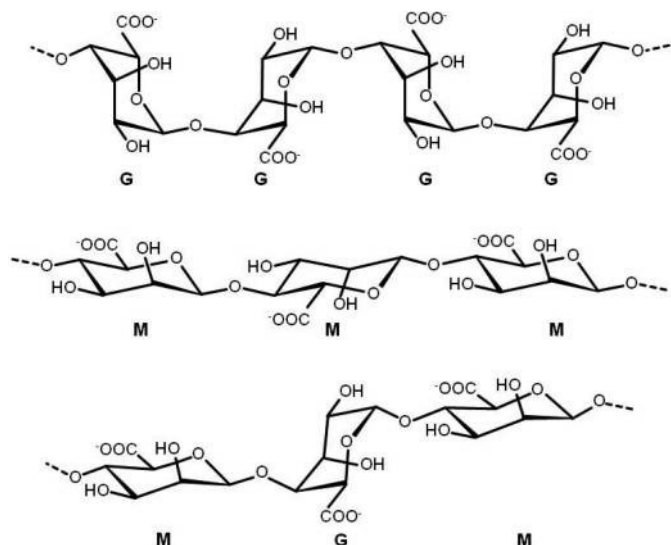


Figure 7. Chemical structures of alternating alginate blocks of G-blocks and M-blocks. Reprinted with permission from *Alginate: Properties and biomedical applications* (108), by K. Yong Lee, et.al. 2012, United States, Elsevier.

Alginate hydrogels are relatively stiff due to the electrostatic repulsion that exists between the charged groups on the polymer chain, and a degree of control of their mechanical properties is afforded by the careful selection of alginate source based on monomeric composition, as well as its blocks distribution. Indeed, crosslinking polycationic molecules will bind specifically to certain blocks. For example, Sr²⁺ will bind specifically to G-blocks, while Ca²⁺ will bind to G- and MG-blocks and Ba²⁺ will bind to G- and M-blocks. Alginate mechanical properties (swelling, stiffness, rigidity) can be tuned by some factors during gel formation as crosslinker type, but also by the

crosslinking density, viscosity of extracted Na-alginate, molecular weight distribution and M/G blocks ratio^{[19][82]}.

The biocompatibility of alginate is another important characteristic that has increased its use as a base polymer for hydrogel fabrication in tissue engineering applications. During extraction from the algae or bacteria, alginate must be highly purified to avoid the presence of impurities and contaminants (e.g., proteins, endotoxins, heavy metals, etc.) that could elicit an immune response. However, this polymer is generally accepted as eliciting minimal cytotoxic and inflammatory responses, a feature that is not shared by other polysaccharides such as chitosan and polycationic polymers that include poly-L-lysine and polyethylenimine (PEI). Because of these reasons, alginate has been used broadly in different biomedical applications, including in pharmaceuticals, as wound dressing material, in cell culture and tissue regeneration application and for protein and cell delivery^[83].

2.3.3 Proposed Strategy

In this study, we are proposing that the combination of alginate, polyP and chondrocytes into a single solution delivered dropwise into a crosslinking bath of polycationic molecules will allow the encapsulation of cells within a crosslinked network of alginate and polyP based on the polyanionic nature of both alginate and polyP (Figure 8). In essence, this would be replicating elements of the organization of chondrons in cartilage tissue, as chondrons contain high levels of polysaccharides and most of the polyP content of AC.

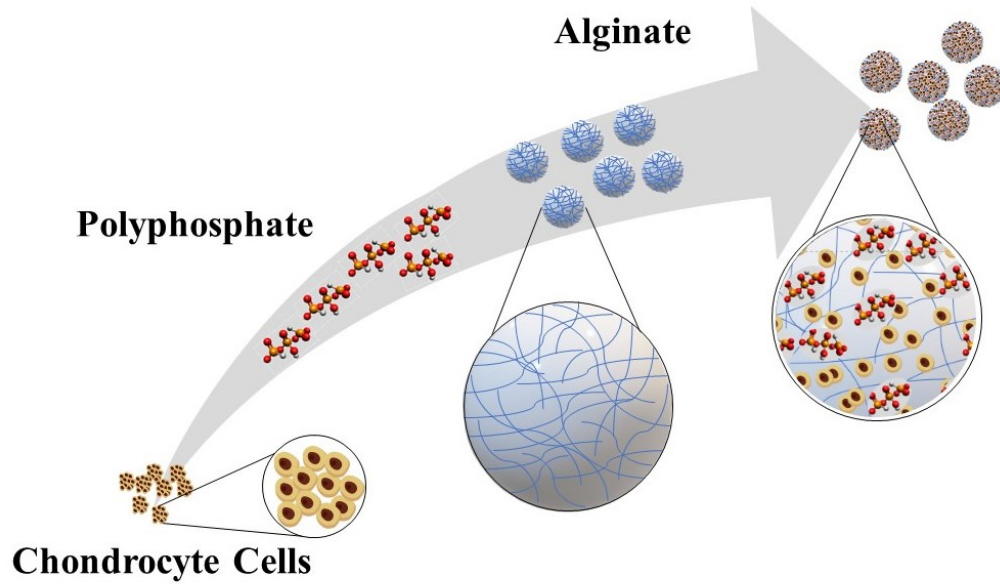


Figure 8. Schematic representation of the main constituents in this study for cartilage tissue engineering. Bovine chondrocytes as native cell, polyP as the biomolecule and alginate beads as scaffold to provide an adequate 3-D environment. Adapted from *Cartilage Regeneration and Tissue Engineering* (369), by M. Sancho-Tello, et.al., 2019, Spain, Elsevier^[39].

CHAPTER 3 - MATERIALS AND METHODS

3.1 Materials

Sodium alginate (Protanal LF 10/60; low viscosity; high G content between 65 and 75%) was a kind gift from FMC Corporation (Philadelphia, PA). Sodium polyphosphate was a kind gift from Budenheim (Germany). Chitosan, Dulbecco's Modified Eagle Medium (DMEM), fetal bovine serum (FBS), sodium citrate dihydrate, L-cysteine hydrochloride, papain from papaya latex, antibiotic-antimycotic solution, and anhydrous magnesium chloride (MgCl_2) were purchased from Sigma-Aldrich (St. Louis, MO). Calcium chloride ($\text{CaCl}_2 \cdot 2\text{H}_2\text{O}$) was purchased from ACP Chemicals (CA). Phosphate Buffered Saline (PBS) pellets was obtained from VWR (Radnor, PA). Strontium chloride hexahydrate ($\text{SrCl}_2 \cdot 6\text{H}_2\text{O}$), polyethyleneimine (PEI), and Cobalt (II) chloride hexahydrate, 98% ($\text{CoCl}_2 \cdot 6\text{H}_2\text{O}$) were purchased from Alfa Aesar (Haverhill, MA). Ethylenediamine tetraacetic acid (EDTA), and Poly(dimethylsiloxane) (PDMS) were purchased from Fisher Scientific (Waltham, MA). Sodium hydroxide and sodium chloride were purchased from I-Chem (St. Louis, MO).

3.2 Alginate bead formation

Alginate beads were formed under sterile conditions as described below for all experiments. Briefly, each experiment required the selection of the appropriate alginate concentration, type and concentration of crosslinker, and duration of crosslinking step in order to answer specific questions. A solution of sodium alginate (2-6 %w/v) in PBS (1X) was prepared with or without 50 mM polyP (concentration on a phosphate basis rather than a polymer basis). The solution was sterile filtered with a 0.2 μm filter and then mixed with an equal volume of DMEM (1.0 g/L

glucose). The concentration of multivalent cations in DMEM is insufficient to observe gelation at this step. When cells were incorporated within the beads, the cells were first added to the DMEM prior to mixing with the alginate solution. Cells were added to the DMEM at a concentration of approximately 1-4 million per mL. After the solution was well mixed, a 7.5 μL volume of this final alginate-DMEM solution with and without polyP and/or cells was dropped into a crosslinking solution prepared at the prescribed concentration (e.g., 50-250 mM Ca^{2+} , or Sr^{2+}) to form a single bead. Beads were kept in the crosslinking bath for 15-60 minutes depending on the experiment and the crosslinking solution was removed, followed by a single washing step in DMEM solution or PBS depending. Beads were then used for experiments.

3.3 Quantification of inorganic polyphosphate retention in beads

PolyP retention within alginate beads over time provides information on the interactions between this inorganic biomolecule and the hydrogel. Alginate beads were incubated in DMEM (1.0 g/L glucose) for given periods of time from 15 minutes to 7 days at 37 °C, 100% humidity and 5% CO_2 . The beads (3 per sample) were then dissolved in 55 mM sodium citrate and an aliquot of the solution (10 μL) was diluted 10 times in ddH₂O/sodium citrate mixture. (40 μL of ddH₂O, and 50 μL sodium citrate) and then incubated with 10 μL of 4', 6-diamidino-2-phenylindole (DAPI; 1 mg/mL) all together in a well plate. Binding of DAPI with the polyP in the solution was measured fluorimetrically with a Tecan Infinity M 1000 spectrofluorometer at excitation and emission wavelengths of 415 and 550 nm. Each sample contained 3 beads (7.5 μL) and experiments were performed at least in triplicates for each condition. Seven and a half μL aliquots of the alginate solution with and without polyP prior to crosslinking, as well as aliquots of the buffer without alginate were used as controls and a standard curve was prepared with polyP. PolyP retention was

expressed as a percentage of the polyP level measured in the alginate solution prior to crosslinking, and release was expressed as 100% minus the measured retention.

3.4 Alginate bead swelling and degradation

Two of the physical properties that were analysed for the alginate beads prepared in different crosslinking solution were the swelling and subsequent hydrogel degradation over time. For these experiments, beads were weighed immediately after washing and incubated in either PBS to accelerate the degradation of the alginate beads (since PBS does not contain Ca^{2+} , Sr^{2+} , or other crosslinking polycations, the crosslinkers diffuse out of the hydrogel at a faster rate than in culture medium or biological fluids), or DMEM (1.0 g/L glucose) at 37 °C, 100% humidity and 5% CO_2 . The weight of each bead was measured every day. Each sample was prepared using a total volume of alginate solution of 200 μL . Each condition was performed at least in triplicate. Swelling was evaluated as the initial mass of the hydrogel.

3.5 Compression test on alginate hydrogels

For compression testing, alginate hydrogel discs were prepared through a slightly different gelation process than for bead formation. Polydimethylsiloxane (PDMS) molds with 8 mm diameter holes were prepared and placed onto filter paper previously soaked with the crosslinking solution. The cavity was filled with alginate solution and a filter paper soaked with the crosslinking solution was placed on top of the cavity. The sample was submerged in crosslinking solution and incubated for a period of 30 minutes. The compression test was performed with an Instron 3000 Universal Tester (along with Bluehill 2 Materials testing software) under unconfined compression with the platen moving at 0.05 mm/min with a 150 N load cell. Force-displacement data were acquired and

analyzed to produce stress-strain curves. The slopes from data between 5% +/- 1% and 10% +/- 1% strain were calculated to provide compression moduli at 5 and 10% strain respectively.

3.6 Chondrocyte cells isolation and culture

Bovine chondrocyte cells were extracted by enzymatic digestion of cartilage excised from the phalangeal-metacarpal joint of cow legs by dissection under sterile condition. Cow legs were purchased from Tom Henderson Meats & Abattoir. Excised cartilage was collected in a petri dish filled with 15 mL of Dulbecco's Modified Eagle's Medium (DMEM) (4.5g/L glucose with 1 %v/v antibiotic-antimycotic). Cartilage tissue was cultured for 2 days (37 °C, 100% humidity and 5% CO₂) to ensure the absence of microorganism contamination and subsequently digested by the addition of 2.5 mL of 0.1 %w/v Pronase in DMEM and incubating for one hour, washing the tissue three times with 10 mL DMEM (no additives) and adding 10 mL of 0.5 %w/v Collagenase in DMEM for 24 hours. After the enzymatic digestion, the cell-rich digest was filtered through a 100 µL strainer to separate undigested cartilage from the cells. The cell solution was centrifuged at 300 RCF for 3 minute and the supernatant was removed carefully, leaving a cell pellet at the bottom of the tube. The supernatant was removed and the cell pellet washed with an adequate volume of DMEM (1.0g/L glucose) cells were counted in a hemocytometer. After the total cell number was determined, the cell solution was centrifuged one more time, the supernatant removed, and the cell concentration adjusted with DMEM (1.0 g/L glucose) (0.5M/mL, 1M/mL and 2M/mL). The cells were encapsulated in alginate beads as detailed in section 3.2 or cultured in tissue culture plates depending on the experiment. Unless specified otherwise, cells were cultured at 37 °C in a 100% humidity and 5% CO₂ environment in DMEM (1.0 g/L glucose) supplemented with 1 %v/v antibiotic-antimycotic and 1 %v/v insulin-transferrin-selenium (ITS). Select experiments were

performed with 2 or 10 %v/v fetal bovine serum instead of ITS. The culture medium was changed every 48 hours.

3.7 Biological assays

3.7.1 Live/Dead viability test

A Live/Dead viability test was carried out in chondrocyte-encapsulated alginate beads to verify the cytotoxicity of certain materials and culture conditions. First, the culture medium was removed from each well and samples were washed with the same volume of DMEM (1 g/L glucose) without any additive for 5 minutes before being removed. A dye solution was prepared with 1 μ M Calcein-AM and 2 μ M Propidium iodide (PI) in DMEM and 500 μ L was added to each well. Samples were incubated for 20 minutes and then visualized using an Olympus IX81 epifluorescence microscope at a 5x magnification with FITC (live cells; calcein) and TRITC (dead cells; PI) filters. Five images were taken for each sample. The total of live and dead cells were counted for each frame and ratios of each over the total number of cells were calculated.

3.7.2 Biochemical content of alginate beads

3.7.2.1 Papain digestion

A papain digestion buffer containing 55 mM sodium citrate, 5 mM cysteine hydrochloride and 5 mM EDTA in PBS with pH adjusted to 7.4 was prepared and supplemented with 80 μ g/mL of papain immediately prior to the experiment. Beads were incubated in an aliquot of the papain digestion solution at 60 °C for 24 hours. The solutions were then frozen at -20 °C until further testing was performed.

3.7.2.2 DNA content assay

DNA content in a culture represents an estimate of the number of cells present. A single bovine single chondrocyte has been evaluated as having 7.7 pg of DNA. While cells undergoing mitosis have twice as much DNA and dead cells would still contribute to the DNA content of the culture, this approach provides a relatively good estimate of cell numbers for cultures that do not proliferate rapidly or have large numbers of dead cells. A Quant-it PicoGreen kit for dsDNA quantification was used according to the supplier's directions. A 25 μ L aliquot of papain digest was mixed with 25 μ L of TE buffer (1X) and 50 μ L of the PicoGreen dye in TE buffer. Solution fluorescence was measured using a spectrofluorometer (Tecan infinite M 1000) at excitation and emission wavelengths of 480 and 520 nm, respectively. A calibration curve was prepared with Lambda DNA in TE buffer.

3.7.2.3 Sulfated GAG content assay

The dimethylmethylene blue (DMMB) assay is a spectrophotometric procedure that measure sGAG content in biological fluids. The basic principle of this assay is the change in the absorption spectrum showed by the dye 1,9-dimethylmethylene (a thiazine chromotrope agent) caused by the induction of metachromasia when bound to sulfated GAGs permitting a fast detection of GAGs^[84]. A 10 μ L aliquot of papain digest was mixed with 200 μ L of DMMB solution (1.6 mg/mL DMMB in ethanol, 40 mM Glycine, and 40 mM NaCl; pH adjusted to 1.25 with HCl). A calibration curve was prepared with chondroitin sulfate. The absorbance was read using a BioTek Epoch plate reader at wavelengths of 525 and 590 nm. The absorbance values obtained at 525 nm were divided by those at 590 nm for the same sample and the sGAG concentrations were determined from the standard curve. The data was normalized to DNA.

3.8 Statistical analysis

The Student t-test was performed to determine if statistically significant differences were present in experiments when only two conditions were compared. One-way analysis of variance (ANOVA) was used for all experiments with more than 2 conditions. Tukey's Post hoc test was used for pairwise comparison and two-tailed p-values < 0.05 were considered significant. Each condition was performed in biological triplicates unless specified otherwise and many experiments were repeated twice as indicated in the figure captions. Technical replicates were performed for each test according to standard practice in the lab. The results were expressed as means \pm standard error.

CHAPTER 4 – RESULTS AND DISCUSSION PART 1:

PolyP retention within ionically Ca^{2+} and Sr^{2+} crosslinked alginate beads

This section details our early findings toward the development of optimal chondrocyte culture conditions within ionically crosslinked alginate beads, as well as investigations of the effect of polyP incorporation in alginate beads on chondrocyte responses, and our attempts to tailor polyP retention profile and alginate beads properties through the selection of ionic crosslinkers.

Preliminary experiments were performed prior to the work detailed below to obtain cell-encapsulated alginate beads under sterile conditions. A protocol involving filtration of the solutions and autoclaving of each tool used in the process was developed.

4.1 Effects of the incorporation of polyP in calcium-alginate beads

In a first experiment, we hypothesized that incorporating polyanionic polyP within alginate bead would allow its retention within the hydrogel structure through ionic interactions with the cationic crosslinker, in this case Ca^{2+} . The polyP was incorporated in chondrocyte-encapsulated calcium-alginate beads at concentrations of a 0, 1.0, and 2.5 mM. The beads were formed from a 1 %wt. alginate solution dropped into a 100 mM CaCl_2 bath and the cell concentration was adjusted at 0.50 million/mL of the alginate solution. As can be seen in Figure 9, the DNA content inside the beads increases significantly over time in culture. DNA content is used as an indirect measure of the number of cells present in each bead, whereby 1 cell is estimated to contain 7.7 pg of DNA^[85]. While the increase appears less important between days 7 and 14 than in the first 7 days of culture, it should be noted that, under these culture conditions, chondrocytes migrated outside the beads starting between days 5 and 7 and proliferated rapidly onto the plate surfaces. The DNA from the cells that had escaped the beads was not measured because of the rapid chondrocyte proliferation

expected on tissue culture plastic made any comparison of cell numbers in and outside the beads irrelevant. Unexpectedly, no significant difference in DNA content was observed between beads prepared with polyP and control beads prepared without polyP at any time point. Previous work evaluating the effects of soluble polyP on chondrocytes showed decreased DNA content over time compared to untreated controls^[86]. It was speculated that this result could indicate (i) the absence of an effect of polyP on chondrocytes in this particular system, or (ii) the rapid release of polyP from the hydrogel bead, and/or (iii) an insufficient amount of polyP for bioactivity.

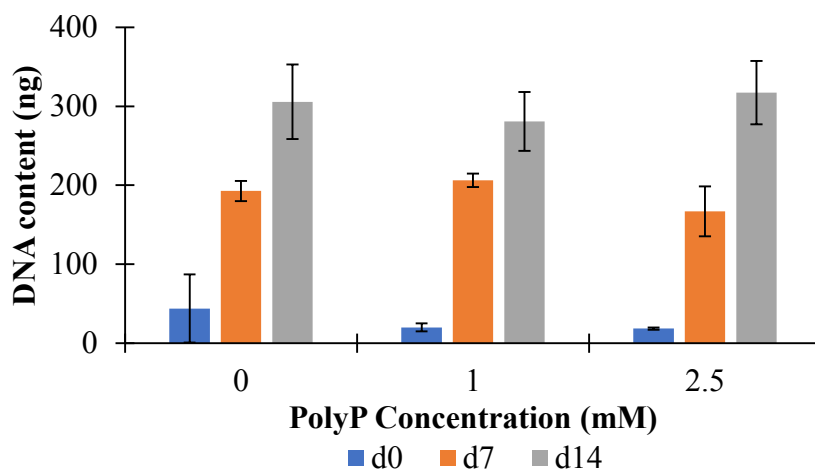


Figure 9. DNA content of chondrocyte-encapsulated alginate beads formed to incorporate 0.0, 1.0, and 2.5 mM polyP at days 0, 1, and 14 in culture. The experiment was performed in biological triplicates. Data are presented as means \pm standard deviation.

These results were confirmed by light microscopy imaging of the alginate beads after different time points in culture. As seen in Figure 10, chondrocytes were initially present as single cells dispersed throughout the hydrogel; however, large cell agglomerations became evident by day 7 in culture, confirming DNA evidence of proliferation. Once again, no differences in cell numbers were observed through our extensive observations of all samples and throughout the depth of the beads as a function of initial polyP loading in the alginate beads.

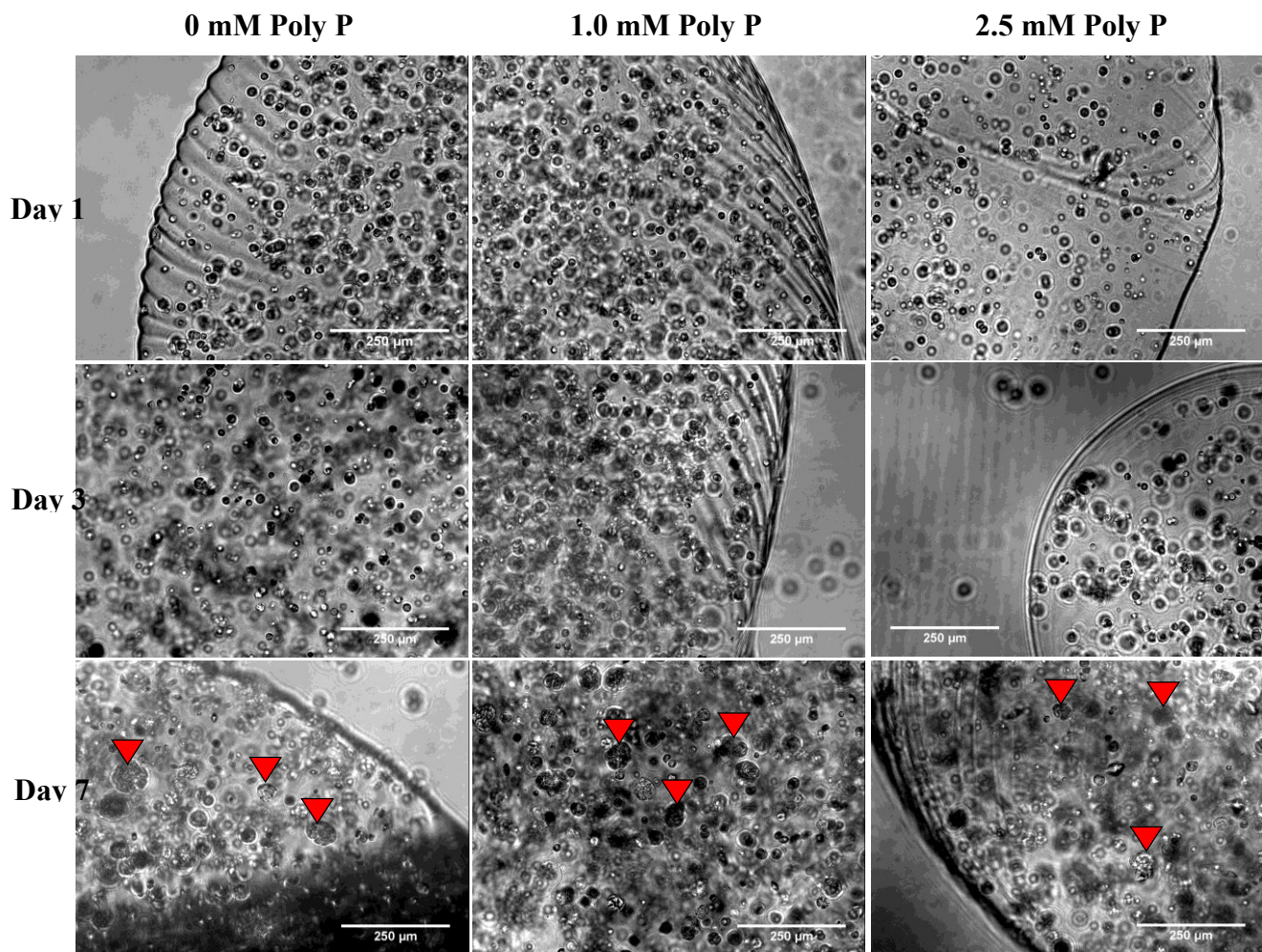


Figure 10. Representative light microscopy images of calcium-alginate beads formed with different initial concentrations of polyP with chondrocytes entrapped in the 3D structure after different time points in culture. Red arrowheads highlight some of the large cell agglomerates that start appearing between 3 and 7 days in culture.

Figure 11 shows the accumulation of sGAG (normalized by the DNA content), one of the two main ECM components of cartilage tissue, by encapsulated chondrocytes in the alginate beads formed without and with polyP. These results show a significant, but small, increase in sGAG accumulation in beads prepared with 2.5 mM polyP compared to controls with 0 mM polyP at day 7; however, no significant effects were observed at day 14. Substantially increased and sGAG accumulation had previously been reported for chondrocytes treated with soluble polyP^[86]. Day 0

is not included because sGAG content at that early time point is below the limit of detection of the assay.

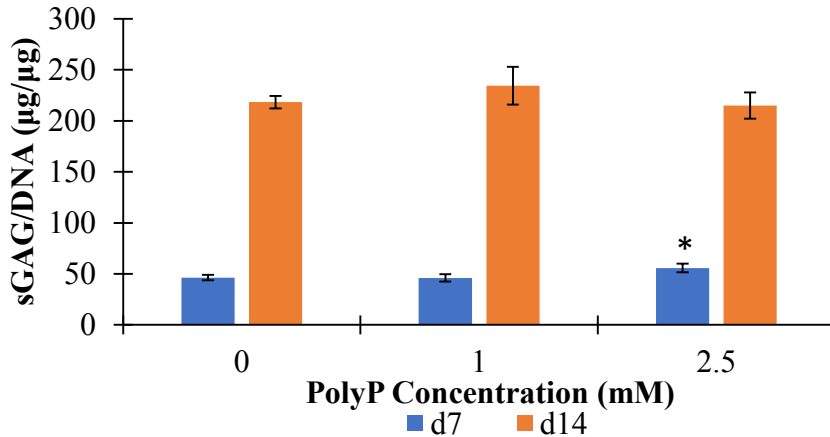


Figure 11. sGAG accumulation by chondrocytes encapsulated in alginate beads prepared with 0, 1, and 2.5 mM polyP at days 7, and 14. The sGAG data are normalized by the DNA content of the beads. The experiment was performed in biological triplicates. Data is presented as means \pm standard deviation ($p < 0.05$). * indicates a statistically significant difference between the 2.5 mM and 0 mM polyP control condition.

Taken together, the results of this experiment (Figures 9-11) highlighted two key aspects that should be investigated in more detail in order to achieve the objectives of this project. First, an excessive amount of chondrocyte proliferation was observed. We felt that it was important to identify culture conditions that controlled this cell response because excessive cell proliferation is typically associated with damaged and diseased cartilage, while chondrocytes in healthy cartilage have a low mitogenic activity [8][87]. Efforts in the group are also ongoing to incorporate cell binding molecules within the alginate beads, since alginate does not present cell binding motifs recognized by mammalian cells. Second, while a small significant difference in sGAG content within alginate beads formed with the highest concentration of polyP was observed at day 7, it was

gone by day 14. Efforts to increase polyP concentration in the beads and/or improve retention were deemed necessary to elicit prolonged bioactivity in chondrocytes. It was deemed unlikely that the reason for the absence of polyP effects was related to the system used, partly because polyP effects on chondrocytes has previously been investigated in a 3D system.

4.2 Effects of culture conditions on chondrocytes encapsulated in calcium-alginate beads

To modulate the excessive chondrocyte proliferation initially observed in calcium-alginate beads, we first investigated the impact of culture medium conditions on cell proliferation. We speculated that the high FBS concentration may be causing the important chondrocyte proliferation observed. Chondrocytes were encapsulated in 1 %wt. calcium-alginate beads at a concentration of 0.5 million per mL of alginate solution. Each hydrogel bead was formed by dropping 7.5 μ L of the alginate-chondrocyte solution into a 100 mM CaCl_2 bath to cross-link the alginate. The beads were cultured in media supplemented with 10% FBS (control), 2% FBS, and 1% ITS. ITS stands for insulin-transferrin-selenium and is a serum-free minimal medium supplement often used for the culture of chondrocytes and chondrogenic cells. In Figure 12, the DNA content in beads is shown to increase significantly over time in the 10% FBS culture condition as was observed previously in Figure 9. Conversely, in the 2% FBS and 1% ITS culture conditions, DNA content increase over time was much more modest. This difference lead to significantly higher DNA content in beads cultured in 10% FBS than the other two conditions by day 14.

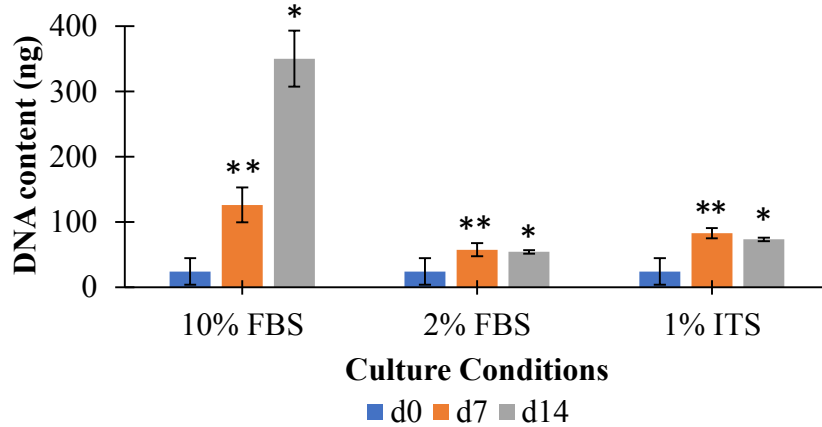


Figure 12. DNA content of chondrocyte-encapsulated alginate beads cultured in 10% FBS, 2% FBS and 1% ITS culture conditions at days 0, 7, and 14. The experiment was performed in biological triplicates. Data are presented as means \pm standard deviation. * indicates a statistically significant increase in DNA content compared the control condition (10% FBS). ** indicates a statistically significant difference in DNA content between samples at day 7.

Light microscopy imaging of the alginate beads at day 7 is shown in Figure 13 and confirms the excessive chondrocyte proliferation in the 10% FBS culture condition as exemplified by the presence of large cell agglomerates. In the 2% FBS and 1% ITS conditions these cell agglomerates are not observed, in agreement with the DNA content data in Figure 12.

The sGAG content (normalized by the DNA content) accumulated in alginate beads is shown in Figure 14. A significant increase in sGAG/DNA over time (i.e. from day 7 to day 14) is observed for each of the three conditions. A comparison between conditions at day 14 shows a significantly higher accumulation of sGAG normalized by DNA in both the 2% FBS and 1% ITS culture conditions compared to the 10% FBS control condition.

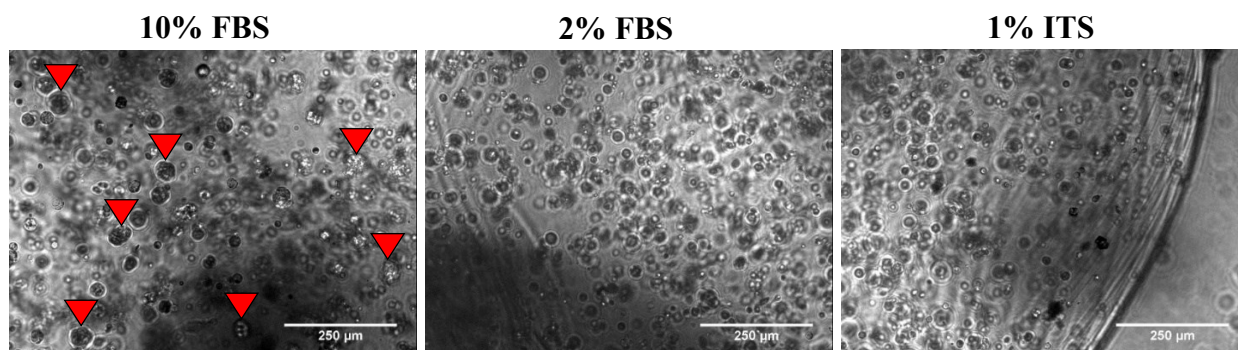


Figure 13. Representative light microscopy images of calcium-alginate beads in different culture conditions (10% FBS, 2% FBS, and 1% ITS) with chondrocytes entrapped in the 3D structure after 7 days in culture. Red arrowheads highlight some of the large cell agglomerates that start appearing between 3 and 7 days in culture.

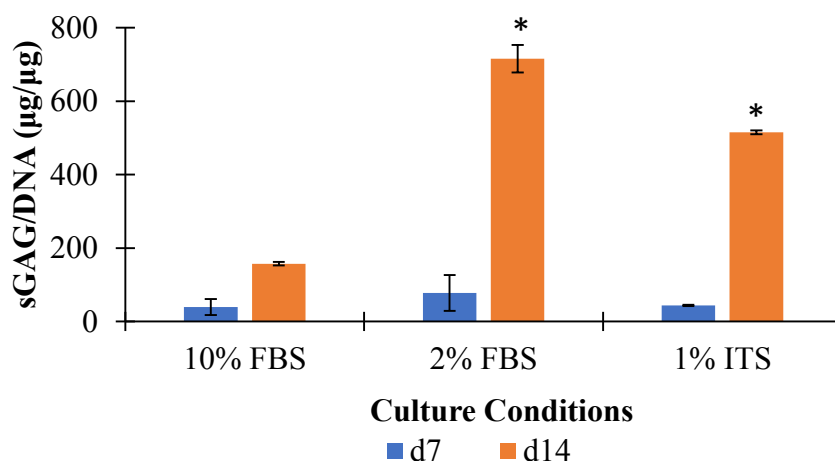


Figure 14. sGAG accumulation by chondrocytes encapsulated in alginate beads in 10% FBS, 2% FBS, and 1% ITS culture conditions at days 7, and 14. The sGAG data are normalized by the DNA content of the beads. The experiment was performed in biological triplicates. Data is presented as means \pm standard deviation ($p < 0.05$; $n=3$). * indicates a statistically significant difference compared to the control condition 10% FBS.

The results of this experiment are in accordance with a previous study that shows that chondrocyte proliferation is increases proportionally with FBS concentration in the medium and

that it is minimal in 1% ITS^[88]. Based on the results, and because FBS would cause complications towards clinical translation due to the fact that it leads to interactions between the hydrogel and animal sourced biomolecules, it was decided that ITS would be used as a culture supplement for most further studies in this thesis. ITS holds potential as a serum-free medium supplement for translation to clinical applications^[89], It also addresses the issue of excessive chondrocyte proliferation identified early in our studies and leads to increased sGAG accumulation per cell (it is generally assumed that each chondrocyte contains 7.7 pg of DNA^[85]). This increased sGAG accumulation per cell was expected because proliferation and ECM accumulation are considered mutually exclusive cell processes^[90]. Additionally, it does away with issues of batch to batch variability associated with the use of FBS for *in vitro* studies.

4.3 Effect of NaCl on chondrocytes morphology

Owing to the high concentration of negatively charged sGAG in cartilage ECM, high concentrations of inorganic cations such as calcium, sodium, and potassium accumulate in the fluid phase of the tissue. The presence of these cations in concentrations higher than that found in the blood leads to the high water content of the tissue via osmotic pressure, which in turn plays a role in the biomechanical behavior of the tissue^[23]. During our efforts to optimize alginate bead formation, we observed potentially improved cell responses (e.g. cell morphology was more rounded) with the addition of NaCl inside the alginate beads. To verify this potential effect based on observations, we conducted an experiment whereby chondrocytes were cultured in 2D on tissue culture plates in DMEM, which contains 109.51 mM NaCl, alone or supplemented with different concentrations of NaCl (i.e., 150 mM, and 300 mM) in solution. These two concentrations of NaCl

were selected to represent the lower and upper ranges of sodium concentrations in articular cartilage^[91].

Chondrocytes cultured in 2D change their morphology to an elongated, fibroblastic-like shape within 1-3 days of attaching to tissue culture plastic as can be seen in Figure 15 for the control condition cultured in a medium not supplemented with NaCl. This is accompanied by dedifferentiation, which includes a decreased expression of collagen type II and aggrecan and increased expression of collagen type I, and an increased proliferation rate^{[92][93]}. Lower proliferation, as observed by decreased cell density on the culture surface, and a generally more rounded morphology were observed when the medium was supplemented with additional NaCl. This suggests that an increased concentration of NaCl to mimic the cationic concentration found in native AC (320 mM on average)^{[94][95]} may help prevent dedifferentiation in vitro. This may offer avenues for improved chondrocyte culture conditions and for the redifferentiation of passaged chondrocytes, an active area of research aimed at producing large quantities of cells with chondrogenic potential for clinical applications in cartilage repair. When NaCl was supplemented at a high concentration of 300 mM, smaller yet still round cells were observed, leading us to speculate that they may be suffering from the increased osmotic pressure associated with the medium supplementation. This work was beyond the scope of the project presented in this thesis and was not pursued beyond these results; however, these findings are interesting and should be investigated further.

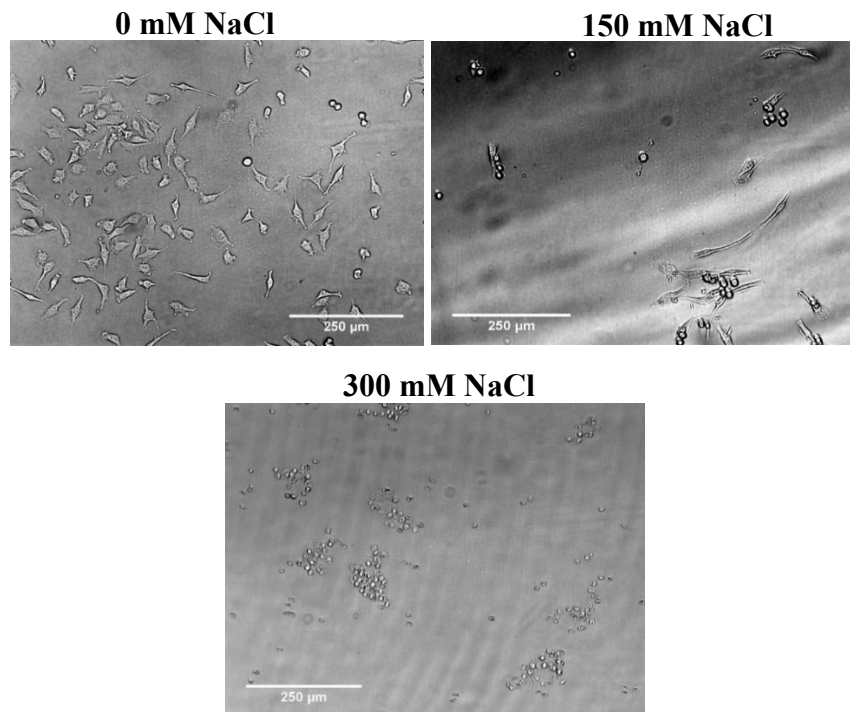


Figure 15. Morphology of bovine chondrocytes in monolayer culture on tissue culture plastic in DMEM alone or supplemented with different concentrations of NaCl imaged by light microscopy 24 hours after the introduction of the NaCl.

4.4 Effect of bead formation on polyP content

The second issue raised in section 4.1 as a potential explanation for the fact that only a small increase in sGAG content was observed in alginate beads containing polyP at day 7 compared to those prepared in absence of polyP, and that no effect of polyP was noted by day 14, was the possibility that the initial polyP concentration may be too low and/or that polyP diffuses out of the beads too rapidly. This finding had highlighted the need for an assay to quantify polyP inside alginate beads, in order to study its retention/release over time.

Direct quantification of polyP has previously been achieved based on the interaction between dissolved polyP and DAPI, which leads to a shift in the emission fluorescence wavelength

to the yellow-green range of the spectrum compared to DAPI binding with DNA, which results in fluorescence emitted in the blue range of the spectrum [96][97]. This approach was tested on the alginate solution (7.5 μ L) spiked with 2.5 mM, and 25.0 mM polyP prior to and after bead formation and washing (see Figure 16). The polyP levels measured in the solution before gelation were very close to theoretical levels based on the polyP content added to each solution (i.e., 19 and 1.9 μ g for the 2.5 and 25.0 mM conditions respectively). These data suggest that the method can accurately estimate polyP levels in an alginate solution. Beads were also formed in a CaCl_2 bath for 30 minutes and washed once with PBS before being transferred to a digestion buffer that leads to the breakdown of the gel structure. The results showed that approximately 55% of the polyP added to the solution is released during the bead formation and washing steps for the 25.0 mM polyP condition, while 27% of the initial polyP content is released for the 2.5 mM polyP condition. These results suggest the need to optimize the bead formation protocol to reduce polyP release during this step.

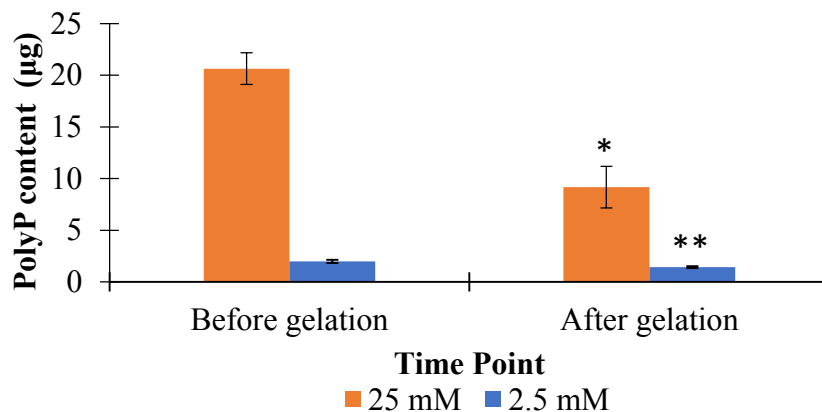


Figure 16. PolyP content within spiked an alginate solution (7.5 μ L) before forming the bead (solution) and after forming the bead in CaCl_2 for 30 minutes and washing once with PBS. PolyP was spiked at 2.5 and 25.0 mM. The experiment was performed in five replicates. Data are presented as means \pm standard deviation. * indicates a statistically significant difference compared

to before gelation for 25.0 mM polyP condition. ** indicates a statistically significant difference compared to before gelation for 2.5 mM polyP condition

PolyP was also quantified in the buffers and media used to incubate the beads after formation. After these experiments, it was decided that polyP quantification would be carried out as the polyP content retained in the beads and measured from digests because more variable results were obtained from the release. It is unclear what the source of this experimental variability was; however, we speculated that some level of precipitation may occur once the polyP is released from the beads and into the medium and that this may be a factor.

4.5 PolyP release profile of calcium-alginate beads

Following the establishment of a method to quantify polyP content within alginate beads over time, efforts were made to improve the retention of polyP within the bead structure during bead formation and washing steps. It was found that washing with DMEM rather than PBS leads to increased retention as can be seen in Figure 17, whereby nearly 69% of the 19 μg of polyP is retained in the 1% calcium-alginate beads. We also found that increasing the alginate concentration leads to a significant increase in initial polyP retention to almost 100% of the quantity initially loaded with a 2.5% alginate solution. This result was not unexpected because the alginate concentration has previously been shown to play an important role in encapsulation efficiency, as well as size, and shape of alginate beads ^[64]. Interestingly, at all alginate concentrations, the polyP release profile exhibited a burst release within the first 24 hours of incubation followed by a more gradual polyP release for at least 7 days. While a large proportion of the polyP was lost during the burst release phase, this result was considered encouraging for the ability to release polyP over a relatively long period; however, achieving release of a greater proportion of the cargo over a period

of at least 1 to 2 months would be considered optimal for cartilage tissue engineering applications, given the time required to form new tissue. These results also suggest that only a small proportion of the polyP added interacts with the alginate through ionic bonds with calcium. It is unclear at this point if this effect is caused by considerably different calcium binding affinities for the alginate polymer or polyP, which could result in relatively few bonds forming between the two types of molecules. The effect of alginate concentration suggests that increasing the ratio of alginate monomers to phosphate groups (in other words the ratio of alginate to polyP charge), leads to increased retention. This may indicate saturation of the possible alginate-calcium-polyP "binding sites" occurs. For example, calcium binds specifically to guluronate blocks and mannuronate-guluronate blocks in alginate^[98] and it is possible that alginate-calcium-polyP binding only occurs at specific monomeric sequences in the alginate polymer.

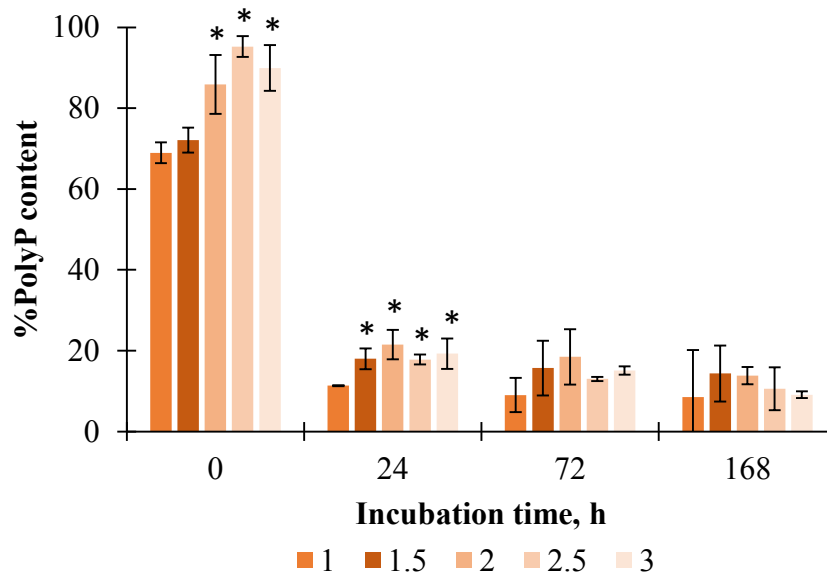


Figure 17. PolyP content within calcium-alginate beads prepared at different weight concentrations (1.0, 1.5, 2.0, 2.5, and 3.0 %wt.) after different times in DMEM. The initial polyP loading was 25 mM. The experiment was performed in quadruplets. Data are presented as means

± standard deviation. * indicates a statistically significant difference compared to control condition (1%wt. alginate).

One potential explanation for the limited number of alginate-calcium-polyP binding events may be that despite the infiltration of the gel structure by calcium ions, the hydrogel could remain anionic in nature because of the high charge density of the alginate polymer. This would reduce the number of potential ionic interactions for anionic polyP and its associated prolonged retention. To test this possibility, small concentrations of calcium were added to the polyP/alginate solution prior to gelation via the PBS. This approach was intended to ensure that an increased amount of positive charges was present within the bead structure at the time of gelation by dropping into a CaCl₂ bath. It was noticed that some level of gelation occurred within the alginate by this addition, which could be reversed by mixing. As can be seen in Figure 18, this approach did not result in increased polyP retention within the beads, as the cumulative release at 24 hours was the same with and without addition of calcium to the alginate-polyP solution prior to gelation step. This result suggests that the overall charge of the hydrogel may not have been an important contributing factor to low prolonged polyP retention within calcium alginate beads. Alternatively, it could also indicate that the addition was insufficient to change the ionic nature of the hydrogel. Having said that, adding more calcium would make it difficult to extrude the alginate-polyP solution and was not explored as a strategy. Developing a strategy for the slow release of calcium within the hydrogel could provide such an opportunity, but would require substantial amount of optimization and may not contribute to improved release kinetics.

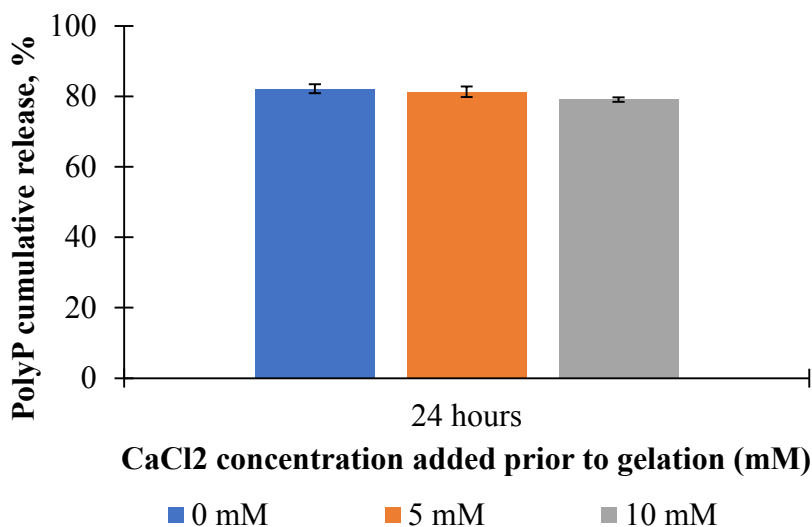


Figure 18. PolyP cumulative release profile of calcium-alginate beads prepared at different CaCl₂ concentrations (0, 5, and 10 mM) after 24 hours in DMEM. The initial polyP loading was 25 mM. The experiment was performed in triplicates. Data are presented as means \pm standard deviation.

Given the fact that an important polyP burst release was observed within 24h of incubation (>70% of the initial polyP incorporated), an in depth analysis of polyP release within the first 24 hours following gelation was undertaken. This experiment was carried out at 2% wt. alginate in 100 mM CaCl₂; the data obtained from this short-term experiment was fitted with the most commonly used drug release models: the zero order, first order, Higuchi, Kors-Peppas, and Hixson models. . This comparison of the drug release models revealed that the Higuchi model (Figure 19) provided the best fit based on a R² value of 0.9625 (zero order:0.7989; first order: 0.9522; Kors-Peppas: 0.9142; Hixson: 0.9113) for the calcium samples and 0.9082 (zero order:0.6983; first order: 0.8991; Kors-Peppas: 0.8907; Hixson: 0.8379) for the strontium samples. Higuchi’s model explains a drug release based on Fick’s law as a diffusion process from a matrix system^[99]. Therefore, these results suggest that the polyP portion that is released during the burst release phase does so via diffusion from the hydrogel and is likely not interacting with the alginate polymer. The

Higuchi model was developed with a number of assumptions in mind, including the fact that the matrix system does not degrade over time. Given the fact that this experiment was carried out over a short period of time and that calcium-alginate hydrogel degradation in DMEM takes place over a much longer period, it was assumed that this condition was met. It should also be emphasized that this model has been used broadly to study drug release from alginate beads^{[100][101]}. The slower polyP release observed during longer term incubations suggests that some of the polyP did interact with the hydrogel, albeit a small fraction of that added to the solution.

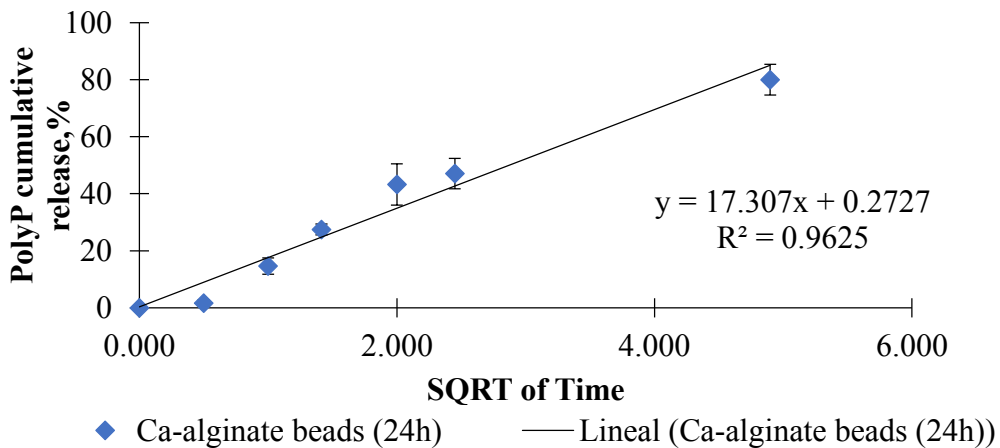
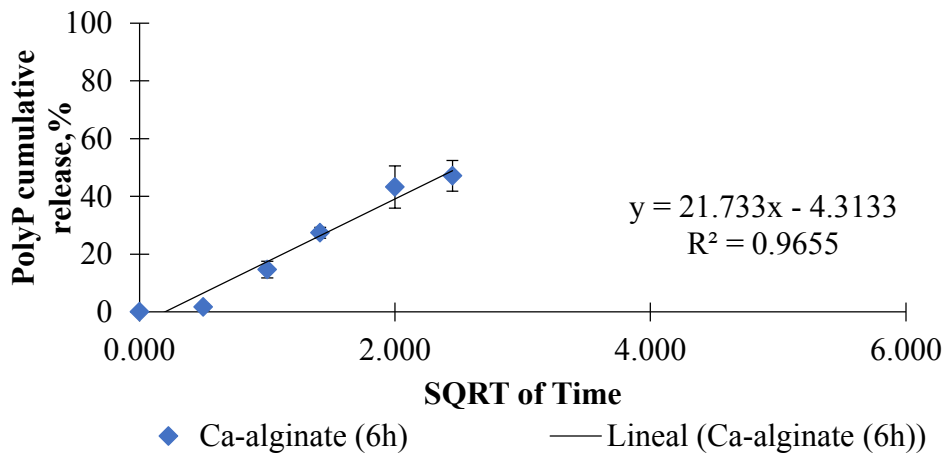


Figure 19. Higuchi release profile of polyP from Ca-alginate beads. The first graph shows release until 6h while the second graph shows the release until 24h. The experiment was performed in triplicates. Data are presented as means \pm standard deviation.

4.6 Swelling of Alginate Beads

Based on our findings suggesting that a large proportion of the polyP loaded into calcium-alginate beads is released rapidly via a diffusion mechanism, we sought to develop a strategy to slow diffusion through the gel. Biomolecule release behaviour from alginate hydrogels is intrinsically related to gel mechanical properties, degradation rate, and swelling^[82] and these properties are affected directly by the choice of crosslinking cations and the crosslinking density^[80]. For example, a number of divalent cations have been investigated for the crosslinking of alginate and were found to exhibit varying binding strengths. Studies have reported that cationic binding strength to the guluronate blocks is as follows: $Mg^{2+} \ll Ca^{2+} < Sr^{2+} < Ba^{2+}$, while Ca^{2+} also binds to guluronate-mannuronate blocks and Ba^{2+} also binds to mannuronate blocks^[102]. Based on this information and because strontium is a cation that has been associated with positive biological effects on cells of the musculoskeletal system^{[103][104][105]}, substitution of calcium by strontium in the crosslinking bath was investigated. The effect of this substitution on the swelling behaviour of alginate beads was evaluated first to verify previous reports in the literature. Calcium-alginate beads do swell over time and become weaker, before degrades fully^[106]. It was hypothesized that decreased swelling via crosslinker substitution would lead to decreased polyP release by diffusion. In Figure 20, swelling (expressed as the hydrogel weight at time 0) and degradation over time are analyzed for alginate gels prepared with 1.0, 1.5 and 2.0%wt. alginate solutions and using three different crosslinking solutions (100 mM $CaCl_2$, 50 mM $CaCl_2$:50 mM $SrCl_2$, and 100 mM $SrCl_2$). In this

experiment, the samples were incubated in PBS to accelerate the degradation rate. PBS does not contain Ca^{2+} or Sr^{2+} ions, such that there is a driving force for diffusion of these ions outside the hydrogel, leading to faster degradation of alginate beads due to breakdown of the ionic bonds^{[62][107]}. The results show that substitution of calcium for strontium does indeed lead to a significant lower bead mass, indicative of decrease swelling. Further, strontium-alginate beads exhibit increased stability and decreased degradation rate in comparison with calcium-alginate beads, as evaluated by the time required for the mass to fall to 0. Higher alginate concentration also appeared to provide increased hydrogel stability, but did not affect swelling.

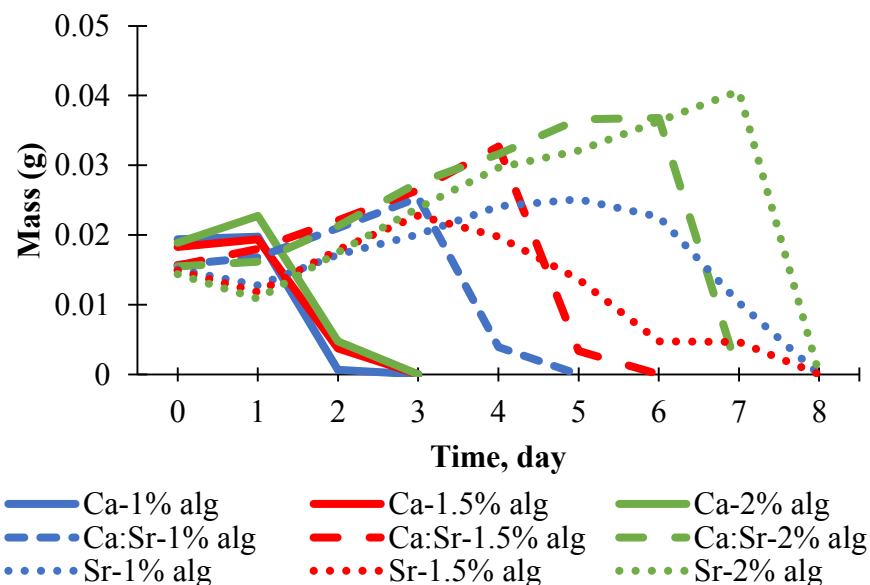


Figure 20. Hydrogel mass over time during incubation in PBS. Alginate beads formed by crosslinking with calcium and strontium cations (100 mM CaCl_2 , 50:50 CaCl_2 : SrCl_2 mM and 100 mM SrCl_2) and alginate concentrations (1.0, 1.5, and 2.0 %wt.). Two experiments were performed and each experiment was performed with triplicate samples.

A similar swelling and degradation rate experiment was also performed with incubation in DMEM culture medium rather than PBS. As can be seen in Figure 21, a slower degradation of the

alginate beads is observed under cell culture conditions, with full hydrogel degradation not occurring for any condition in the first 17 days. The trends observed in Figure 20 appear to hold for this more realistic incubation condition with the substitution of calcium for strontium leading to decreased swelling.

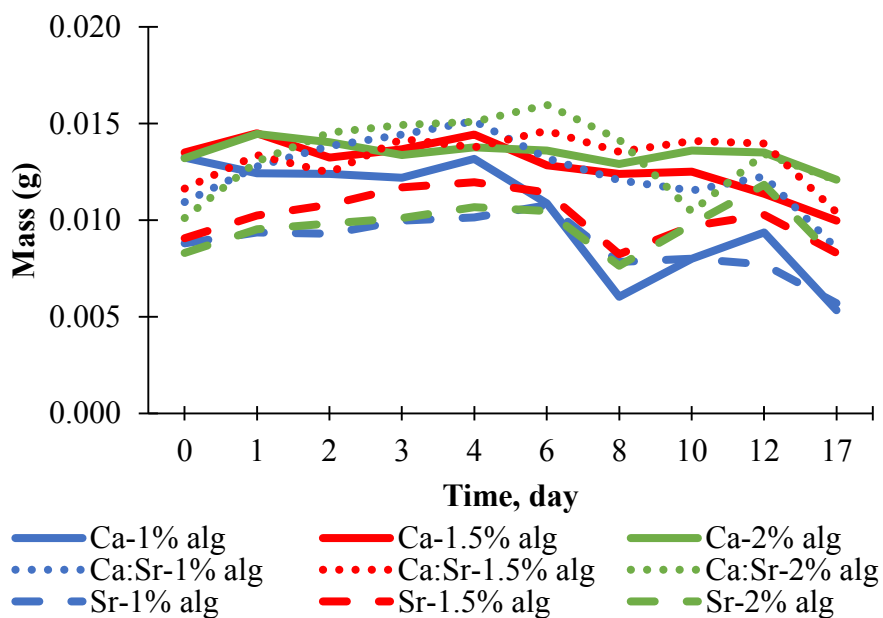


Figure 21. Hydrogel mass over time during incubation in DMEM. Alginate beads were formed by crosslinking with calcium and strontium cations (100 mM Ca, 50:50 Ca:Sr mM and 100 mM Sr) and alginate concentrations (1.0, 1.5, and 2.0 %wt.). The experiment was performed in triplicates.

Based on these results, we investigated the effect of substituting calcium for strontium on polyP release from alginate beads. The alginate concentration was fixed at 2 %wt. for this experiment based on previous results. As can be seen in Figure 22, data measured at time 0 show that increased substitution of calcium for strontium within the crosslinking bath results in decreased retention of polyP following gelation and washing. Nevertheless, replacement of a fraction or all of the calcium by strontium in the crosslinking bath did not affect the polyP retention from 24 hours onwards.

An additional experiment to identify if this loss of polyP retention was due to the washing step or the process of bead formation was carried out and results shown in Figure 23 clearly indicate that the bulk of the early release takes place immediately upon casting the bead (casting time of 0), with only a slight effect of incubation in the crosslinking bath (casting times of 15 and 30 minutes) or adding a washing step. It is unclear at this point what causes this very rapid release from the structure.

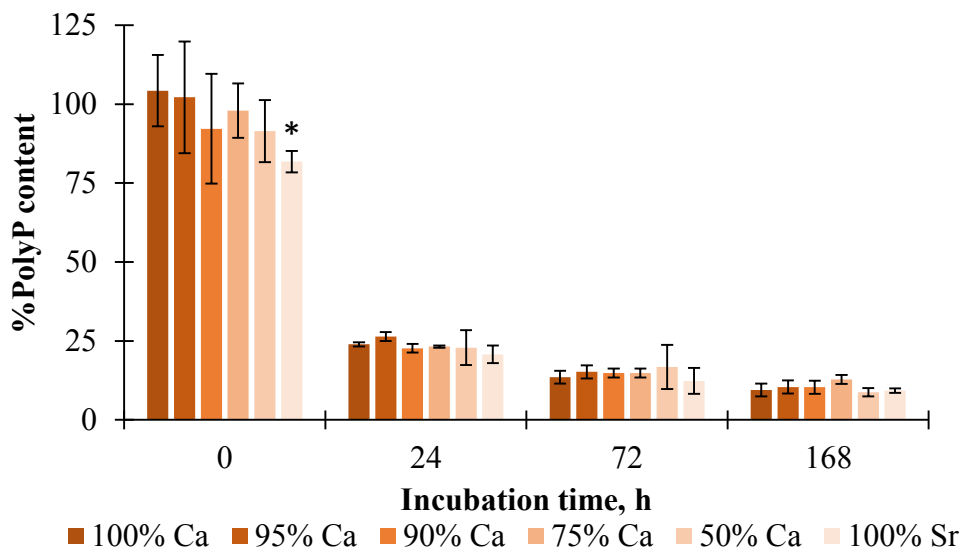


Figure 22. PolyP content within alginate beads prepared in crosslinking baths comprising different ratios of calcium and strontium after different times in DMEM. The initial polyP loading was 25 mM. The experiment was performed in quadruplets from 2 independent experiments. Data are presented as means \pm standard deviation. * indicates a statistically significant difference compared to the Ca-alginate bead condition.

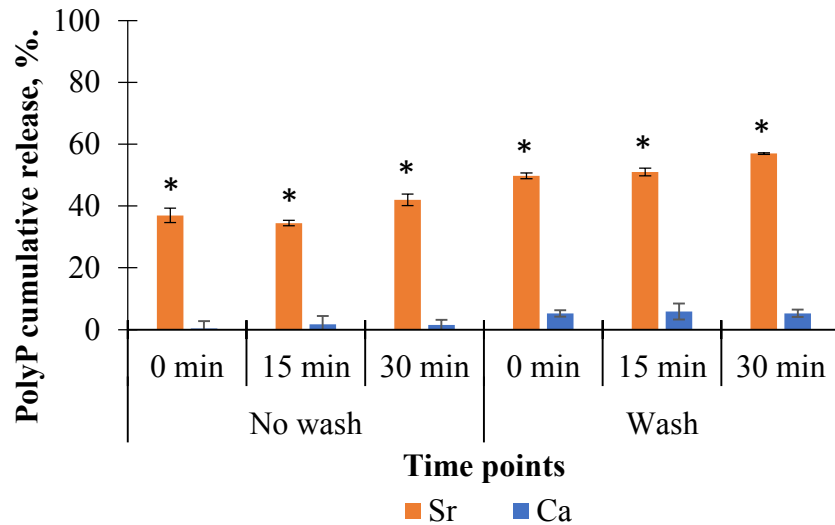


Figure 23. PolyP content inside strontium-alginate and calcium-alginate beads (7.5 μ L) after gelation. Casting times of ~0, 15 and 30 min were investigated with and without a washing step with culture medium. A polyP concentration of 25 mM was used. The experiment was performed in quadruplets. Data are presented as means \pm standard deviation. * indicates a statistically significant difference compared to the Ca-alginate bead condition for each time point.

A closer look at the burst release stage of the polyP release profile in the first 24 hours appears to suggest that strontium-alginate beads exhibit a more important burst release than calcium-alginate beads as evidenced by a larger slope in the Higuchi plot compared to that in Figure 19, but that polyP levels stabilize by 24 hours (Figure 24). This effect was unexpected because of the decreased swelling associated with the substitution of calcium for strontium in the crosslinking bath. It may be attributed to the fact that Ca^{2+} cations can bind to both G- and MG-blocks in the alginate polymer, while Sr^{2+} cations only bind G-blocks exclusively^[65]; hence there might be less sites for polyP binding in strontium-alginate beads than calcium-alginate beads.

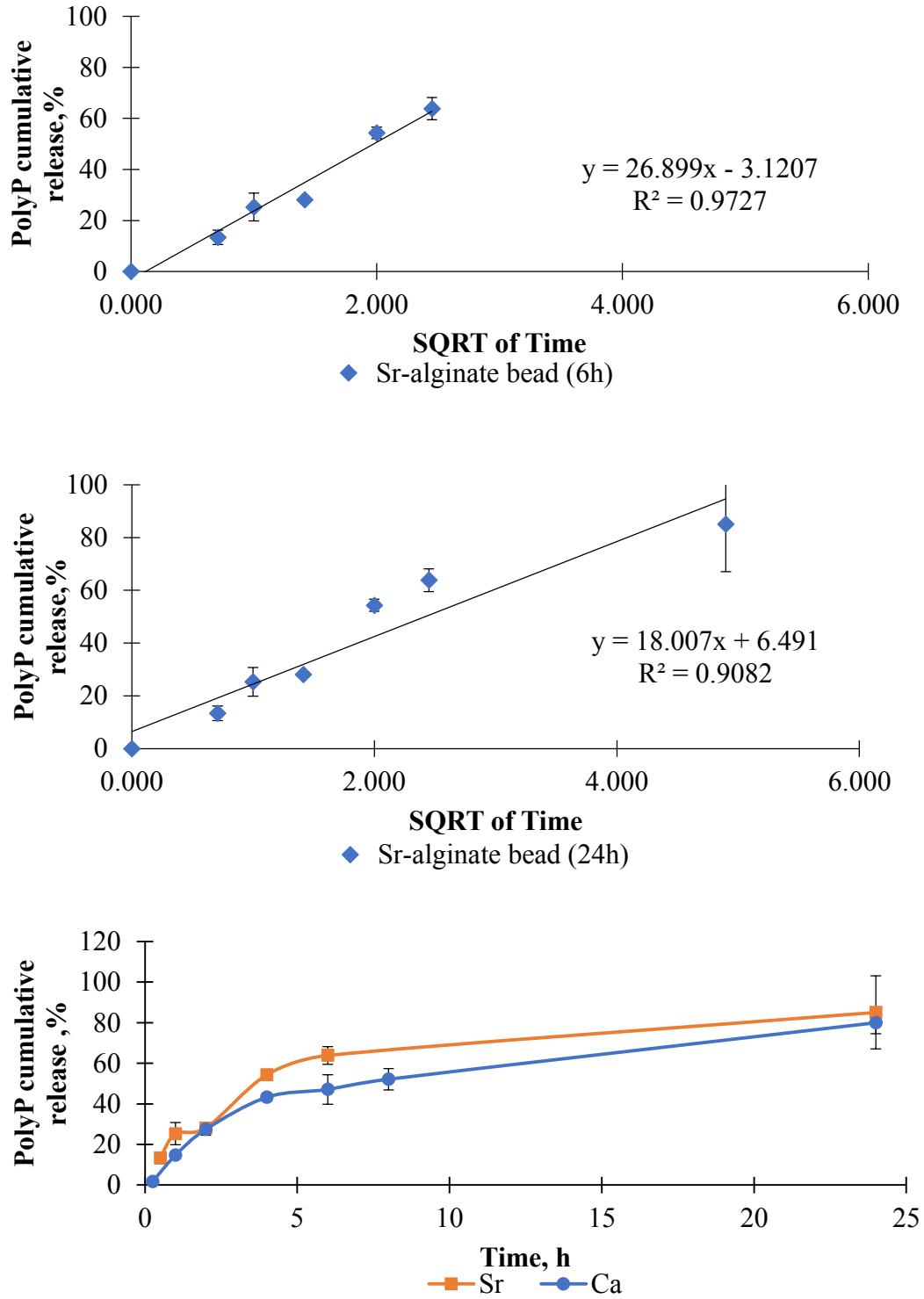


Figure 24. Higuchi release profile of polyP from Sr-alginate beads. The first graph shows release

until 6h while the second graph shows the release until 24h. Last graph shows the release profile for Sr-alginate and Ca-alginate bead. The experiment was performed in triplicates. Data are presented as means \pm standard deviation.

Further efforts to improve the retention of polyP within the strontium-alginate beads included testing the effect of crosslinking baths with different concentrations of SrCl₂. A concentration of 50 mM was investigated because of suggestions in the literature that high crosslinking concentrations result in non-uniform crosslinking through the depth of the hydrogel with poorly crosslinked cores and a concentration of 250 mM was investigated to attempt to increase the cationic density. As can be seen in Figure 25, the polyP release profile from beads crosslinked in 50 mM SrCl₂ remains similar to those crosslinked in 100 mM SrCl₂, while increasing SrCl₂ concentration to 250 mM lead to a significantly decreased release at 2 hours, suggesting a slower burst release. Nevertheless, the percentage of polyP released by 24 hours was comparable. This result suggests that it may be possible to adjust the rate of burst release slightly through adjustments of the crosslinker nature or concentration; however, the ability to substantially impact the release profile and deliver polyP over a period of weeks to months would require a strategy that increases the fraction of polyP added to the alginate solution that crosslinks within the hydrogel structure. This is likely due to the fact that the chain length of the polyP used for this study is relatively short at 40 orthophosphate units; however, this is a parameter that was fixed in our study because it was previously demonstrated that chondrocytes respond optimally to polyP of that chain length than longer inorganic polymers.

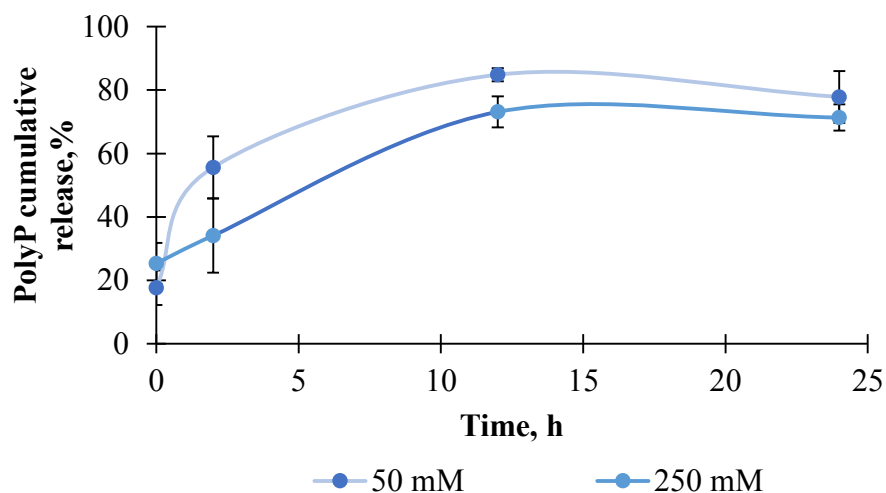


Figure 25. PolyP release profile from alginate beads crosslinked in baths with 50 mM and 250 mM SrCl₂. The experiment was performed in quadruples. Data are presented as means \pm standard deviation.

4.7 Mechanical properties of alginate gels in compression

Despite the lack of benefits to the polyP release profile resulting from the substitution of calcium by strontium in the crosslinking bath, the effect observed on the swelling behaviour of the hydrogels suggested that strontium crosslinking may lead to improved mechanical properties of the hydrogels. Unconfined compression were performed and the data analyzed (Figure 26). Hydrogels prepared in 100 mM CaCl₂, 50:50 mM CaCl₂:SrCl₂, and 100 mM SrCl₂, with alginate solutions at concentrations of 1.0, 2.0, and 3.0 %wt. were prepared as 8 mm discs in PDMS molds. The Young's moduli were calculated at 5 and 10 % strain for each condition and are reported in Figure 27.

These tests showed trends towards increased Young's modulus with increasing alginate concentration. Calcium- calcium/strontium- and strontium-alginate hydrogels showed significant differences between conditions the 1 and 3 %wt., alginate hydrogels at both 5 and 10 % strain.

Similarly, the incorporation of strontium appears to lead to stiffer hydrogels; however, no significant differences were observed between specimens at the same alginate concentration but crosslinked in different solutions. We can conclude that mechanical properties are more dependent on alginate concentration rather than cation used in the crosslinking process. Nevertheless, it is important to specify that these tests were performed with an instrument equipped with a 150 N load cell. Therefore the resolution is insufficient for the forces measured in alginate hydrogels and introduces important errors as evidence by the size of the error bars. These experiments will be repeated with a more adapted equipment as soon as it becomes available.

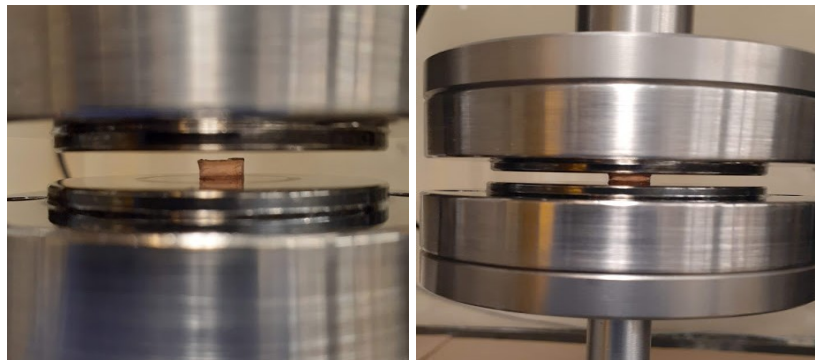


Figure 26. Images of alginate disc compressed by an Instron instrument in an unconfined compression test.

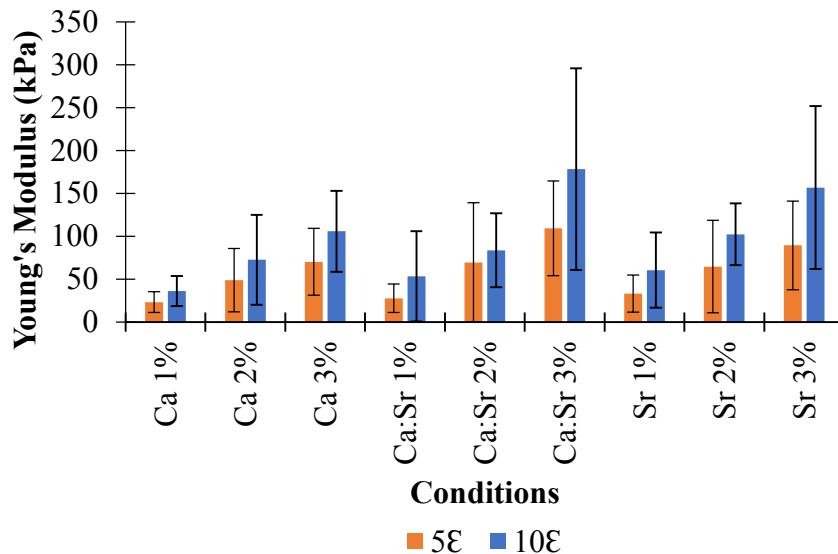


Figure 27. Young’s modulus in compression at 5 and 10 % strain of alginate gels prepared in crosslinking baths of 100 mM CaCl₂, 50:50 mM CaCl₂:SrCl₂ and 100 mM SrCl₂. Alginate concentrations used were 1, 2, and 3 %wt. The experiment was performed in nine replicates from three different experiments. Data are presented as means ± standard deviation.

4.8 Effect of polyP incorporation on the response of chondrocytes encapsulated in alginate beads

Given the sustained release of polyP over a period of at least 7 days at a rate that is comparable to the levels of soluble polyP that were shown to be bioactive on chondrocytes (i.e., 0.5-1.0 mM replaced every 2 days), the effect of polyP incorporation on chondrocytes encapsulated within calcium-, calcium/strontium-, and strontium-alginate beads was investigated. The main differences with the first cell experiment reported in this thesis, beyond the incorporation of strontium, include the incorporation of a higher polyP concentration (25 mM) within a solution with higher concentration of alginate, and the use of ITS in the culture medium rather than FBS. However, the cell concentration was also raised, albeit still to a low level for chondrocytes encapsulated with

hydrogels, to allow for a more accurate measurement of the biochemical content of beads. Each sample consisted of three beads (7.5 μ L) with a primary bovine chondrocyte concentration of 2 million cells per mL. The alginate solution was fixed at 2.0 %wt. and the crosslinking bath at 100 mM CaCl₂, 50:50 CaCl₂:SrCl₂, or 100 mM SrCl₂. Beads were cultured for up to 4 weeks in DMEM (1.0g/L glucose), supplemented with 1% antibiotic-antimycotic solution and 1% ITS. The DNA content in 3 beads per sample over time is shown in figure28. DNA content measurements showed a significant difference at week 1 between the cultures with polyP and without polyP for all three types of alginate crosslinking solutions. This effect was lost by week 2 and no significant differences were observed. A previous study had shown that polyP leads to a lower increase in DNA content in chondrocyte cultures and unpublished data by our group suggests that this is caused by a decrease in the cell proliferation rate. However, in these results a general decrease in DNA content is observed over time in all experimental conditions. This may be ascribed to the use of ITS as a culture supplement rather than FBS as per previous studies that suggest a decreased rate of proliferation^[67]. However, it could also be caused by issues with the diffusion of nutrients through the hydrogel beads, particularly because of the high cell density used for this study compared to our previous experiments, which may lead to cells in the center of the beads being deprived from essential nutrients. It is therefore still unclear if the decreased DNA content in encapsulated chondrocytes exposed to polyP was caused by decreased viability or decreased cell proliferation. Further studies with carefully selected cell concentrations and culture conditions are needed to resolve this question, as well as additional assays to evaluate cytotoxicity and proliferation.

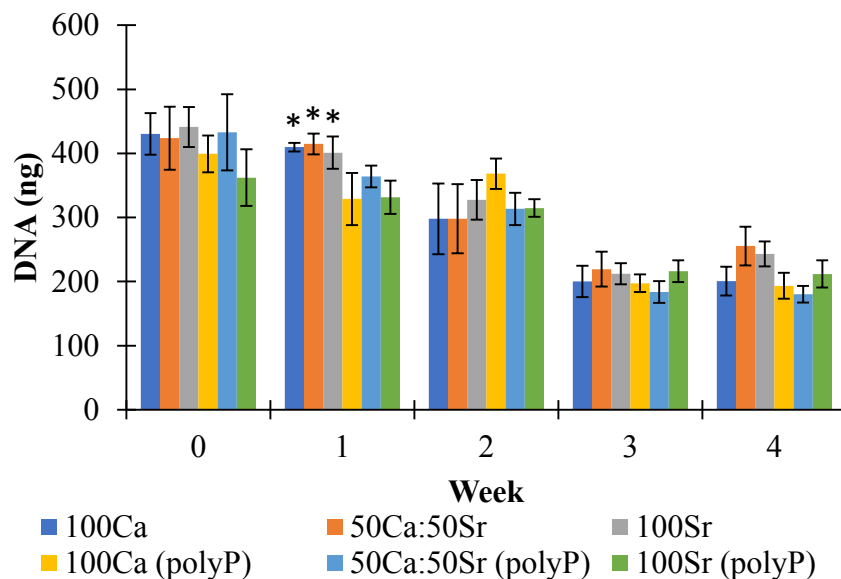


Figure 28. DNA content in three alginate beads (7.5 μ L) formed in crosslinking baths of 100 mM CaCl_2 , 50:50 mM CaCl_2 : SrCl_2 , and 100 mM SrCl_2 and with or without 25 mM polyP at week 0, 1, 2, 3, and 4. The experiment was performed in biological triplicates. Data are presented as means \pm standard deviation. * indicates a statistically significant difference compared to treated conditions at week 1.

The sGAG accumulation was also measured and normalized to the DNA content of each sample (Figure 29). The sGAG content provides information on the amount of ECM produced by the cells and is an important measure of tissue formation by chondrocytes. The normalized sGAG content increases over time until week 3 for all conditions, after which it appears to plateau. At week 1, a significant increase in sGAG/DNA was observed in beads with polyP compared to beads without polyP for the calcium-alginate and strontium-alginate (but not the 50:50) conditions; however, this increase is not considerable. From week 2 onwards, this effect was no longer observed. Based on previous results on the effects of soluble polyP on chondrocyte cultures, an increase in sGAG/DNA content would have been expected by week 2 rather than as early as 1

week. The absence of an important effect is in accordance with the fact that polyP retention is not sustained at sufficient level for a period longer than 1 week.

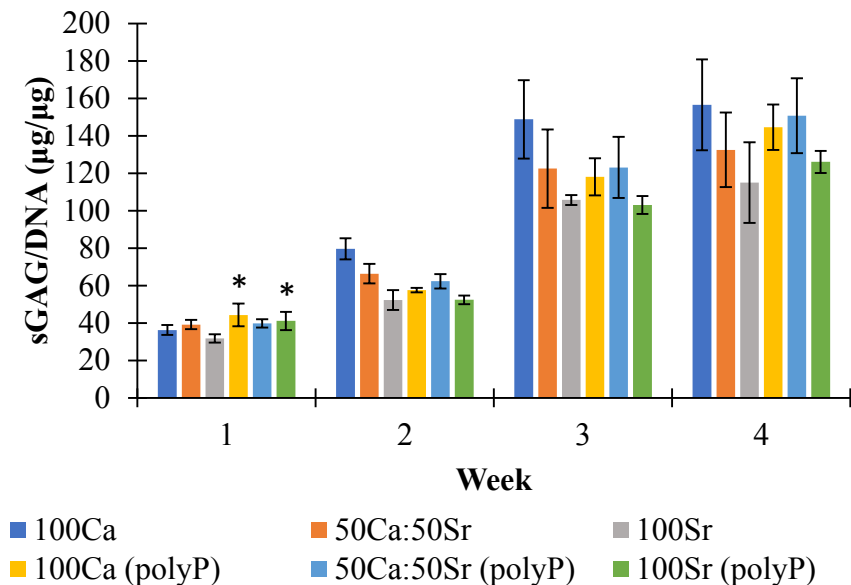


Figure 29. sGAG/DNA content in three alginate beads (7.5 µL) formed in crosslinking baths of 100 mM CaCl₂, 50:50 mM CaCl₂:SrCl₂, and 100 mM SrCl₂ and with or without 25 mM polyP at week 0, 1, 2, 3, and 4. The experiment was performed in biological triplicates. Data are presented as means ± standard deviation. * indicates a statistically significant difference compared to untreated conditions at week 1

Taken together, these results suggest that the current system provides polyP delivery to chondrocytes at bioactive levels for approximately 1 week. While this represents an interesting result and the materials designed offer “short-term” delivery of polyP, there is a need for sustained delivery of polyP to encapsulated chondrocytes over a prolonged period of time spanning multiple weeks to months for this approach to be viable for AC repair applications.

CHAPTER 5 – RESULTS AND DISCUSSION PART 2:

Additional attempts to increase the polyP retention in alginate beads

In this chapter, several strategies that were investigated to improve the polyP release profile from alginate beads for applications in AC repair by slowing its rate of release will be described, culminating with a promising strategy that warrants further investigation.

5.1 Investigation of other bioactive cations (Co^{2+} and Mg^{2+}) as ionic crosslinkers

As was discussed in Chapter 4, different ions have different binding affinities to alginate. Results obtained with the substitution of calcium from the crosslinking bath by strontium, had initially lead us to hypothesize that the decreased retention of polyP at the end of the burst release phase in strontium-alginate hydrogels compared to calcium-alginate hydrogels was caused by a greater proportion of the ionic crosslinks being between two alginate molecules than between alginate and polyP owing to a greater preferential affinity of Sr^{2+} for alginate, compared to Ca^{2+} . To investigate this possibility and potentially increase the proportion of crosslinks between alginate and polyP, we investigated the use of other divalent cations known to be characterized by a lower binding affinity for alginate than Ca^{2+} . Two cations, Co^{2+} and Mg^{2+} , were used to form alginate beads and the short-term polyP release profile from the resulting beads is shown in figure 30.

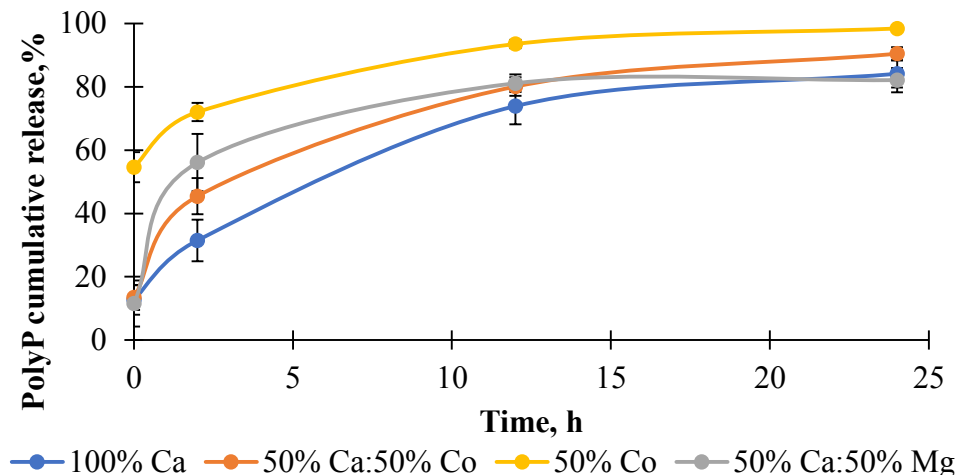


Figure 30. PolyP release profile from alginate beads formed in different crosslinking solution at 100 mM CaCl₂, 50:50 mM CaCl₂:CoCl₂, 100 mM CoCl₂, and 50:50 mM CaCl₂:MgCl₂. Each alginate bead was formed from a solution with 2.0 %wt. alginate and 25 mM polyP. The experiment was performed with triplicate samples. Data are presented as means ± standard deviation.

A more important polyP burst release was observed from alginate beads for all conditions incorporating cobalt or magnesium in the crosslinking bath compared to the control with only CaCl₂. Alginate beads formed with 100 mM MgCl₂ were mechanically weak and could not be processed for incubation as they disintegrated during the pipetting and manipulation. One study^[108] supports this findings and ascribe this result to the weak magnesium-alginate interactions. Based on these results, different strategies to improve polyP retention within alginate hydrogels were investigated.

5.2 Effect of ethanol addition in crosslinking bath on polyP retention

In our research group, small quantities of ethanol have been added to the crosslinking bath as a surfactant to help reduce the size of the alginate bead formed by electrospaying. It appears that the presence of ethanol leads to shrinkage of the bead, which we assumed indicates a higher density of ionic crosslinks. We hypothesized that this denser hydrogel network could reduce the diffusion of polyP and thereby increase its retention over time and/or provide more opportunities for crosslinking between alginate and polyP. An experiment was conducted to determine the release profile of polyP from beads formed in crosslinking baths containing different proportions of ethanol ranging from 5 to 15 %vol. As can be seen in Figure 31, the addition of ethanol to the crosslinking bath has no effect on the polyP release profile from alginate beads and this approach was abandoned.

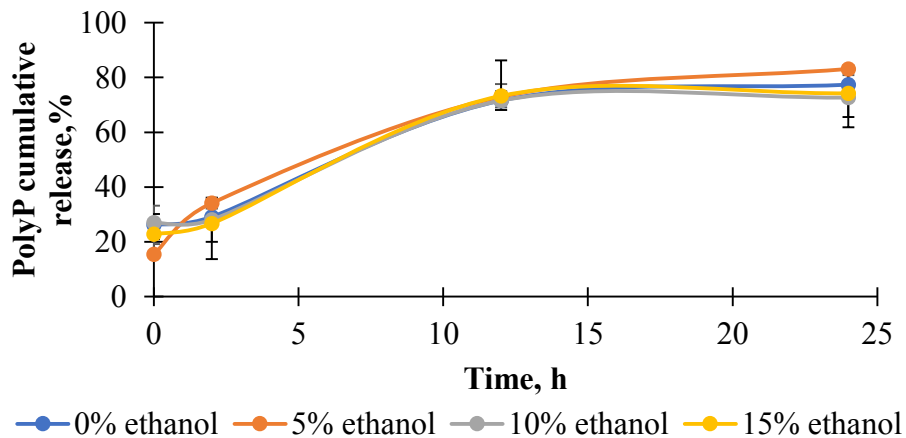


Figure 31. PolyP release profile from alginate beads formed in a 100 mM CaCl₂ crosslinking solution with different concentrations of ethanol. Each alginate bead was formed from a solution with 2.0 %wt. alginate and 25 mM polyP. The experiment was performed with triplicate samples. Data are presented as means ± standard deviation.

5.3 Effect of polycationic polymers on polyP retention

One approach that had initially been considered for the retention of polyP within cell-encapsulating hydrogels was the use of polycationic polymers, such as chitosan, poly-L-lysine, and polyethylenimine (PEI) rather than alginate as the base material, such that polyP could have been used as the crosslinker. This approach was not initially pursued because these polycationic polymers have been associated with cytotoxic and pro-inflammatory effects^{[109][110][111]}. Following our results with alginate detailed thus far, we decided to explore the use of small concentrations of the polycationic polymers as handles to tether polyP onto the calcium-alginate hydrogel.

5.3.1 Chitosan

The first polycationic polymer investigated was chitosan, a linear polysaccharide of glucosamine and N-acetylglucosamine formed by the partial deacetylation of chitin^[112]. Alginate-chitosan beads have previously been shown to exhibit better mechanical properties, limited swelling and decreased drug release at pH 7 compared to calcium-alginate^[113].

PolyP-chitosan-alginate beads were formed by dropping a solution with 25 mM polyP and 2.0 %wt. alginate in a crosslinking solution supplemented with 0, 0.1, 0.2, and 0.4 %wt. chitosan in 100 mM CaCl₂ and evaluating the polyP release profile. Figure 32 shows that there was no significant difference in polyP released at 12 or 24 hours for hydrogels prepared with any chitosan concentration compared to the control prepared in the absence of chitosan; however, at 2 hours, a trend towards decreased polyP release in the presence of chitosan was observed, albeit not a statistically significant effect. This result was intriguing, especially in light of the fact that the pKa of chitosan is approximately 6.5 and that only a relatively small proportion of the amino groups would be positively charged at pH 7.4, the pH of DMEM used in this study. Indeed, it is expected

that the pH would increase rapidly inside the alginate beads following incubation in DMEM and affect the ability of chitosan to retain polyP. Nevertheless, the approach selected here, whereby chitosan was included in the crosslinking bath, could be at cause for the non-significant effect observed here. It may be worth revisiting the use of chitosan as a positively charged linker between alginate and polyP, while using the sample preparation strategy detailed below with PEI.

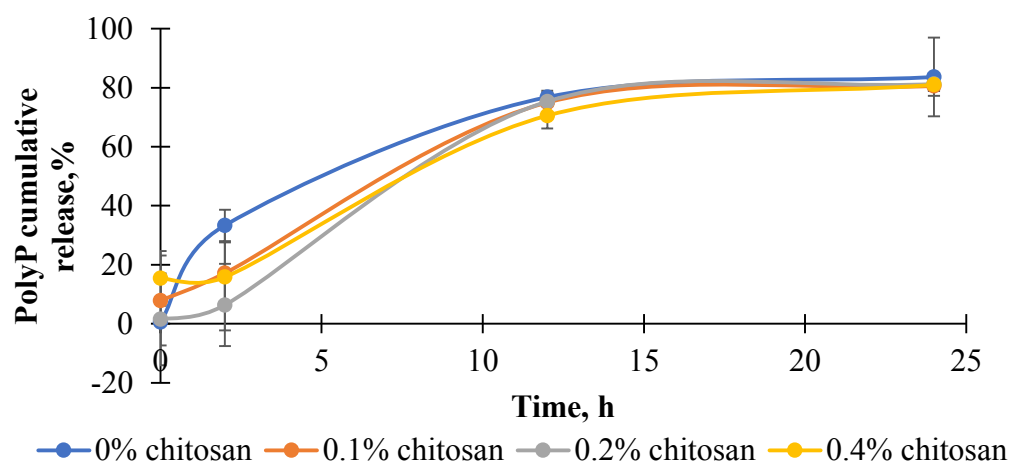


Figure 32. PolyP release profile from alginate beads formed in a 100 mM CaCl₂ crosslinking solution with different concentrations of chitosan. Each alginate bead was formed from a solution with 2.0 %wt. alginate and 25 mM polyP. The experiment was performed in triplicate samples. Data are presented as means ± standard deviation.

5.3.2 Polyethylenimine

PEI is a polycationic polymer containing primary, secondary and tertiary amino groups with a strong anion exchange under a variety of conditions^[114] and a hydrophobic backbone with a closely-spaced amine with weak-base protonation capacity. The pKa values of PEI amino groups are all >9.0, while PEI also has a buffering capacity down to pH 3 covering the physiological range^[115]. This means that it will present a high degree of positive charges at pH 7.4, the pH of

DMEM. In recent years, PEI has been used as a versatile vector for gene delivery and has, therefore, a track record of use with cells^[116]. Here, rather than mix the PEI directly with the crosslinking bath, a different - multistep - approach was attempted. Linear PEI was first mixed with polyP at a molar ratio of positive charges on the PEI to negative charges on the polyP of 1.0:0.9 (assuming that all amines in PEI and all phosphates in polyP are charged). This approach would leave positive charges on the PEI polymer to ionically bind the complexes with the alginate hydrogel. Next, the PEI-polyP complexes were mixed with the alginate solution to form a 2.0 %wt. alginate solution with 25 mM polyP bound with PEI. This solution did not gel owing to the relatively low concentration of PEI-polyP complexes added. The solution was finally dropped into a crosslinking bath consisting of 100 mM CaCl₂ to form a gel. Figure 33 presents the polyP release profile from these PEI-incorporating alginate gels. As can be seen, only approximately 42% of the polyP initially loaded in the beads was released by 24 hours, representing roughly half of that which was released at the same time point from alginate gels prepared without PEI.

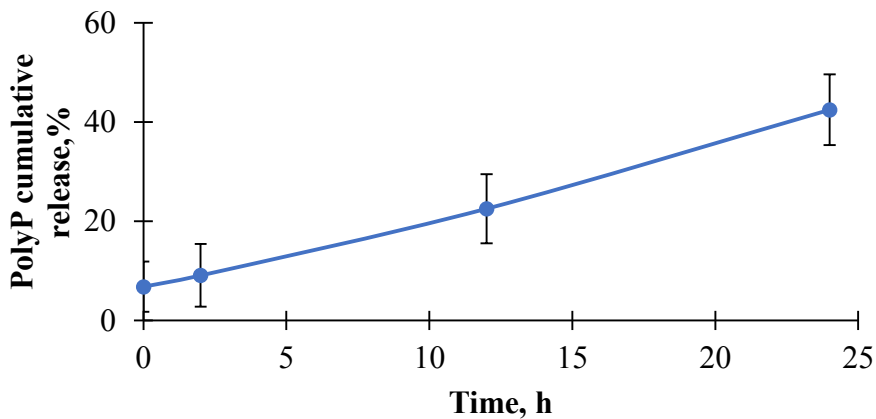


Figure 33. PolyP release profile from alginate beads formed in a 100 mM CaCl₂ crosslinking solution following the addition of polyP-PEI at a 0.9:1.0 charge ratio. Each alginate bead was

formed from a solution with 2.0 %wt. alginate and 25 mM polyP. The experiment was performed in triplicate samples. Data are presented as means \pm standard deviation.

While promising, these results need to be validated with polyP release experiments over prolonged periods of time to fully appreciate the potential of this approach. Further, investigation of different polyP:PEI charge ratio would be necessary to appreciate the potential for control of the release profile. It should be mentioned that our experimental results also suggested that binding of the polyP to PEI interfered with our polyP quantification assay. Indeed, the initial content of polyP measured prior to gelation dropped substantially when introducing PEI. Experiments with only solutions (i.e. no gelation) were conducted next to help us understand this finding (Table 1). This experiment confirmed that the binding of PEI with polyP does impact our ability to detect polyP. A number of approaches were then evaluated to dissociate the polyP from the PEI and recover the ability to measure polyP accurately including chelation with EDTA and increasing the concentration of citrate in the bead digestion buffer. Ultimately, we settled on another modification of the alginate bead digestion buffer. Following the theory of acid dissociation, a change in the pH would potentially help dissociate presumptive ionic bonds between polyP and PEI. In Table 2, this approach was shown to work quite well in solutions, while the extent of the dissociation appeared to be decreased when working with beads (Table3). Therefore, proper controls were used to allow the accurate evaluation of the percentage of polyP released.

Table 1. Measured polyP content when polyP is mixed with PEI and control conditions.

	Average	STDEV
PolyP	18.61	1.35
PBS	0.02	0.05
PEI	-0.01	0.02
PolyP-PEI	8.25	1.38

Table 2. Measured polyP content in solution when polyP is mixed with PEI and alginate and control conditions at different solution pH.

		Average	STDEV
pH 7	PolyP	20.20	1.01
	PolyP-PEI	9.11	0.57
	PolyP-alginate	25.02	1.28
	PolyP-PEI-alginate	12.83	3.29
pH 10	PolyP	20.84	0.48
	PolyP-PEI	10.31	0.64
	PolyP-alginate	23.81	0.84
	PolyP-PEI-alginate	13.09	0.45
pH 11	PolyP	18.95	1.99
	PolyP-PEI	12.01	0.21
	PolyP-alginate	23.91	2.04
	PolyP-PEI-alginate	16.53	2.45
pH 12	PolyP	18.62	1.39
	PolyP-PEI	14.59	0.71
	PolyP-alginate	21.43	1.35
	PolyP-PEI-alginate	19.09	0.65

Table 3. Measured polyP content in beads when polyP is mixed with PEI and alginate and control conditions at different solution pH.

		Average	STDEV
pH 3	PolyP	17.59	1.45
	PBS	0.02	0.02
	PEI	0.01	0.02
	PolyP-PEI	6.35	0.57
pH 10	PolyP	18.70	1.69
	PBS	0.02	0.03
	PEI	-0.02	0.02
	PolyP-PEI	7.45	0.59
pH 12	PolyP	16.52	1.00
	PBS	0.13	0.03
	PEI	-0.01	0.01
	PolyP-PEI	10.86	2.45

Polyp-PEI-calcium-alginate beads are a promising strategy for polyP retention and controlled release. However, PEI has previously been associated with cytotoxicity, which is dependant on the molecular weight and branching ^{[117][118]}. Cytotoxicity was tested using a live/dead assay for chondrocytes encapsulated in (Figure 34 A) calcium-alginate beads, (B) polyP-calcium-alginate beads, (C) PEI-calcium-alginate beads, and (D) polyP-PEI-calcium-alginate beads. The result of this experiment showed the controls in (A) and (B) with a near 100% viability, while in (C) viability dropped to 65%. Interestingly, condition (D; the system of interest including the PEI-polyP complex) showed 93% viability which is the composite of interest for polyP retention. Further tests will be required to determine if the results for the PEI-calcium-alginate beads indicate that cytotoxicity will be an issue for the system over longer time periods.

Nevertheless, these results are encouraging and warrant additional experimentation, notably to select PEI molecules with lower cytotoxicity.

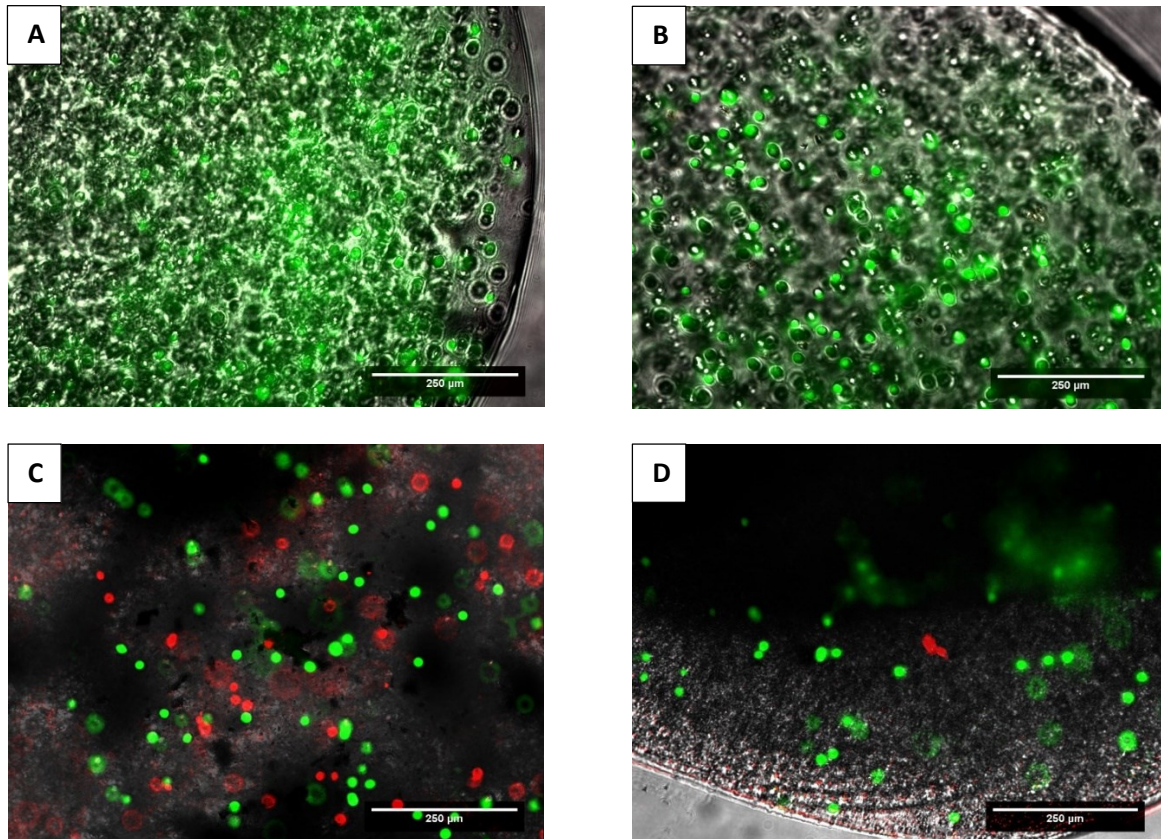


Figure 34. Live/dead assay of Ca-alginate beads (A), polyP-Ca-alginate beads (B), PEI-Ca-alginate beads (C), and PEI-PolyP-Ca- alginate beads (D) at 1million cells per mL and after 24h incubation.

CHAPTER 6 – CONCLUSIONS, LIMITATIONS AND FUTURE WORK

6.1 Conclusions

In this thesis, a protocol was developed to form calcium-alginate beads loaded with 19 μg (i.e. 25 mM) of polyP under sterile conditions. Culture conditions for chondrocytes encapsulated in these alginate beads that prevent excessive proliferation, based on the use of ITS or low FBS supplementation were also investigated. We proceeded to characterize the polyP retention profile in alginate beads over time. It was found that 70-80 % of the cargo is released during a burst release phase within the first 24 hours of incubation, followed by a more gradual release sustained for at least a week. This suggests that only a small proportion of the polyP added actually crosslinks with the alginate meshwork via ionic bonds with the calcium ions. The alginate concentration of hydrogels was found to improve the early retention of polyP. The biological responses of chondrocytes encapsulated within the polyP-alginate beads were significantly impacted, but the effects were lost by week 2. These results still provide a means to ensure the short term release of polyP over a timeframe of days to weeks. While these results may be insufficient for cartilage tissue engineering, they may find applications in the IA delivery of polyP or even in the treatment of skin wounds.

Efforts to reduce the diffusion of polyP during the burst release phase, notably via the substitution of the calcium crosslinker by strontium to reduce hydrogel swelling, were unsuccessful. It became clear through these investigations that the best approach to control the polyP release profile from alginate beads involved developing novel strategies to increase the fraction of polyP that was bound to the alginate meshwork. To achieve this goal and address the limitations associated with the polyP release profile in calcium- and strontium-alginate beads, a

novel strategy involving the tethering of polyanionic polyP onto a linear polycationic PEI polymer via ionic interactions in molar charge ratios of 0.9:1.0, prior to binding of the PEI to alginate via its free positive charges and hydrogel formation in calcium was developed. This approach led to a substantially decreased short term polyP release (40% at 24 hours) and the presence of polyP did reduce the cytotoxicity of PEI. Further work into this strategy is required to assess its potential.

6.2 Limitations

Over the course of the thesis, some issues have limited the progression of the work. The absence of a previous protocol for bead formation and chondrocytes encapsulation under sterile conditions required that efforts be dedicated to the establishment of a reliable procedure. Substantial efforts were dedicated to testing new strategies to retain polyP inside alginate beads for prolonged periods of time. Because a number of different assumptions needed to be tested in order to gain an improved understanding of the complex interactions between alginate, polyP and a range of polycationic crosslinkers, a number of our results do not provide a solution to the issue of an insufficient polyP retention, but rather allow us to eliminate a potential direction. Finally, a compression test was performed with an Instron housed in the Department of Chemical and Biological Engineering. This equipment is equipped with a 150 N load cell, which does not afford the resolution required to properly test hydrogel properties. As such, meaningful compression moduli will need to be obtained from another equipment, once available.

6.3 Future work

This thesis can serve as a basis for the next improvements in regard to polyP delivery to hydrogel encapsulated cells or for the delivery of other bioactive molecules. Alginate beads have been

shown an effective biomaterial for cell encapsulation; however, the polyP interactions with the alginate and crosslinking cations during bead formation and over a prolonged period of time remain to be completely understood. Some approaches that could be investigated further in order to improve the retention of polyP within calcium- and strontium-alginate beads include:

- The crosslinking with a mixture of Ca^{2+} and Ba^{2+} whereby barium can bind to different alginate monomer blocks than calcium and further hinder diffusion and/or increase the proportion of polyP that is crosslinked to the alginate meshwork. This will require special attention to the cytotoxicity of barium.
- The sequestration of polyP as calcium- or strontium-polyP microparticles dispersed within alginate hydrogels to prevent their diffusion out of the material. Other work in the group has established protocols to prepare these particles.
- The sequestration of polyP onto bulky proteins such as albumin (or growth factors) dispersed within alginate hydrogels to prevent their diffusion out of the material. PolyP has been shown to bind to a large number of proteins.

The potential of the polyP-PEI-alginate system also needs to be evaluated further. This will require a longer term evaluation of the polyP release profile, as well as cytotoxicity and an evaluation of cell responses to polyP. Further investigations into the fabrication parameters including the PEI:polyP ratio and incubation times for each step will be required.

In the longer term, the different materials will need to be investigated for applications in cartilage tissue engineering, particularly in the presence of pro-inflammatory cytokines as would be expected in OA joints, and in the IA polyP delivery over prolonged periods.

References

- [1] Arthritis Society of Canada [Internet]. 2009. Available from: <http://www.arthritis.ca/look-at-research/Cochrane-reviews>
- [2] Matsushita T, Tanaka T. [Aging and homeostasis. Aging of articular cartilage and chondrocytes.]. *Clin Calcium*. 2017;27(7):933–9.
- [3] Brandt KD. Osteoarthritis. *Clin Geriatr Med* [Internet]. 1988 May;4(2):279–93. Available from: <http://www.ncbi.nlm.nih.gov/pubmed/3288321>
- [4] Camarero-Espinosa S, Rothen-Rutishauser B, Foster EJ, Weder C. Articular cartilage: from formation to tissue engineering. *Biomater Sci* [Internet]. 2016;4(5):734–67. Available from: <http://xlink.rsc.org/?DOI=C6BM00068A>
- [5] Seidman AJ, Limaïem F. Synovial Fluid Analysis [Internet]. *StatPearls*. 2019. Available from: <http://www.ncbi.nlm.nih.gov/pubmed/30725799>
- [6] Sakata R, Iwakura T, Reddi AH. Regeneration of Articular Cartilage Surface: Morphogens, Cells, and Extracellular Matrix Scaffolds. *Tissue Eng Part B Rev* [Internet]. 2015 Oct;21(5):461–73. Available from: <http://www.ncbi.nlm.nih.gov/pubmed/25951707>
- [7] Song EK, Jeon J, Jang DG, Kim HE, Sim HJ, Kwon KY, et al. ITGEBL1 modulates integrin activity to promote cartilage formation and protect against arthritis. *Sci Transl Med* [Internet]. 2018;10(462). Available from: <http://www.ncbi.nlm.nih.gov/pubmed/30305454>
- [8] Hwang HS, Kim HA. Chondrocyte Apoptosis in the Pathogenesis of Osteoarthritis. *Int J Mol Sci* [Internet]. 2015 Oct 30;16(11):26035–54. Available from:

<http://www.ncbi.nlm.nih.gov/pubmed/26528972>

- [9] Nakasa T, Ochi M. [Cell based therapy for articular cartilage injury]. *Clin Calcium* [Internet]. 2011 Jun;21(6):890–5. Available from: <http://www.ncbi.nlm.nih.gov/pubmed/21628804>
- [10] Makris EA, Gomoll AH, Malizos KN, Hu JC, Athanasiou KA. Repair and tissue engineering techniques for articular cartilage. *Nat Rev Rheumatol* [Internet]. 2015 Jan;11(1):21–34. Available from: <http://www.ncbi.nlm.nih.gov/pubmed/25247412>
- [11] Ng HY, Lee AA, Shen KX. Articular Cartilage: Structure, Composition, Injuries and Repair. *JSM Bone Jt Dis*. 2017;1:1–6.
- [12] Angelova PR, Baev AY, Berezhnov A V, Abramov AY. Role of inorganic polyphosphate in mammalian cells: from signal transduction and mitochondrial metabolism to cell death. *Biochem Soc Trans* [Internet]. 2016 Feb;44(1):40–5. Available from: <http://www.ncbi.nlm.nih.gov/pubmed/26862186>
- [13] Lee WD, Gawri R, Shiba T, Ji A-R, Stanford WL, Kandel RA. Simple Silica Column-Based Method to Quantify Inorganic Polyphosphates in Cartilage and Other Tissues. *Cartilage* [Internet]. 2018;9(4):417–27. Available from: <http://www.ncbi.nlm.nih.gov/pubmed/28357919>
- [14] St-Pierre J-P, Wang Q, Li SQ, Pilliar RM, Kandel RA. Inorganic Polyphosphate Stimulates Cartilage Tissue Formation. *Tissue Eng Part A* [Internet]. 2012;18(11–12):1282–92. Available from: <https://doi.org/10.1089/ten.tea.2011.0356>
- [15] St-Pierre J-P, De Croos JN, Theodoropoulos JS, Petrera M, Sharma P, Li S, et al.

- Inorganic polyphosphate exhibits anabolic effects on articular cartilage. *Osteoarthr Cartil* [Internet]. 2012 Apr 1;20:S39. Available from: <https://doi.org/10.1016/j.joca.2012.02.572>
- [16] Sallis JD, Cheung HS. Inhibitors of articular calcium crystal formation. *Curr Opin Rheumatol* [Internet]. 2003 May;15(3):321–5. Available from: <http://www.ncbi.nlm.nih.gov/pubmed/12707588>
- [17] Rivera-Delgado E, Djuhadi A, Danda C, Kenyon J, Maia J, Caplan AI, et al. Injectable liquid polymers extend the delivery of corticosteroids for the treatment of osteoarthritis. *J Control Release* [Internet]. 2018;284:112–21. Available from: <http://www.ncbi.nlm.nih.gov/pubmed/29906555>
- [18] Pandolfi V, Pereira U, Dufresne M, Legallais C. Alginate-Based Cell Microencapsulation for Tissue Engineering and Regenerative Medicine. *Curr Pharm Des* [Internet]. 2017;23(26):3833–44. Available from: <http://www.ncbi.nlm.nih.gov/pubmed/28911305>
- [19] Capone SH, Dufresne M, Rechel M, Fleury MJ, Salsac AV, Paullier P, et al. Impact of Alginate Composition: From Bead Mechanical Properties to Encapsulated HepG2/C3A Cell Activities for In Vivo Implantation. *PLoS One*. 2013;8(4).
- [20] Kohn R, Larsen B. Preparation of water-soluble polyuronic acids and their calcium salts, and the determination of calcium ion activity in relation to the degree of polymerization. Vol. 26, *Acta chemica Scandinavica*. 1972. p. 2455–68.
- [21] Grasdalen H. Study of the Composition and Sequence of Uronate residues in Alginate. *J Chem Inf Model*. 2013;53(9):1689–99.
- [22] Coates EE, Fisher JP. Cartilage tissue engineering [Internet]. Second Edi. *Tissue*

- Engineering: Principles and Practices. Elsevier Inc.; 2012. 30-1-30–26 p. Available from:
<http://dx.doi.org/10.1016/B978-0-12-381422-7.10053-7>
- [23] Sophia Fox AJ, Bedi A, Rodeo SA. The basic science of articular cartilage: Structure, composition, and function. *Sports Health*. 2009;1(6):461–8.
- [24] Buckwalter, JA ; Mankin,HJ; Grodzinsky A. Articular cartilage and Osteoarthritis. Vol. 54, *Articular Cartilage and Osteoarthritis*. 2005. p. 466–80.
- [25] Brittberg M. Tissue engineering of cartilage. *Tissue Eng [Internet]*. 2008 Jan 1 [cited 2019 Nov 5];533–57. Available from:
<https://www.sciencedirect.com/science/article/pii/B9780123708694000185>
- [26] Luo Y, Sinkeviciute D, He Y, Karsdal M, Henrotin Y, Mobasheri A, et al. The minor collagens in articular cartilage. *Protein Cell [Internet]*. 2017 Aug 17;8(8):560–72. Available from: <http://link.springer.com/10.1007/s13238-017-0377-7>
- [27] Eyre DR. Collagens and Cartilage Matrix Homeostasis. *Clin Orthop Relat Res [Internet]*. 2004 Oct;427:S118–22. Available from: <http://journals.lww.com/00003086-200410001-00020>
- [28] Bruckner P, van der Rest M. Structure and function of cartilage collagens. *Microsc Res Tech [Internet]*. 1994 Aug 1;28(5):378–84. Available from:
<http://doi.wiley.com/10.1002/jemt.1070280504>
- [29] Smeriglio P, Dhulipala L, Lai JH, Goodman SB, Dragoo JL, Smith RL, et al. Collagen VI Enhances Cartilage Tissue Generation by Stimulating Chondrocyte Proliferation. *Tissue Eng Part A [Internet]*. 2015 Feb;21(3–4):840–9. Available from:

<https://www.liebertpub.com/doi/10.1089/ten.tea.2014.0375>

- [30] Eyre DR, Apon S, Wu J-J, Ericsson LH, Walsh KA. Collagen type IX: Evidence for covalent linkages to type II collagen in cartilage. *FEBS Lett* [Internet]. 1987 Aug 17;220(2):337–41. Available from: <http://doi.wiley.com/10.1016/0014-5793%2887%2980842-6>
- [31] Wu JJ, Woods PE, Eyre DR. Identification of cross-linking sites in bovine cartilage type IX collagen reveals an antiparallel type II-type IX molecular relationship and type IX to type IX bonding. *J Biol Chem*. 1992;267(32):23007–14.
- [32] Eyre D. Collagen of articular cartilage. - PubMed - NCBI. *Arthritis Res Ther* [Internet]. 2002;4(1):30–5. Available from: <https://www.ncbi.nlm.nih.gov/pubmed/11879535>
- [33] Lohmander S. Proteoglycans of joint cartilage. *Baillieres Clin Rheumatol* [Internet]. 1988 Apr;2(1):37–62. Available from: <https://linkinghub.elsevier.com/retrieve/pii/S0950357988800049>
- [34] Couchman JR, Pataki CA. An Introduction to Proteoglycans and Their Localization. *J Histochem Cytochem* [Internet]. 2012 Dec 26;60(12):885–97. Available from: <http://journals.sagepub.com/doi/10.1369/0022155412464638>
- [35] Zhang F, Zhang Z, Linhardt RJ. Glycosaminoglycans. In: *Handbook of Glycomics* [Internet]. Elsevier; 2010. p. 59–80. Available from: <https://linkinghub.elsevier.com/retrieve/pii/B9780123736000000032>
- [36] Lories RJ, Luyten FP. Overview of Joint and Cartilage Biology. In: *Genetics of Bone Biology and Skeletal Disease* [Internet]. Elsevier; 2013. p. 35–51. Available from:

<https://linkinghub.elsevier.com/retrieve/pii/B9780123878298000032>

- [37] Hunziker EB. The structure of articular cartilage. *Regen Med Biomater Repair Connect Tissues* [Internet]. 2010 Jan 1 [cited 2019 Nov 5];83–105. Available from: <https://www.sciencedirect.com/science/article/pii/B9781845694173500032>
- [38] Akkiraju H, Nohe A. Role of chondrocytes in cartilage formation, progression of osteoarthritis and cartilage regeneration. *J Dev Biol*. 2015;3(4):177–92.
- [39] Sancho-Tello M, Milián L, Mata Roig M, Martín de Llano JJ, Carda C. Cartilage Regeneration and Tissue Engineering. *Adv Biomech Tissue Regen* [Internet]. 2019 Jan 1 [cited 2019 Nov 5];361–78. Available from: <https://www.sciencedirect.com/science/article/pii/B9780128163900000182>
- [40] Buckwalter JA, Mankin HJ. Articular cartilage: tissue design and chondrocyte-matrix interactions. *Instr Course Lect* [Internet]. 1998;47:477–86. Available from: <http://www.ncbi.nlm.nih.gov/pubmed/9571449>
- [41] Poole AR, Kojima T, Yasuda T, Mwale F, Kobayashi M, Lavery S. Composition and structure of articular cartilage: A template for tissue repair. *Clin Orthop Relat Res*. 2001;1(391 SUPPL.):26–33.
- [42] Buckwalter JA, Mow VC, Ratcliffe A. Restoration of Injured or Degenerated Articular Cartilage. *JAAOS - J Am Acad Orthop Surg* [Internet]. 1994;2(4). Available from: https://journals.lww.com/jaaos/Fulltext/1994/07000/Restoration_of_Injured_or_Degenerated_Articular.2.aspx
- [43] Vaishya R, Pariyo GB, Agarwal AK, Vijay V. Non-operative management of

- osteoarthritis of the knee joint. *J Clin Orthop Trauma* [Internet]. 2016;7(3):170–6.
Available from: <http://dx.doi.org/10.1016/j.jcot.2016.05.005>
- [44] Martel-Pelletier J, McCollum R, Fujimoto N, Obata K, Cloutier JM, Pelletier JP. Excess of metalloproteases over tissue inhibitor of metalloprotease may contribute to cartilage degradation in osteoarthritis and rheumatoid arthritis. *Lab Invest* [Internet]. 1994;70(6):807—815. Available from: <http://europepmc.org/abstract/MED/8015285>
- [45] Pelletier J-P, Mineau F, Faure M-P, Martel-Pelletier J. Imbalance between the mechanisms of activation and inhibition of metalloproteases in the early lesions of experimental osteoarthritis. *Arthritis Rheum* [Internet]. 1990 Oct;33(10):1466–76.
Available from: <http://doi.wiley.com/10.1002/art.1780331003>
- [46] Mankin HJ. The response of articular cartilage to mechanical injury. *J Bone Joint Surg Am* [Internet]. 1982 Mar;64(3):460–6. Available from:
<http://www.ncbi.nlm.nih.gov/pubmed/6174527>
- [47] Rönn K, Reischl N, Gautier E, Jacobi M. Current Surgical Treatment of Knee Osteoarthritis. *Arthritis*. 2011;2011:1–9.
- [48] Harris JD, Cole BJ. Knee Articular Cartilage Restoration Procedures. *Noyes' Knee Disord Surgery, Rehabil Clin Outcomes* [Internet]. 2017 Jan 1 [cited 2019 Nov 5];912–21.
Available from:
<https://www.sciencedirect.com/science/article/pii/B9780323329033000317>
- [49] Barr AJ, Conahan PG. Disease-modifying osteoarthritis drugs (DMOADs): what are they and what can we expect from them? [Internet]. *Medicographia*. 2013. p. 189–96.
Available from: <http://www.medicographia.com/2013/10/disease-modifying->

osteoarthritis-drugs-dmoads-what-are-they-and-what-can-we-expect-from-them/.

- [50] Thysen S, Luyten FP, Lories RJU. Targets, models and challenges in osteoarthritis research. *Dis Model Mech* [Internet]. 2015 Jan 1;8(1):17–30. Available from: <http://dmm.biologists.org/cgi/doi/10.1242/dmm.016881>
- [51] Watt FE, Gulati M. New Drug Treatments for Osteoarthritis: What is on the Horizon? *Eur Med journal Rheumatol* [Internet]. 2017 Mar 2;2(1):50–8. Available from: <http://www.ncbi.nlm.nih.gov/pubmed/30364878>
- [52] Bellamy N. Outcome measurement in osteoarthritis clinical trials. *J Rheumatol Suppl* [Internet]. 1995 Feb;43:49–51. Available from: <http://www.ncbi.nlm.nih.gov/pubmed/7752137>
- [53] Li MH, Xiao R, Li JB, Zhu Q. Regenerative approaches for cartilage repair in the treatment of osteoarthritis. *Osteoarthr Cartil*. 2017;25(10):1577–87.
- [54] Fitzgerald K, Susko A. The pain-relieving qualities of exercise in knee osteoarthritis. *Open Access Rheumatol Res Rev* [Internet]. 2013 Oct;81. Available from: <http://www.dovepress.com/the-pain-relieving-qualities-of-exercise-in-knee-osteoarthritis-peer-reviewed-article-OARRR>
- [55] Crawford DC, Miller LE, Block JE. Conservative management of symptomatic knee osteoarthritis: a flawed strategy? *Orthop Rev (Pavia)* [Internet]. 2013 Feb 22;5(1):2. Available from: <http://www.pagepress.org/journals/index.php/or/article/view/or.2013.e2>
- [56] Hofstede SN, Vliet Vlieland TP, van den Ende CH, Marang-van de Mheen PJ, Nelissen RG, van Bodegom-Vos L. Designing a strategy to implement optimal conservative

- treatments in patients with knee or hip osteoarthritis in orthopedic practice: a study protocol of the BART-OP study. *Implement Sci* [Internet]. 2014 Dec 18;9(1):22. Available from: <http://implementationscience.biomedcentral.com/articles/10.1186/1748-5908-9-22>
- [57] Manheimer E, Cheng K, Wieland LS, Shen X, Lao L, Guo M, et al. Acupuncture for hip osteoarthritis. *Cochrane database Syst Rev* [Internet]. 2018;5:CD013010. Available from: <http://www.ncbi.nlm.nih.gov/pubmed/29729027>
- [58] Manheimer E, Cheng K, Linde K, Lao L, Yoo J, Wieland S, et al. Acupuncture for peripheral joint osteoarthritis. *Cochrane database Syst Rev* [Internet]. 2010 Jan 20;(1):CD001977. Available from: <http://www.ncbi.nlm.nih.gov/pubmed/20091527>
- [59] Giangarra CE, Manske RC, Fitzgerald GK, Irrgang JJ. Articular Cartilage Procedures of the Knee. *Clin Orthop Rehabil a Team Approach* [Internet]. 2018 Jan 1 [cited 2019 Nov 5];405-410.e1. Available from: <https://www.sciencedirect.com/science/article/pii/B9780323393706000615>
- [60] Davies R, Kuiper N. Regenerative Medicine: A Review of the Evolution of Autologous Chondrocyte Implantation (ACI) Therapy. *Bioengineering* [Internet]. 2019 Mar 13;6(1):22. Available from: <https://www.mdpi.com/2306-5354/6/1/22>
- [61] Carr BC, Goswami T. Knee implants - Review of models and biomechanics. *Mater Des*. 2009;30(2):398–413.
- [62] Ahadian S, Savoji H, Khademhosseini A. Recent advances in hydrogels for tissue engineering. *Chem Eng Prog*. 2018;114(5):59–75.

- [63] Armiento AR, Stoddart MJ, Alini M, Eglin D. Biomaterials for articular cartilage tissue engineering: Learning from biology. *Acta Biomater* [Internet]. 2018;65:1–20. Available from: <https://doi.org/10.1016/j.actbio.2017.11.021>
- [64] Kwon H, Paschos NK, Hu JC, Athanasiou K. Articular cartilage tissue engineering: the role of signaling molecules. *Cell Mol Life Sci* [Internet]. 2016 Mar 25;73(6):1173–94. Available from: <https://linkinghub.elsevier.com/retrieve/pii/S0142961216301296>
- [65] Huang BJ, Hu JC, Athanasiou KA. Cell-based tissue engineering strategies used in the clinical repair of articular cartilage. *Biomaterials* [Internet]. 2016 Aug;98(5):1–22. Available from: <https://linkinghub.elsevier.com/retrieve/pii/S0142961216301296>
- [66] Vinatier C, Guicheux J. Cartilage tissue engineering: From biomaterials and stem cells to osteoarthritis treatments. *Ann Phys Rehabil Med* [Internet]. 2016;59(3):139–44. Available from: <http://dx.doi.org/10.1016/j.rehab.2016.03.002>
- [67] Kumble KD, Kornberg A. Inorganic Polyphosphate in Mammalian Cells and Tissues. *J Biol Chem* [Internet]. 1995 Mar 17;270(11):5818–22. Available from: <http://www.jbc.org/lookup/doi/10.1074/jbc.270.11.5818>
- [68] Morrissey JH, Choi SH, Smith SA. Polyphosphate: An ancient molecule that links platelets, coagulation, and inflammation. *Blood*. 2012;119(25):5972–9.
- [69] Leyhausen G, Lorenz B, Zhu H, Geurtsen W, Bohnensack R, Müller WEG, et al. Inorganic Polyphosphate in Human Osteoblast-like Cells. *J Bone Miner Res* [Internet]. 1998 May 1;13(5):803–12. Available from: <http://doi.wiley.com/10.1359/jbmr.1998.13.5.803>

- [70] Hacchou Y, Uematsu T, Ueda O, Usui Y, Uematsu S, Takahashi M, et al. Inorganic Polyphosphate: a Possible Stimulant of Bone Formation. *J Dent Res* [Internet]. 2007 Sep 20;86(9):893–7. Available from:
<http://journals.sagepub.com/doi/10.1177/154405910708600917>
- [71] Kawazoe Y, Shiba T, Nakamura R, Mizuno A, Tsutsumi K, Uematsu T, et al. Induction of Calcification in MC3T3-E1 Cells by Inorganic Polyphosphate. *J Dent Res* [Internet]. 2004 Aug 20;83(8):613–8. Available from:
<http://journals.sagepub.com/doi/10.1177/154405910408300806>
- [72] Smith SA, Mutch NJ, Baskar D, Rohloff P, Docampo R, Morrissey JH. Polyphosphate modulates blood coagulation and fibrinolysis. *Proc Natl Acad Sci* [Internet]. 2006 Jan 24;103(4):903–8. Available from: <http://www.pnas.org/cgi/doi/10.1073/pnas.0507195103>
- [73] Wang Q, St-Pierre J-P, Kandel RA, Li SQ, Pilliar RM. Inorganic Polyphosphate Stimulates Cartilage Tissue Formation. *Tissue Eng Part A*. 2012;18(11–12):1282–92.
- [74] Shiba T, Nishimura D, Kawazoe Y, Onodera Y, Tsutsumi K, Nakamura R, et al. Modulation of Mitogenic Activity of Fibroblast Growth Factors by Inorganic Polyphosphate. *J Biol Chem* [Internet]. 2003 Jul 18;278(29):26788–92. Available from:
<http://www.jbc.org/lookup/doi/10.1074/jbc.M303468200>
- [75] Xie L, Jakob U. Inorganic polyphosphate, a multifunctional polyanionic protein scaffold. *J Biol Chem* [Internet]. 2019 Feb 8;294(6):2180–90. Available from:
<http://www.jbc.org/lookup/doi/10.1074/jbc.REV118.002808>
- [76] Itoh H, Shiba T. Polyphosphate Synthetic Activity of Polyphosphate:AMP Phosphotransferase in *Acinetobacter johnsonii* 210A. *J Bacteriol* [Internet]. 2004 Aug

- 1;186(15):5178–81. Available from: <http://jb.asm.org/cgi/doi/10.1128/JB.186.15.5178-5181.2004>
- [77] Viera Rey DF, St-Pierre J-P. Fabrication techniques of tissue engineering scaffolds. In: Handbook of Tissue Engineering Scaffolds: Volume One [Internet]. Elsevier; 2019. p. 109–25. Available from: <https://linkinghub.elsevier.com/retrieve/pii/B978008102563500006X>
- [78] Mantha S, Pillai S, Khayambashi P, Upadhyay A, Zhang Y, Tao O, et al. Smart Hydrogels in Tissue Engineering and Regenerative Medicine. Materials (Basel) [Internet]. 2019 Oct 12;12(20):3323. Available from: <https://www.mdpi.com/1996-1944/12/20/3323>
- [79] Eslahi N, Abdorahim M, Simchi A. Smart Polymeric Hydrogels for Cartilage Tissue Engineering: A Review on the Chemistry and Biological Functions. Biomacromolecules. 2016;17(11):3441–63.
- [80] Lee KY, Mooney DJ. Alginate: Properties and biomedical applications. Prog Polym Sci [Internet]. 2012 Jan 1 [cited 2018 Feb 23];37(1):106–26. Available from: <https://www.sciencedirect.com/science/article/pii/S0079670011000918>
- [81] Partovinia A, Vatankhah E. Experimental investigation into size and sphericity of alginate micro-beads produced by electrospraying technique: Operational condition optimization. Carbohydr Polym [Internet]. 2019 Apr;209:389–99. Available from: <https://linkinghub.elsevier.com/retrieve/pii/S0144861719300190>
- [82] Huang S-L, Lin Y-S. The Size Stability of Alginate Beads by Different Ionic Crosslinkers. Adv Mater Sci Eng [Internet]. 2017;2017:1–7. Available from: <https://www.hindawi.com/journals/amse/2017/9304592/>

- [83] Lee KY, Mooney DJ. Alginate: Properties and biomedical applications. *Prog Polym Sci*. 2012;37(1):106–26.
- [84] Coulson-Thomas VJ, ferreira tarsis. Dimethylmethylen Blue Assay (DMMB). *Bio-protocol* [Internet]. 2014;4(18):e1236. Available from: <https://doi.org/10.21769/BioProtoc.1236>
- [85] Kim Y-J, Sah RLY, Doong J-YH, Grodzinsky AJ. Fluorometric assay of DNA in cartilage explants using Hoechst 33258. *Anal Biochem* [Internet]. 1988 Oct;174(1):168–76. Available from: <https://linkinghub.elsevier.com/retrieve/pii/0003269788905325>
- [86] St-Pierre JP, Wang Q, Li SQ, Pilliar RM, Kandel RA. Inorganic polyphosphate stimulates cartilage tissue formation. *Tissue Eng - Part A*. 2012;18(11–12):1282–92.
- [87] Hashimoto S, Takahashi K, Amiel D, Coutts RD, Lotz M. Chondrocyte apoptosis and nitric oxide production during experimentally induced osteoarthritis. *Arthritis Rheum* [Internet]. 1998 Jul;41(7):1266–74. Available from: <http://doi.wiley.com/10.1002/1529-0131%28199807%2941%3A7%3C1266%3A%3AAID-ART18%3E3.0.CO%3B2-Y>
- [88] Liu X, Liu J, Kang N, Yan L, Wang Q, Fu X, et al. Role of Insulin-Transferrin-Selenium in Auricular Chondrocyte Proliferation and Engineered Cartilage Formation in Vitro. *Int J Mol Sci* [Internet]. 2014 Jan 21;15(1):1525–37. Available from: <http://www.mdpi.com/1422-0067/15/1/1525>
- [89] Liu X, Zhang T, Wang R, Shi P, Pan B, Pang X. Insulin-Transferrin-Selenium as a Novel Serum-free Media Supplement for the Culture of Human Amnion Mesenchymal Stem Cells. *Ann Clin Lab Sci* [Internet]. 2019;49(1):63–71. Available from: <http://www.ncbi.nlm.nih.gov/pubmed/30814079>

- [90] Casale J, Crane JS. Biochemistry, Glycosaminoglycans. StatPearls. 2020.
- [91] Urban JPG, Hall AC, Gehl KA. Regulation of matrix synthesis rates by the ionic and osmotic environment of articular chondrocytes. *J Cell Physiol* [Internet]. 1993 Feb;154(2):262–70. Available from: <http://doi.wiley.com/10.1002/jcp.1041540208>
- [92] Rosenzweig DH, Matmati M, Khayat G, Chaudhry S, Hinz B, Quinn TM. Culture of Primary Bovine Chondrocytes on a Continuously Expanding Surface Inhibits Dedifferentiation. *Tissue Eng Part A* [Internet]. 2012 Dec;18(23–24):2466–76. Available from: <https://www.liebertpub.com/doi/10.1089/ten.tea.2012.0215>
- [93] Gibson GJ, Schor SL, Grant ME. Effects of matrix macromolecules on chondrocyte gene expression: synthesis of a low molecular weight collagen species by cells cultured within collagen gels. *J Cell Biol* [Internet]. 1982 Jun 1;93(3):767–74. Available from: <https://rupress.org/jcb/article/93/3/767/21257/Effects-of-matrix-macromolecules-on-chondrocyte>
- [94] Shapiro EM, Borthakur A, Dandora R, Kriss A, Leigh JS, Reddy R. Sodium visibility and quantitation in intact bovine articular cartilage using high field (23)Na MRI and MRS. *J Magn Reson* [Internet]. 2000 Jan;142(1):24–31. Available from: <http://www.ncbi.nlm.nih.gov/pubmed/10617432>
- [95] Paunipagar BK, Rasalkar D. Imaging of articular cartilage. *Indian J Radiol Imaging* [Internet]. 2014 Jul;24(3):237–48. Available from: <http://www.ncbi.nlm.nih.gov/pubmed/25114386>
- [96] Martin P, Van Mooy BAS. Fluorometric quantification of polyphosphate in environmental plankton samples: Extraction protocols, matrix effects, and nucleic acid interference. *Appl*

- Environ Microbiol. 2013;79(1):273–81.
- [97] Diaz JM, Ingall ED. Fluorometric quantification of natural inorganic polyphosphate. Environ Sci Technol. 2010;44(12):4665–71.
- [98] Mørch ÝA, Donati I, Strand BL. Effect of Ca²⁺, Ba²⁺, and Sr²⁺ on Alginate Microbeads. Biomacromolecules [Internet]. 2006 May;7(5):1471–80. Available from: <https://pubs.acs.org/doi/10.1021/bm060010d>
- [99] Ramteke K.H., Dighe P.A., Kharat A. R. PSV. Mathematical Models of Drug Dissolution: A Review. J Philos Hist. 2008;2(1):1–28.
- [100] Bajpai SK, Tankhiwale R. Examination of the Higuchi Model for the Release of Vitamin B₂ from Multilayered Calcium Alginate/Chitosan Beads in Varying pH Medium. J Macromol Sci Part A [Internet]. 2006 Jun;43(7):1013–20. Available from: <http://www.tandfonline.com/doi/abs/10.1080/10601320600739985>
- [101] Bhopatkar D, Anal AK, Stevens WF. Ionotropic alginate beads for controlled intestinal protein delivery: Effect of chitosan and barium counter-ions on entrapment and release. J Microencapsul [Internet]. 2005 Feb 3;22(1):91–100. Available from: <http://www.tandfonline.com/doi/full/10.1080/02652040400026434>
- [102] Dalheim MØ, Omtvedt LA, Bjørge IM, Akbarzadeh A, Mano JF, Aachmann FL, et al. Mechanical Properties of Ca-Saturated Hydrogels with Functionalized Alginate. Gels. 2019 Apr;5(2):23.
- [103] Liu J, Rawlinson SCF, Hill RG, Fortune F. Strontium-substituted bioactive glasses in vitro osteogenic and antibacterial effects. Dent Mater [Internet]. 2016 Mar;32(3):412–22.

Available from: <https://linkinghub.elsevier.com/retrieve/pii/S0109564115005163>

- [104] Iskandar L, Rojo L, Di Silvio L, Deb S. The effect of chelation of sodium alginate with osteogenic ions, calcium, zinc, and strontium. *J Biomater Appl* [Internet]. 2019 Oct 19;34(4):573–84. Available from: <http://journals.sagepub.com/doi/10.1177/0885328219861904>
- [105] Yu D, Ding H, Mao Y, Liu M, Yu B, Zhao X, et al. Strontium ranelate reduces cartilage degeneration and subchondral bone remodeling in rat osteoarthritis model. *Acta Pharmacol Sin* [Internet]. 2013 Mar 21;34(3):393–402. Available from: <http://www.nature.com/articles/aps2012167>
- [106] Bajpai SK, Sharma S. Investigation of swelling/degradation behaviour of alginate beads crosslinked with Ca²⁺ and Ba²⁺ ions. *React Funct Polym* [Internet]. 2004 May;59(2):129–40. Available from: <https://linkinghub.elsevier.com/retrieve/pii/S1381514804000161>
- [107] Bajpai SK, Kirar N. Swelling and drug release behavior of calcium alginate/poly (sodium acrylate) hydrogel beads. *Des Monomers Polym* [Internet]. 2016 Jan 2;19(1):89–98. Available from: <http://www.tandfonline.com/doi/full/10.1080/15685551.2015.1092016>
- [108] Topuz F, Henke A, Richtering W, Groll J. Magnesium ions and alginate do form hydrogels: a rheological study. *Soft Matter* [Internet]. 2012;8(18):4877. Available from: <http://xlink.rsc.org/?DOI=c2sm07465f>
- [109] He W, Guo Z, Wen Y, Wang Q, Xie B, Zhu S, et al. Alginate-Graft-PEI as a Gene Delivery Vector with High Efficiency and Low Cytotoxicity. *J Biomater Sci Polym Ed* [Internet]. 2012 Jan 13;23(1–4):315–31. Available from:

<https://www.tandfonline.com/doi/full/10.1163/092050610X550359>

- [110] Patnaik S, Aggarwal A, Nimesh S, Goel A, Ganguli M, Saini N, et al. PEI-alginate nanocomposites as efficient in vitro gene transfection agents. *J Control Release* [Internet]. 2006 Sep;114(3):398–409. Available from: <https://linkinghub.elsevier.com/retrieve/pii/S0168365906003154>
- [111] Rajaram A, Schreyer DJ, Chen DXB. Use of the polycation polyethyleneimine to improve the physical properties of alginate–hyaluronic acid hydrogel during fabrication of tissue repair scaffolds. *J Biomater Sci Polym Ed* [Internet]. 2015 May 3;26(7):433–45. Available from: <http://www.tandfonline.com/doi/abs/10.1080/09205063.2015.1016383>
- [112] Hari PR, Chandy T, Sharma CP. Chitosan/calcium?alginate beads for oral delivery of insulin. *J Appl Polym Sci* [Internet]. 1996 Mar 14;59(11):1795–801. Available from: <http://doi.wiley.com/10.1002/%28SICI%291097-4628%2819960314%2959%3A11%3C1795%3A%3AAID-APP16%3E3.0.CO%3B2-T>
- [113] Segale L, Giovannelli L, Mannina P, Pattarino F. Calcium Alginate and Calcium Alginate-Chitosan Beads Containing Celecoxib Solubilized in a Self-Emulsifying Phase. *Scientifica (Cairo)* [Internet]. 2016;2016:1–8. Available from: <http://www.hindawi.com/journals/scientifica/2016/5062706/>
- [114] Virgen-Ortíz JJ, dos Santos JCS, Berenguer-Murcia Á, Barbosa O, Rodrigues RC, Fernandez-Lafuente R. Polyethylenimine: a very useful ionic polymer in the design of immobilized enzyme biocatalysts. *J Mater Chem B* [Internet]. 2017;5(36):7461–90. Available from: <http://xlink.rsc.org/?DOI=C7TB01639E>
- [115] Benjaminsen R V., Matthebjerg MA, Henriksen JR, Moghimi SM, Andresen TL. The

possible "proton sponge " effect of polyethylenimine (PEI) does not include change in lysosomal pH. *Mol Ther.* 2013;21(1):149–57.

- [116] Zakeri A, Kouhbanani MAJ, Beheshtkhoo N, Beigi V, Mousavi SM, Hashemi SAR, et al. Polyethylenimine-based nanocarriers in co-delivery of drug and gene: a developing horizon. *Nano Rev Exp* [Internet]. 2018 Jan 3;9(1):1488497. Available from: <https://www.tandfonline.com/doi/full/10.1080/20022727.2018.1488497>
- [117] Barkat MA, A.B. H, Beg S, Ahmad FJ, editors. *Multifunctional Nanocarriers for Contemporary Healthcare Applications* [Internet]. IGI Global; 2018. (Advances in Medical Technologies and Clinical Practice). Available from: <http://services.igi-global.com/resolvedoi/resolve.aspx?doi=10.4018/978-1-5225-4781-5>
- [118] Khansarizadeh M, Mokhtarzadeh A, Rashedinia M, Taghdisi S, Lari P, Abnous K, et al. Identification of possible cytotoxicity mechanism of polyethylenimine by proteomics analysis. *Hum Exp Toxicol* [Internet]. 2016 Apr 30;35(4):377–87. Available from: <http://journals.sagepub.com/doi/10.1177/0960327115591371>